

CALIBRATION OF CONVENTIONAL MEASUREMENT TRANSFORMERS  
AGAINST HARMONIC COMPONENTS BY USING FIELD MEASUREMENTS  
OF OPTICAL TRANSDUCERS AND RESISTIVE-CAPACITIVE VOLTAGE  
TRANSFORMERS

A THESIS SUBMITTED TO  
THE GRADUATE SCHOOL OF NATURAL AND APPLIED SCIENCES  
OF  
MIDDLE EAST TECHNICAL UNIVERSITY

BY

COŞKUN AZİZ TÜRKMEN

IN PARTIAL FULFILLMENT OF THE REQUIREMENTS  
FOR  
THE DEGREE OF MASTER OF SCIENCE  
IN  
ELECTRICAL AND ELECTRONICS ENGINEERING

MAY 2010

Approval of the thesis:

**CALIBRATION OF CONVENTIONAL MEASUREMENT TRANSFORMERS  
AGAINST HARMONIC COMPONENTS BY USING FIELD MEASUREMENTS  
OF OPTICAL TRANSDUCERS AND RESISTIVE-CAPACITIVE VOLTAGE  
TRANSFORMERS**

submitted by **COŞKUN AZİZ TÜRKMEN** in partial fulfillment of the requirements  
for the degree of **Master of Science in Electrical and Electronics Engineering De-  
partment, Middle East Technical University** by,

Prof. Dr. Canan ÖZGEN \_\_\_\_\_  
Dean, Graduate School of **Natural and Applied Sciences**

Prof. Dr. İsmet ERKMEN \_\_\_\_\_  
Head of Department, **Electrical and Electronics Engineering**

Prof. Dr. Muammer Ermiş \_\_\_\_\_  
Supervisor, **Electrical and Electronics Engineering Dept.,  
METU**

**Examining Committee Members:**

Prof. Dr. Nezih Güven \_\_\_\_\_  
Electrical and Electronics Engineering, METU

Prof. Dr. Muammer Ermiş \_\_\_\_\_  
Electrical and Electronics Engineering, METU

Prof. Dr. Ahmet Rumeli \_\_\_\_\_  
Electrical and Electronics Engineering, METU

Prof. Dr. Mirzahan Hizal \_\_\_\_\_  
Electrical and Electronics Engineering, METU

M.Sc. Cem Özgür Gerçek \_\_\_\_\_  
TÜBİTAK - Uzay

**Date:** \_\_\_\_\_

**I hereby declare that all information in this document has been obtained and presented in accordance with academic rules and ethical conduct. I also declare that, as required by these rules and conduct, I have fully cited and referenced all material and results that are not original to this work.**

Name, Last Name: COŞKUN AZİZ TÜRKMEN

Signature :

## **ABSTRACT**

### **CALIBRATION OF CONVENTIONAL MEASUREMENT TRANSFORMERS AGAINST HARMONIC COMPONENTS BY USING FIELD MEASUREMENTS OF OPTICAL TRANSDUCERS AND RESISTIVE-CAPACITIVE VOLTAGE TRANSFORMERS**

Türkmen, Coşkun Aziz

M.S., Department of Electrical and Electronics Engineering

Supervisor : Prof. Dr. Muammer Ermiş

May 2010, 147 pages

It is known from the literature that conventional voltage and current transformers measure inaccurate values for voltage and current harmonics which are parts of power quality. Maximum bandwidth of conventional current transformers, which are used in electricity transmission and distribution systems, is 1.5-2 kHz and it is lower for conventional voltage transformers. Also, it is known that; voltages in some frequency spectrum are measured higher and voltages in another frequency spectrum are measured lower by the conventional voltage transformers. Furthermore, because of the phase shift of fundamental component caused by the conventional current and voltage transformers, losses and efficiency can not be calculated accurately. In this work, through the simultaneous measurements taken at the same feeder by both conventional transformers and new technology measurement transformers; amplitude and phase shift errors which are caused by conventional transformers depending on frequency and so harmonics, are examined and evaluated. Amplitude coefficients and phase shifts are determined for different types of conventional transformers to be able

to calibrate measurement deviation. Through this work, measured data by conventional transformers will be accurate and realistic in terms of harmonic components. This matter is important to determine whether the accurate limits which will be set in the future possibly concerning with harmonics and interharmonics, are surpassed or not; also for punitive sanction.

Keywords: optical voltage and current transducers, resistive-capacitive voltage transformer (RCVT), instrument transformers, harmonic measurements, power quality

## ÖZ

### KONVANSİYONEL ÖLÇÜ TRANSFORMATÖRLERİNİN, OPTİK DÖNÜŞTÜRÜCÜLER VE REZİSTİF-KAPASİTİF GERİLİM TRANSFORMATÖRLERİ İLE YAPILAN SAHA ÖLÇÜMLERİ KULLANILARAK HARMONİKLERE YÖNELİK KALİBRASYONU

Türkmen, Coşkun Aziz

Yüksek Lisans, Elektrik-Elektronik Mühendisliği Bölümü

Tez Yöneticisi : Prof. Dr. Muammer Ermiş

Mayıs 2010, 147 sayfa

Güç kalitesi bileşenleri olan gerilim ve akım harmoniklerinin okunmasında mevcut gerilim ve akım ölçü transformatörlerinin yanlış sonuçlar verdiği literatürdeki bilgilerden anlaşılmaktadır. Elektrik iletim ve dağıtım sistemlerinde kullanılan konvansiyonel akım ölçü transformatörlerinin bant genişlikleri en çok 1.5-2 kHz değerine ulaşabilmektedir. Konvansiyonel gerilim transformatörleri için ise bu değer daha da düşüktür. Bu transformatörlerin bazı frekans aralığındaki gerilimleri olduğundan daha fazla, bazılarını ise daha az ölçtüğü de bilinmektedir. Ayrıca konvansiyonel akım ve gerilim transformatörlerinin ana bileşen ölçümünde yaptıkları faz kaymaları yüzünden kayıplar ve verimlilik de sağlıklı bir şekilde hesaplanamamaktadır. Bu çalışmada mevcut konvansiyonel ölçü transformatörleri ve yeni teknoloji ölçü transformatörleriyle eşzamanlı ve aynı fiderde yapılan ölçümler sayesinde, konvansiyonel ölçü transformatörlerinin frekansa ve dolayısıyla harmoniklere bağlı olarak yaptıkları genlik ve faz ölçüm sapmaları ortaya çıkarılmış ve değerlendirilmiştir. Bu ölçüm sapmalarını kalibre edebilmek amacıyla farklı konvansiyonel ölçü transformatörü tipleri

için genlik katsayıları ve faz kaymaları belirlenmiştir. Bu çalışma sayesinde konvansiyonel ölçü transformatörleri ile toplanacak olan veriler de harmonik bileşen açısından artık doğru ve gerçekçi olabilecektir. Bu husus, harmonik ve interharmoniklerle ilgili olarak gelecekte konulması muhtemel hassas sınırların aşılıp aşılmadığının tespiti ve cezai yaptırım durumları için büyük önem arz etmektedir.

**Anahtar Kelimeler:** optik gerilim ve akım dönüştürücüleri, rezistif-kapasitif gerilim transformatörü (RCVT), ölçü transformatörleri, harmonik ölçümü, güç kalitesi

*To Headbangers*

## ACKNOWLEDGMENTS

I would like to express my deepest gratitude to my supervisor Prof. Dr. Muammer Ermiř for his guidance, advice, encouragements, criticism and insight throughout this thesis.

I would like to express my deepest thanks to Prof. Dr. Iřık adırcı for her guidance and support throughout this thesis.

I also thank all personnel of TÜBİTAK-Uzay Power Electronics Group for their guidance throughout my research work and the research environment, which they provided.

I would like to thank project manager Cem Özgür Gerçek for his dedicated efforts, companionship and cooperation throughout this thesis.

I am especially thankful to my colleagues Erinç Altıntaş, Burhan Halilođlu, Özgür Ünsar and Serkan Sönmez for their companionship and dedicated efforts during building the mobile platforms and field measurements; Dilek Küçük, Serkan Buhan and Neslihan Köse for the development of the measurement software.

I also would like to thank Yener Akkaya for his support and guidance at substations of TEİAŞ.

I would like to thank my family for their life-long guidance and continuous morale support.

Finally, i am thankful to TÜBİTAK BİDEB for the scholarship.

This thesis is fully supported by the Public Research Grant Committee (KAMAG) of TÜBİTAK within the scope of the National Power Quality Project (105G129).

# TABLE OF CONTENTS

ABSTRACT . . . . .	iv
ÖZ . . . . .	vi
ACKNOWLEDGMENTS . . . . .	ix
TABLE OF CONTENTS . . . . .	x
LIST OF TABLES . . . . .	xii
LIST OF FIGURES . . . . .	xv
CHAPTER	
1 INTRODUCTION . . . . .	1
1.1 Scope of the Thesis . . . . .	8
2 MEASUREMENT TRANSFORMERS FOR EHV, HV AND MV AP- PLICATIONS . . . . .	10
2.1 Conventional Current Transformers . . . . .	10
2.2 Conventional Voltage Transformers . . . . .	15
2.2.1 Capacitive Voltage Transformers . . . . .	17
2.2.2 Inductive Voltage Transformers . . . . .	22
2.2.3 Capacitive Voltage Dividers . . . . .	26
2.3 Resistive - Capacitive Voltage Transformers (RCVTs) . . . . .	27
2.4 Optical Voltage and Current Transducers (NXVCT and NXCT) . . . . .	37
2.4.1 Optical Current Transducer . . . . .	44
2.4.2 Optical Voltage Transducer . . . . .	46
3 MOBILE MEASUREMENT INFRASTRUCTURE . . . . .	49
3.1 Trailer of the Columns . . . . .	49
3.2 Trailer of the Electronic System . . . . .	56

3.3	Measurement Software . . . . .	60
4	SIMULATION MODEL OF A CVT . . . . .	65
4.1	General Model of the CVT . . . . .	65
4.2	Effect of $L_c$ . . . . .	70
4.3	Effect of Ferroresonance Suppression Circuit . . . . .	71
5	FIELD TEST RESULTS . . . . .	72
5.1	RCVT versus NXVCT . . . . .	72
5.2	Voltage Measurements . . . . .	73
5.2.1	Voltage Measurements at 34.5 kV . . . . .	73
5.2.2	Voltage Measurements at 154 kV . . . . .	80
5.2.3	Voltage Measurements at 380 kV . . . . .	83
5.3	Current Measurements . . . . .	86
5.3.1	Current Measurements at 34.5 kV . . . . .	87
5.3.2	Current Measurements at 154 kV . . . . .	96
5.3.3	Current Measurements at 380 kV . . . . .	98
6	CONCLUSION . . . . .	100
	REFERENCES . . . . .	104
APPENDICES		
A	ROUTINE TEST REPORT FOR RCVT by TRENCH GROUP . . . . .	107
B	ROUTINE TEST REPORT FOR NXVCT by NxtPhase T&D Corporation . . . . .	123

## LIST OF TABLES

### TABLES

Table 1.1	Current Distortion Limits for General Distribution Systems (120V - 69000V) [6] . . . . .	2
Table 1.2	Current Distortion Limits for General Subtransmission Systems (69001V - 161000V) [6] . . . . .	3
Table 1.3	Current Distortion Limits for General Transmission Systems (> 161 kV) [6] . . . . .	3
Table 1.4	Voltage Distortion Limits [6] . . . . .	4
Table 1.5	Current Harmonic Limits for Distribution Systems (1 - 34.5 kV) [29]	4
Table 1.6	Current Harmonic Limits for Subtransmission Systems (34.5 - 154 kV) [29] . . . . .	4
Table 1.7	Current Harmonic Limits for Transmission Systems (> 154 kV) [29]	5
Table 1.8	Voltage Harmonic Limits for 380 kV Transmission Systems [30] . .	5
Table 1.9	Voltage Harmonic Limits for 20-154 kV Transmission Systems [30]	6
Table 2.1	Limits of current error and phase displacement for measuring current transformers (classes from 0.1 to 1) [1] . . . . .	14
Table 2.2	Limits of error for protective current transformers [1] . . . . .	14
Table 2.3	Limits of voltage error and phase displacement for measuring voltage transformers [2] . . . . .	16
Table 2.4	Limits of voltage error and phase displacement for protective voltage transformers [2] . . . . .	17
Table 2.5	Voltage Transformer Technology Comparison [7] . . . . .	35
Table 2.6	Limits of current error and phase displacement for measuring current transformers for special application [1] . . . . .	38

Table 4.1	Frequency Response of the CVT . . . . .	66
Table 4.2	Frequency Response of the CVT without $L_c$ . . . . .	70
Table 4.3	Frequency Response of the CVT without FSC . . . . .	71
Table 5.1	Comparison of NXVCT and RCVT at 380 kV . . . . .	72
Table 5.2	Sample data of RCVT and IVT against fundamental component at 34.5 kV . . . . .	77
Table 5.3	Sample data of RCVT and IVT against 3 <sup>rd</sup> harmonic at 34.5 kV when ground cable is connected to the control room . . . . .	78
Table 5.4	Sample data of RCVT and IVT against 3 <sup>rd</sup> harmonic at 34.5 kV when ground cable is connected to the trailer of the electronic system . . .	79
Table 5.5	Sample data of RCVT and IVT against 5 <sup>th</sup> harmonic at 34.5 kV . . .	80
Table 5.6	Sample data of RCVT and IVT against 7 <sup>th</sup> harmonic at 34.5 kV . . .	80
Table 5.7	Sample data of NXVCT and CVT against fundamental component at 154 kV . . . . .	81
Table 5.8	Sample data of NXVCT and CVT against 3 <sup>rd</sup> harmonic at 154 kV .	82
Table 5.9	Sample data of NXVCT and CVT against 5 <sup>th</sup> harmonic at 154 kV . .	83
Table 5.10	Sample data of NXVCT and CVT against 7 <sup>th</sup> harmonic at 154 kV . .	83
Table 5.11	Sample data of NXVCT and CVT against fundamental component at 380 kV . . . . .	84
Table 5.12	Sample data of NXVCT and CVT against 3 <sup>rd</sup> harmonic at 380 kV .	84
Table 5.13	Sample data of NXVCT and CVT against 5 <sup>th</sup> harmonic at 380 kV . .	85
Table 5.14	Sample data of NXVCT and CVT against 7 <sup>th</sup> harmonic at 380 kV . .	86
Table 5.15	Phase shift error of conventional CT at fundamental component at 34.5 kV . . . . .	95
Table 5.16	Phase shift error of conventional CT at 3 <sup>rd</sup> harmonic component at 34.5 kV . . . . .	96
Table 5.17	Phase shift error of conventional CT at other harmonic component at 34.5 kV . . . . .	96
Table 5.18	Phase shift error of conventional CT at 154 kV . . . . .	98

Table 5.19 Phase shift error of conventional CT at 380 kV . . . . . 99

## LIST OF FIGURES

### FIGURES

Figure 2.1	Current Transformer. (a) Connection Diagram. (b) Equivalent Circuit (linear model). (c) Phasor Diagram . . . . .	12
Figure 2.2	Components of a CVT . . . . .	18
Figure 2.3	Equivalent circuit of a CVT . . . . .	19
Figure 2.4	Active FSC . . . . .	20
Figure 2.5	Passive FSC . . . . .	21
Figure 2.6	Frequency response of a typical CVT [11] . . . . .	22
Figure 2.7	Three phase system including IVTs and capacitances . . . . .	23
Figure 2.8	IVT with a resistor on the primary side for damping ferroresonance	23
Figure 2.9	Zero sequence components at an IVT with a neutral resistor on the primary . . . . .	24
Figure 2.10	A discharge gap between the neutral point and ground on the secondary side [11] . . . . .	25
Figure 2.11	IVT having discharge gaps on each secondary windings [11] . . . . .	26
Figure 2.12	Equivalent circuit of a capacitive voltage divider (CVD) . . . . .	27
Figure 2.13	420kV RCVT in the substation of Temelli in Ankara . . . . .	28
Figure 2.14	Schematic view of the RCVT . . . . .	29
Figure 2.15	Equivalent Circuit of the RCVT . . . . .	30
Figure 2.16	Termination of a 50 $\Omega$ coaxial cable on an RCVT . . . . .	33
Figure 2.17	Comparison of amplitude errors of RCVT and conventional transformers [19] . . . . .	34
Figure 2.18	Accuracy of RCVT over frequency range [19] . . . . .	36

Figure 2.19 Comparison of phase shifts of RCVT and conventional transformers [19] . . . . .	36
Figure 2.20 Phase deviation of RCVT over frequency range [19] . . . . .	37
Figure 2.21 Schematic of an NXVCT column . . . . .	39
Figure 2.22 420 kV NXVCT at substation of Temelli in Ankara . . . . .	40
Figure 2.23 Accuracy of NXVT [22] . . . . .	41
Figure 2.24 Accuracy of NXCT [21] . . . . .	41
Figure 2.25 General Connection scheme of an NXVCT system [21] . . . . .	42
Figure 2.26 The Electronic System - Back and Front View of the Cabinet . . . . .	43
Figure 2.27 Fiber Optic Current Sensor Optical Block Diagram [21] . . . . .	44
Figure 3.1 420 kV NXVCT columns are at transportation position . . . . .	50
Figure 3.2 420 kV NXVCT column while tilting up for connection . . . . .	51
Figure 3.3 420 kV NXVCT column is tilted up . . . . .	51
Figure 3.4 420 kV RCVT columns are raised by the lift . . . . .	52
Figure 3.5 Movable Cable Duct and Hydraulic System . . . . .	53
Figure 3.6 Connection Cabinet on the Trailer . . . . .	53
Figure 3.7 Temperature Sensors and Coiled up Cables . . . . .	54
Figure 3.8 Trailer which is used at 36 kV measurements . . . . .	55
Figure 3.9 36 kV RCVT and NXCT Columns at field measurement . . . . .	56
Figure 3.10 Trailer of the Electronic System . . . . .	57
Figure 3.11 Cabinets in the trailer . . . . .	58
Figure 3.12 Interface PCBs . . . . .	58
Figure 3.13 GPS and Wireless Antennas . . . . .	59
Figure 3.14 DAQ Card . . . . .	60
Figure 3.15 Setting Screen of the Software . . . . .	61
Figure 3.16 Display Screen of the Software . . . . .	62
Figure 3.17 Illustration of harmonic and interharmonic groups for a 50 Hz supply [5] . . . . .	63

Figure 3.18 Illustration of harmonic and interharmonic subgroups for a 50 Hz supply [5] . . . . .	64
Figure 4.1 Schematic of the CVT used for the simulation . . . . .	66
Figure 4.2 Response of CVT to 50 Hz input . . . . .	67
Figure 4.3 Response of CVT to 150 Hz input . . . . .	67
Figure 4.4 Response of CVT to 250 Hz input . . . . .	68
Figure 4.5 Response of CVT to 350 Hz input . . . . .	68
Figure 4.6 Response of CVT to 550 Hz input . . . . .	69
Figure 4.7 Response of CVT to 1 kHz input . . . . .	69
Figure 4.8 Response of CVT to 50 Hz input without $L_c$ . . . . .	70
Figure 5.1 An output of NXVCT at 380 kV . . . . .	73
Figure 5.2 An output of RCVT at 380 kV . . . . .	73
Figure 5.3 Trailers used in measurements at 34.5 kV . . . . .	74
Figure 5.4 A sample data of conventional transformer at 34.5 kV . . . . .	75
Figure 5.5 A sample data of RCVT at 34.5 kV . . . . .	75
Figure 5.6 Simplified connection diagram of conventional voltage transformers.	76
Figure 5.7 A sample data of conventional transformer at 34.5 kV . . . . .	77
Figure 5.8 A sample data of RCVT at 34.5 kV . . . . .	77
Figure 5.9 A sample data of conventional transformer at 34.5 kV when ground is connected to the trailer . . . . .	78
Figure 5.10 A sample data of RCVT at 34.5 kV when ground is connected to the trailer . . . . .	78
Figure 5.11 A sample data of conventional transformer at 34.5 kV when ground is connected to the trailer . . . . .	79
Figure 5.12 A sample data of RCVT at 34.5 kV when ground is connected to the trailer . . . . .	79
Figure 5.13 Trailers used in measurements at 154 kV . . . . .	81
Figure 5.14 A sample data of conventional transformer at 154 kV . . . . .	82

Figure 5.15 A sample data of NXVCT at 154 kV . . . . .	82
Figure 5.16 Trailers used in measurements at 380 kV . . . . .	84
Figure 5.17 A sample data of conventional transformer at 380 kV . . . . .	85
Figure 5.18 A sample data of NXVCT at 380 kV . . . . .	85
Figure 5.19 A sample data of conventional transformer at 34.5 kV . . . . .	87
Figure 5.20 A sample data of NXCT at 34.5 kV . . . . .	87
Figure 5.21 Deviation of $I_{conv}/I_{NXCT}$ against amplitude of fundamental component for 3 <sup>rd</sup> harmonic component . . . . .	88
Figure 5.22 Deviation of $I_{conv}/I_{NXCT}$ against amplitude of harmonic component for 3 <sup>rd</sup> harmonic component . . . . .	88
Figure 5.23 Deviation of $I_{conv}/I_{NXCT}$ against percentage of harmonic component for 3 <sup>rd</sup> harmonic component . . . . .	89
Figure 5.24 Deviation of $I_{conv}/I_{NXCT}$ against amplitude of fundamental component for 5 <sup>th</sup> harmonic component . . . . .	89
Figure 5.25 Deviation of $I_{conv}/I_{NXCT}$ against amplitude of harmonic component for 5 <sup>th</sup> harmonic component . . . . .	90
Figure 5.26 Deviation of $I_{conv}/I_{NXCT}$ against percentage of harmonic component for 5 <sup>th</sup> harmonic component . . . . .	90
Figure 5.27 Deviation of $I_{conv}/I_{NXCT}$ against amplitude of fundamental component for 7 <sup>th</sup> harmonic component . . . . .	91
Figure 5.28 Deviation of $I_{conv}/I_{NXCT}$ against amplitude of harmonic component for 7 <sup>th</sup> harmonic component . . . . .	91
Figure 5.29 Deviation of $I_{conv}/I_{NXCT}$ against percentage of harmonic component for 7 <sup>th</sup> harmonic component . . . . .	92
Figure 5.30 Deviation of $I_{conv}/I_{NXCT}$ against amplitude of fundamental component for 11 <sup>th</sup> harmonic component . . . . .	92
Figure 5.31 Deviation of $I_{conv}/I_{NXCT}$ against amplitude of harmonic component for 11 <sup>th</sup> harmonic component . . . . .	93
Figure 5.32 Deviation of $I_{conv}/I_{NXCT}$ against percentage of harmonic component for 11 <sup>th</sup> harmonic component . . . . .	93

Figure 5.33 Deviation of $I_{conv}/I_{NXCT}$ against amplitude of fundamental component for 13 <sup>th</sup> harmonic component . . . . .	94
Figure 5.34 Deviation of $I_{conv}/I_{NXCT}$ against amplitude of harmonic component for 13 <sup>th</sup> harmonic component . . . . .	94
Figure 5.35 Deviation of $I_{conv}/I_{NXCT}$ against percentage of harmonic component for 13 <sup>th</sup> harmonic component . . . . .	95
Figure 5.36 Deviation of $I_{conv}/I_{NXVCT}$ against amplitude of fundamental component for 3 <sup>rd</sup> harmonic component . . . . .	97
Figure 5.37 Deviation of $I_{conv}/I_{NXVCT}$ against amplitude of fundamental component for 5 <sup>th</sup> harmonic component . . . . .	97
Figure 5.38 Deviation of $I_{conv}/I_{NXVCT}$ against amplitude of fundamental component for 5 <sup>th</sup> harmonic component . . . . .	98

# CHAPTER 1

## INTRODUCTION

Since the beginning of the transmission and distribution of electrical energy with high and medium voltages, instrument transformers have been used to transform the high values of current and voltages to measurable values. Instrument transformers transform voltage or current depending on the basis of magnetic circuits which produces an image of the primary side value on the secondary side.

For the measurements in transmission and distribution systems, conventional current and voltage transformers have been used for years. These transformers have high reliability due to the magnetic basis they depend on. But the today requirements of diagnostic, protection and revenue metering measurements on the transfer performances cannot be fulfilled with the conventional transformers[7]. To be able to satisfy today's requirements, digital technology has been used in control, metering and protection units. The implementation of digital technology and automation within power supply industries began in 1970's by the use of computers for power system control. The digital protection relays have been developed in 1980's and in the 1990's all automation, control and protection were done with digital technology[8].

Harmonic is one of the key parameters of power quality. This is because, loads may be damaged due to current and/or voltage harmonics. For example; harmonics increase iron and core losses at electric motors and generators, which increases the temperature of the machine. So, harmonics decrease the efficiency of the machine and also they cause premature aging of the organic insulation. Effect of harmonics to the transformers is not only increased audible noise, but also, current harmonics increase copper losses and stray flux losses, where voltage harmonics cause an increase

in iron losses. The overall effect is an increase in transformer heating. Harmonics have effect even in power cables; they increase voltage stress and corona probability which can lead to insulation failure. Harmonics affect the operation of electronic equipment, too. Since voltage zero-crossing and phase-to-phase intersection points may be shifted by harmonics, the electronic equipment may operate inaccurately.

The permissible limits of harmonics are determined by IEEE[6]. Current harmonics are limited according to the ratio of maximum short circuit current to maximum demand load current in addition to voltage level of the system; where voltage harmonics are limited according to the voltage level. The limits are listed in Table 1.1, Table 1.2 and Table 1.3 for current harmonics and in Table 1.4 for voltage harmonics.

Table 1.1: Current Distortion Limits for General Distribution Systems (120V - 69000V) [6]

Maximum Harmonic Current Distortion in Percent of $I_L$						
Individual Harmonic Order (Odd Harmonics)						
$I_{sc}/I_L$	$< 11$	$11 \leq h < 17$	$17 \leq h < 23$	$23 \leq h < 35$	$35 \leq h$	TDD
$< 20^*$	4.0	2.0	1.5	0.6	0.3	5.0
$20 < 50$	7.0	3.5	2.5	1.0	0.5	8.0
$50 < 100$	10.0	4.5	4.0	1.5	0.7	12.0
$100 < 1000$	12.0	5.5	5.0	2.0	1.0	15.0
$> 1000$	15.0	7.0	6.0	2.5	1.4	20.0
Even harmonics are limited to 25% of the odd harmonic limits above.						
Current distortions that result in a dc offset are not allowed.						
* All power generation equipment is limited to these values of current distortion, regardless of actual $I_{sc}/I_L$						
where						
$I_{sc}$ = maximum short-circuit current at Point of Common Coupling (PCC)						
$I_L$ = maximum demand load current (fundamental component) at PCC						
TDD: Total Demand Distortion, harmonic current distortion in % of maximum demand load current						

Table 1.2: Current Distortion Limits for General Subtransmission Systems (69001V - 161000V) [6]

Maximum Harmonic Current Distortion in Percent of $I_L$						
Individual Harmonic Order (Odd Harmonics)						
$I_{sc}/I_L$	< 11	$11 \leq h < 17$	$17 \leq h < 23$	$23 \leq h < 35$	$35 \leq h$	TDD
< 20*	2.0	1.0	0.75	0.3	0.15	2.5
20 < 50	3.5	1.75	1.25	0.5	0.25	4.0
50 < 100	5.0	2.25	2.0	0.75	0.35	6.0
100 < 1000	6.0	2.75	2.5	1.0	0.5	7.5
> 1000	7.5	3.5	3.0	1.25	0.7	10.0
Even harmonics are limited to 25% of the odd harmonic limits above.						
Current distortions that result in a dc offset are not allowed.						
* All power generation equipment is limited to these values of current distortion, regardless of actual $I_{sc}/I_L$						
where $I_{sc}$ = maximum short-circuit current at PCC $I_L$ = maximum demand load current (fundamental component) at PCC TDD: Total Demand Distortion, harmonic current distortion in % of maximum demand load current						

Table 1.3: Current Distortion Limits for General Transmission Systems (> 161 kV) [6]

Maximum Harmonic Current Distortion in Percent of $I_L$						
Individual Harmonic Order (Odd Harmonics)						
$I_{sc}/I_L$	< 11	$11 \leq h < 17$	$17 \leq h < 23$	$23 \leq h < 35$	$35 \leq h$	THD
< 50*	2.0	1.0	0.75	0.3	0.15	2.5
$\geq 50$	3.0	1.5	1.15	0.45	0.22	3.75
Even harmonics are limited to 25% of the odd harmonic limits above.						
Current distortions that result in a dc offset are not allowed.						
* All power generation equipment is limited to these values of current distortion, regardless of actual $I_{sc}/I_L$						
where $I_{sc}$ = maximum short-circuit current at PCC $I_L$ = maximum demand load current (fundamental component) at PCC						

In Turkey, electricity market is regulated by EPDK [27] and the regulations are enforced by TEIAS [28]. Harmonic limits are also determined by EPDK in Transmission System Supply Reliability and Quality Regulation [29] and Electricity Market

Table 1.4: Voltage Distortion Limits [6]

Bus Voltage at PCC	Individual Voltage Distortion (%)	Total Voltage Distortion THD (%)
$v \leq 69kV$	3.0	5.0
$69kV < v \leq 161kV$	1.5	2.5
$v > 161kV$	1.0	1.5
NOTE: HV systems can have up to 2% THD where the cause is an HVDC terminal that will attenuate by the time it is tapped for a user.		

Supply Regulation [30]. Current harmonic limits are shown in Table 1.5, Table 1.6 and Table 1.7 where voltage harmonic limits are shown in Table 1.8 and Table 1.9.

Table 1.5: Current Harmonic Limits for Distribution Systems (1 - 34.5 kV) [29]

Maximum Harmonic Current Distortion in Percent of $I_L$						
Individual Harmonic Order (Odd Harmonics)						
$I_{sc}/I_L$	< 11	$11 \leq h < 17$	$17 \leq h < 23$	$23 \leq h < 33$	$33 \leq h$	TDD
< 20	4.0	2.0	1.5	0.6	0.3	5
20 < 50	7.0	3.5	2.5	1.0	0.5	8
50 < 100	10.0	4.5	4.0	1.5	0.7	12
100 < 1000	12.0	5.5	5.0	2.0	1.0	15
> 1000	15.0	7.0	6.0	2.5	1.4	20
Even harmonics are limited to 25% of the odd harmonic limits above.						

Table 1.6: Current Harmonic Limits for Subtransmission Systems (34.5 - 154 kV) [29]

Maximum Harmonic Current Distortion in Percent of $I_L$						
Individual Harmonic Order (Odd Harmonics)						
$I_{sc}/I_L$	< 11	$11 \leq h < 17$	$17 \leq h < 23$	$23 \leq h < 33$	$33 \leq h$	TDD
< 20	2.0	1.0	0.8	0.3	0.15	2.5
20 < 50	3.5	1.8	1.25	0.5	0.25	4.0
50 < 100	5.0	2.3	2.0	0.75	0.35	6.0
100 < 1000	6.0	2.8	2.5	1.0	0.5	7.5
> 1000	7.5	3.5	3.0	1.25	0.7	10.0
Even harmonics are limited to 25% of the odd harmonic limits above.						

Table 1.7: Current Harmonic Limits for Transmission Systems (> 154 kV) [29]

Maximum Harmonic Current Distortion in Percent of $I_L$						
Individual Harmonic Order (Odd Harmonics)						
$I_{sc}/I_L$	< 11	$11 \leq h < 17$	$17 \leq h < 23$	$23 \leq h < 33$	$33 \leq h$	TDD
< 20	1.0	0.5	0.4	0.15	0.07	1.3
20 < 50	1.8	0.9	0.6	0.25	0.12	2.0
50 < 100	2.5	1.2	1.0	0.4	0.17	3.0
100 < 1000	3.0	1.4	1.25	0.5	0.25	3.75
> 1000	3.8	1.8	1.3	0.6	0.35	5.0

Even harmonics are limited to 25% of the odd harmonic limits above.

Table 1.8: Voltage Harmonic Limits for 380 kV Transmission Systems [30]

Odd Harmonics (Non-triplen)		Odd Harmonics (triplen)		Even Harmonics	
Harmonic Order	Harmonic Voltage (%)	Harmonic Order	Harmonic Voltage (%)	Harmonic Order	Harmonic Voltage (%)
5	1.25	3	1.0	2	0.75
7	1.0	9	0.4	4	0.6
11	0.7	$15 \leq h$	0.2	6	0.4
13	0.7			8	0.4
$17 \leq h \leq 25$	0.4			10	0.4
$25 < h$	$0.2+0.2(25/h)$			$12 \leq h$	0.2

THD : 2 %

Up to this point, effects of harmonics and the permissible limits are defined. But the fundamental problem arises at harmonic measurements, because the conventional instrument transformers are designed and tested for fundamental frequency component, not for harmonic frequencies. In the literature, there are both theoretical and practical information about harmonic measurements by conventional instrument transformers. According to IEEE [6], conventional current transformers can measure harmonics up to 10 kHz with an accuracy of 3%. But this is a very general idea because the accuracy depends on several parameters like, amplitude of current, percentage of harmonic current, accuracy class of current transformer, etc. Also, this idea does not include phase shift errors, which is the major disadvantage of current transformers; especially at power calculations. The situation at voltage harmonic measurements is

Table 1.9: Voltage Harmonic Limits for 20-154 kV Transmission Systems [30]

Odd Harmonics (Non-triplen)		Odd Harmonics (triplen)		Even Harmonics	
Harmonic Order	Harmonic Voltage (%)	Harmonic Order	Harmonic Voltage (%)	Harmonic Order	Harmonic Voltage (%)
5	1.5	3	1.5	2	1.0
7	1.5	9	0.75	4	0.8
11	1.0	15	0.3	6	0.5
13	1.0	$21 \leq h$	0.2	8	0.4
17	0.75			10	0.4
19	0.75			$12 \leq h$	0.2
23	0.5				
25	0.5				
$25 < h$	$0.2+0.3(25/h)$				
THD : 3 %					

even worse. According to IEEE [6]; inductive (magnetic) voltage transformers are designed to operate at fundamental frequency and harmonic frequency resonance between winding inductances and capacitances can cause large ratio and phase errors. Harmonic measurements, taken by capacitive voltage transformers, are worse than inductive voltage transformers because the lowest frequency resonance peaks appear at frequencies of less than 200 Hz.

According to an article about current transformers [9], conventional current transformers are reliable when the purpose of the measurement is to determine the harmonic current magnitude. Because the resonance frequencies between parasitic capacitances of the winding and inductances are usually higher than the harmonic frequencies to be measured. But phase angle error affects the accuracy when harmonic powers are measured.

Another article about harmonic measurements [15] uses ratio correction factors for conventional current and voltage transformers to minimize the error at harmonic measurements. But it calculates the ratio correction factor theoretically, ignoring external factors.

An article about ferroresonance problem of conventional voltage transformers [12]

concludes that; ferroresonance filters affect the frequency response of the voltage transformer adversely and results in erroneous output in harmonic measurements.

A new technique is developed at an article [16] for harmonic voltage measurements using a capacitive voltage transformer. It denotes the deficient frequency response of a capacitive voltage transformer and installs current sensors in the voltage transformer to measure the current flow through the capacitive voltage transformer. Then, it compares the measurements against an inductive voltage transformer and implies that the results are almost the same. But the problem is, frequency response of an inductive voltage transformer is not accurate enough to measure harmonics; although it is better than the frequency response of an capacitive one.

Another article about problems of voltage transformers [11] defines the importance of grounding way of voltage transformers in addition to their deficient frequency response. Grounding way of voltage instrument transformers is important because zero-sequence triplen harmonic currents due to unbalanced loads flow between the neutral point and the ground. This current induces voltage across the neutral to ground impedance which concludes inaccurate triplen harmonic measurements. Also, the grounding way is important for protection against the ferroresonance. So, an optimum way of grounding shall be chosen.

An article about instrument transformers [17] indicates that the accuracy of current transformers is sufficient for the first 25 harmonics and the frequency response is virtually constant up to 1500 Hz with a negligible phase shift error. The article also explains that, inductive voltage transformers can be used for harmonic measurements if they are supported by transfer function correction algorithms. The same article also concludes that; capacitive voltage transformers are not suitable for harmonic measurements even supported by correction algorithms because of the fluctuating frequency response.

Finally, an article about harmonic voltage measurement in Norwegian Power System [18] indicates that, frequency response of different capacitive voltage transformers which have different manufacturers, are different, too; where the same type capacitive voltage transformers have similar, but not the same, frequency response. Also, the paper indicates that inductive voltage transformers have small errors up to 29<sup>th</sup>

harmonic.

Depending on the digital world, new technology current and voltage transducers have been developed to take more accurate measurements especially at high voltage level. Main advantages of new technology transducers against conventional ones are wider bandwidth and lower numbers of variances which result in better transient state performance and more accurate harmonic measurement. Two types of transducers are used in this thesis; one of them is resistive - capacitive voltage transformer (RCVT, purchased from TRENCH) and the other is optical voltage and current transducer (NXVCT and NXCT, purchased from NxtPhase). RCVT can measure voltage only; where NXCT can measure current and NXVCT can measure both voltage and current.

## **1.1 Scope of the Thesis**

Monitoring voltage and current is essential in today's world for following the power flow, investigating the power quality and pricing the energy. To be able to respond to demands, accurate measurements are needed and so voltage and current transducers in addition to meters shall give adequate data. Depending on the today's digital world, meters are capable of giving enough accurate measurements. However, the transducers are not sufficient as the meters, especially for harmonic and transient state measurements.

This thesis focuses on the calibration of conventional voltage and current transformers at medium, high and extra high voltage levels. The specific point of the thesis is; measuring the voltage and current directly from the primary side of the conventional one and comparing the measurements of conventional instrument transformers against high-accuracy, new technology transducers.

The transducers which are used in this thesis do not have the defined problems of conventional ones. Simultaneous field measurements are taken to denote the differences between the conventional ones and the new technology ones. The field work is focused on steady state measurements for calibration against harmonics and also reactor and power transformer switching for comparison against transient events. But throughout this thesis, only calibration against harmonics will be studied.

In chapter 2, the theory of conventional current and voltage transformers will be explained including sources of error. Then, the theory of used transducers will be explained in details depending on both manufacturer's datasheets and the literature. The differences between them and conventional ones will be defined, depending on their basis. Accuracy of the used new technology transducers will be analyzed and also, how they remove the errors will be denoted.

In chapter 3, the measurement system developed during this thesis will be investigated. To be able to measure as many feeders as possible, a mobile system has been implemented on trailers. Firstly, the mobile platforms will be presented followed by the detailed explanations of their parts. The electronic system used in measurements will be considered in this chapter, too. Also the connections between the transducer columns and the electronic system will be presented. A high-level software has been developed during the thesis for measurements including the calibration data of the used transducers. Information about this software and used algorithms will be given in this chapter, too.

In chapter 4, simulation work will be presented. A simulation model of a capacitive voltage transformer, which field measurement is taken, has been developed depending on the manufacturer's data. The simulation results against frequency components will be considered and compared with the results of the field measurement. Also, effects of its components on the accuracy of the measurement will be investigated in this chapter.

In chapter 5, results of field measurements will be considered. The phase shift and amplitude error maps of conventional transformers will be derived for both current and voltage transformers. Found issues will be compared with the expected and the literature.

Finally, in chapter 6, conclusions will be presented. Also, further work will be discussed in this chapter.

## **CHAPTER 2**

### **MEASUREMENT TRANSFORMERS FOR EHV, HV AND MV APPLICATIONS**

This thesis focuses on calibration of conventional transformers against harmonic components by the field measurements of Resistive-Capacitive Voltage Transformer (RCVT) and Optical Voltage and Current Transducer (NXVCT). At this point, general theory of conventional instrument transformers and sources of error will be provided followed by the theory of RCVT and NXVCT. Conventional transformers can be divided into two groups; current transformers and voltage transformers. Also, voltage transformers should be grouped into three; capacitive voltage transformers, inductive voltage transformers and capacitive voltage dividers.

As can be realized from the names, RCVT can be used for voltage measurements only, where NXVCT is capable of both voltage and current measurements. RCVT is chosen due to its wider bandwidth and easier installation than the NXVCT. Bandwidth of RCVT is 1 MHz, where it is 20 kHz for NXVCT. But the measurement system developed throughout this study can take accurate data up to 51.2 kHz due to the Nyquist Theorem, where 102.4 kHz is used as sampling rate; which is high enough for harmonic measurements.

#### **2.1 Conventional Current Transformers**

Monitoring and recording of current is very important at today's power system planning and maintenance from the point of power calculations especially. For correct calculations and system installations, accurate current measurements are needed, not

only for the fundamental component but also for the harmonic components. It is known from the literature that; current transformers with accuracy class 0.5 or better provide reasonably accurate measurements of current harmonics magnitudes, however phase angle error may lead to unacceptable errors when current transformers are used to measure active power. Also, even high accuracy current transformers (CTs) may yield unsatisfactory results to determine power flow direction [9, 10]. Also, one of the fundamental concerns is the saturation of the core of the current transformer against distorted, high currents; like fault currents. The saturation of the core depends on the physical design of the CT, the amount of steel in the core, the connected burden, the winding resistance, the remanence flux in the iron core, the fault level and the system X/R ratio, which can cause larger DC offset to occur [23]. As seen from the dependencies, the analysis of CT saturation is very complex and unique to the power system it is installed.

The basic equation of a current transformer is based on Ampere's Law,

$$N_p \cdot i_p = N_s \cdot i_s \quad (2.1)$$

where  $N_p$ ,  $N_s$  are primary and secondary number of turns;  $i_p$  and  $i_s$  are primary and secondary currents, respectively. An equivalent load, called burden, is connected across the secondary terminals with the impedance,  $Z_B = R_B + j\omega L_B$ , as shown in Figure 2.1.

Where;

$(N_p/N_s)I_p$  is the transferred form of primary current phasor  $I_p$  to the secondary side,

$r_p'$  is the primary winding resistance referred to secondary side,

$l_p'$  is the primary leakage inductance referred to secondary side,

$r_s$  is the secondary winding resistance,

$l_s$  is the secondary leakage inductance,

$L_m$  is the magnetizing inductance,

$R_m$  is the magnetic core resistance and equal to  $V_s^2/\Delta P_{Fe}$ ,

$\Delta P_{Fe}$  models the magnetic core hysteresis and eddy current losses.

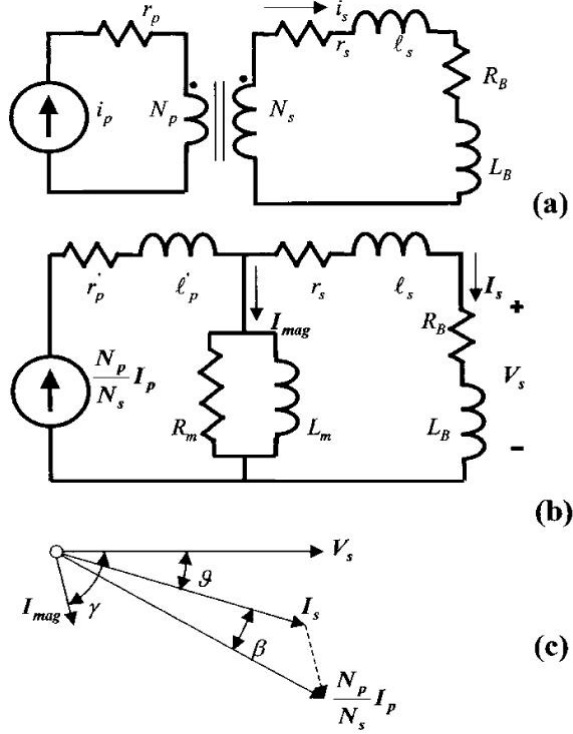


Figure 2.1: Current Transformer. (a) Connection Diagram. (b) Equivalent Circuit (linear model). (c) Phasor Diagram

From Figure 2.1(b) and Kirchhoff's current law, it is seen that;

$$\frac{N_p}{N_s} I_p = I_s + I_{mag} \quad (2.2)$$

Also, the secondary voltage phasor is seen again from the Figure 2.1 (b) and equal to;

$$V_s = (R_B + j\omega L_B) I_s \quad (2.3)$$

From Equation 2.3, it is seen that the measured current is \$I\_s\$; instead of \$(N\_p/N\_s)I\_p\$. The formulation of these two current values is given in Equation 2.2 and it is seen that the difference is due to the magnetizing current. Since the flux is a nonlinear function of the magnetizing current, the magnetic error is nonlinear and it is a function of burden, frequency and nominal ratio. This dependency may also be seen from the Figure 2.1(b); frequency affects the impedances of the inductances and the burden is in parallel with magnetizing circuit so the current division between these branches depends on the frequency and burden. Finally, nominal ratio determines the transfer

of primary current to the secondary side, which also affects the magnetizing current. So, there are mainly two errors;

1. phase angle error

$$\beta \approx \tan^{-1} \left[ \frac{I_{mag} \sin(\gamma - \vartheta)}{\frac{N_p}{N_s} I_p - I_{mag} \cos(\gamma - \vartheta)} \right] \quad (2.4)$$

2. magnitude error characterized by the ratio correction factor (RCF)

$$\begin{aligned} RCF &= \frac{N_p |I_p|}{N_s |I_s|} \\ &\approx \sqrt{1 + \left( \frac{N_s I_{mag}}{N_p I_p} \right)^2 - 2 \frac{N_s I_{mag}}{N_p I_p} \cos(\gamma - \vartheta)} \end{aligned} \quad (2.5)$$

These two errors, especially  $\beta$ , affects the measurement accuracy of powers. Also, as mentioned above, magnetizing error depends on frequency, which results various percentage of errors at current harmonic measurements. The magnetizing current, and so the magnetizing error, also depends on the geometry and material of the core. That is; the lower the ferromagnetic core permeability the larger becomes the magnetizing current and the phase angle error. The larger the air-gap of a clamp on CT, the larger the magnetizing current and the harmonic currents present in the secondary current will be reflected in the spectrum of the magnetizing current even for a perfectly linear CT [9].

The properties of the current transformers are determined by the standard IEC 60044-1 [1]. The accuracy classes are also determined by this standard which are given in Table 2.1 for measuring current transformers. The limits of amplitude error and phase displacement are valid for the rated frequency only; that is the fundamental frequency. Errors increase at harmonics, as the frequency increases. According to the IEEE Standard 519-1992 [6], the current instrument transformers have accuracies better than 3% in the frequency range up to 10 kHz unless they are saturated.

The current error and phase displacement at rated frequency shall not exceed the values in Table 2.1; when the secondary burden is any value between 25% to 100% of the rated burden. The secondary burden used for test purposes shall have a power factor of 0.8 lagging except that; when the burden is less than 5 VA, a burden having

Table 2.1: Limits of current error and phase displacement for measuring current transformers (classes from 0.1 to 1) [1]

Accuracy class	± Percentage current (ratio) error at percentage of rated current shown below				± Phase displacement at percentage of rated current shown below							
					minutes				centiradians			
	5	20	100	120	5	20	100	120	5	20	100	120
0,1	0,4	0,2	0,1	0,1	15	8	5	5	0,45	0,24	0,15	0,15
0,2	0,75	0,35	0,2	0,2	30	15	10	10	0,9	0,45	0,3	0,3
0,5	1,5	0,75	0,5	0,5	90	45	30	30	2,7	1,35	0,9	0,9
1,0	3,0	1,5	1,0	1,0	180	90	60	60	5,4	2,7	1,8	1,8

power factor 1.0 shall be used. The test burden shall not be less than 1 VA for any cases [1].

In Turkey, generally current transformers having at least two secondaries are installed in substations; one for metering and one for protection. Protection type transformers can not measure current as accurate as the ones in Table 2.1 but there is no saturation problem at higher current levels than the rated current, that is why, these current transformers can measure transient surge currents and short-circuit currents better than the measuring CTs and so, they are called protection type current transformers. There are two accuracy classes for protection type current transformers as shown in Table 2.2.

Table 2.2: Limits of error for protective current transformers [1]

Accuracy class	Current error at rated primary current %	Phase displacement at rated primary current		Composite error at rated accuracy limit primary current %
		minutes	centiradians	
5P	±1	±60	±1,8	5
10P	±3	-	-	10

As seen from the Table 2.2 above, limits of phase displacement are not specified for class 10P protective current transformers. Mostly class 5P current transformers are installed in substations in Turkey.

The most important characteristic of current transformers is that; they can operate between 20 % to 120 % of its rated current as seen from the Table 2.1; this is not valid for voltage transformers.

## 2.2 Conventional Voltage Transformers

Voltage transformers are used to obtain effective and secure secondary voltage for metering, control and protection equipments at all voltage levels. For high voltage and extra high voltage applications, electromagnetic voltage transformers are not economical due to their larger size and cost. Thus, capacitive voltage transformers are preferred at high and extra high voltage levels.

The main disadvantage of voltage transformers is ferromagnetic resonance and to avoid this problem, a resistor or nonlinear resistor is connected across the neutral point and the ground on the primary side of the voltage transformer (VT). But this configuration suffers in harmonic measurements. Especially triplen harmonics will be measured much higher than the actual. The grounding way of neutral point on the secondary side will affect the harmonic measurements, too. On the secondary side, a discharge air-gap is used instead of direct grounding. In such a case, 3<sup>rd</sup> harmonic voltage will be a little higher than the actual value. To be able to measure harmonic voltages as accurate as possible, neutral point must be grounded directly on either primary or secondary side of the voltage transformer, which then, increases the ferromagnetic resonance problem [11].

The ferromagnetic resonance, or ferroresonance, is a special case of resonance when a non-linear inductance is connected in series or parallel with a capacitance. The inductance can be the magnetizing inductance of the transformers and the capacitance can be the capacitance of cables, transmission lines, capacitive voltage transformers, capacitor banks and etc. Two types of ferroresonance occurs in voltage transformers and they are named as series ferroresonance and parallel ferroresonance. Series ferroresonance occurs as a result of the series path between a saturable inductor and capacitor; like energizing a capacitor through the magnetizing inductance of the transformer. Most ferroresonance events are series ferroresonance and this is the case seen

at capacitive voltage transformers. Parallel ferroresonance occurs as a result of the parallel path between the system capacitance and the magnetizing inductance of the transformer in addition to an overvoltage in the system. The voltage transformer saturates due to that overvoltage if the voltage regulation of the system is not enough and exchange of energy between the saturated transformer, or namely the magnetizing inductance of the transformer, and the system capacitance occurs which yields in rapid changes in the core flux and results in huge overvoltages in the system. This is the case seen in inductive voltage transformers in an isolated neutral system. Both types of ferroresonance may produce destructive voltages across the transformer terminals and from terminals to ground. It is difficult and almost impossible to predict the probability of ferroresonance because it depends on the system capacitance, cable lengths, characteristics of the transformers, characteristics of the load, etc. So, to avoid the effects of ferroresonance, ferroresonance suppressing circuits (FSCs) have been used on voltage transformer secondaries [12].

As mentioned before, three types of voltage transformers are used in substations; capacitive voltage transformers, inductive voltage transformers and capacitive voltage dividers. But capacitive voltage dividers are used rarely. Capacitive voltage transformers are used for about 90% of voltage measurements due to its high reliability [7]. Specifications of voltage transformers are determined by the international standards IEC 60044-5 [3] for the capacitive voltage transformers and IEC 60044-2 [2] for the inductive voltage transformers. But most of the specifications are the same; like voltage factor and accuracy classes.

Table 2.3: Limits of voltage error and phase displacement for measuring voltage transformers [2]

Class	Percentage voltage (ratio) error $\pm$	Phase displacement $\pm$	
		Minutes	Centiradians
0,1	0,1	5	0,15
0,2	0,2	10	0,3
0,5	0,5	20	0,6
1,0	1,0	40	1,2
3,0	3,0	-	-

The voltage error and phase displacement at rated frequency shall not exceed the values given in Table 2.3 at any voltage between 80% and 120% of rated voltage and with burdens of between 25% and 100% of rated burden at a power factor of 0,8 lagging. Note that, voltage transformers are not capable of measuring a wide voltage range like current transformers.

Table 2.4: Limits of voltage error and phase displacement for protective voltage transformers [2]

Class	Percentage voltage (ratio) error + or -	Phase displacement + or -	
		Minutes	Centiradians
3P	3,0	120	3,5
6P	6,0	240	7,0

The voltage error and phase displacement at rated frequency shall not exceed the values in Table 2.4 at 5% rated voltage and at rated voltage multiplied by the rated voltage factor (1,2, 1,5 or 1,9) with burdens of between 25% and 100% of rated burden at a power factor of 0,8 lagging.

At this point of the thesis, the capacitive voltage transformers (CVTs) will be explained in detail, followed by inductive voltage transformers (IVTs) and finally the capacitive voltage dividers.

### 2.2.1 Capacitive Voltage Transformers

As mentioned before, Capacitive Voltage Transformers (CVTs) are used widely in high voltage networks. The applications at that voltage levels require fast protection equipments. Today's digital technology meets the requirement for relays but CVTs' deficient transient response is a big problem. Because of the storage elements of CVTs, their output can not follow the fast changes at the input side [13].

A CVT is formed by coupling capacitors, compensating inductance, step down transformer and ferroresonance suppression circuit (FSC), as shown in Figure 2.2.

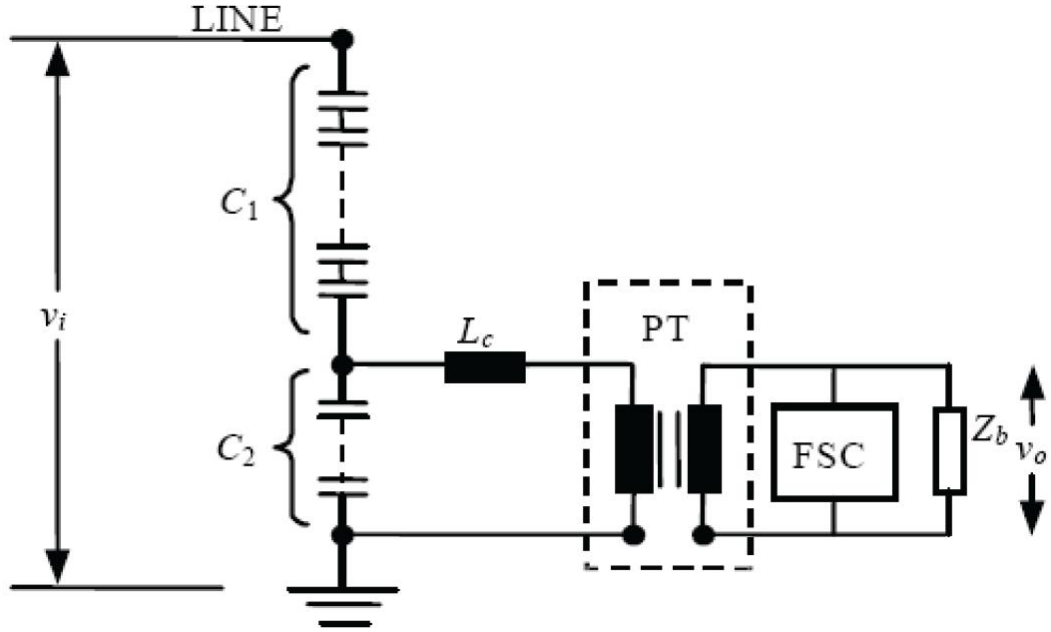


Figure 2.2: Components of a CVT

The coupling capacitors,  $C_1$  and  $C_2$  in Figure 2.2, of the CVT divides the system voltage to an intermediate level. The compensating inductance,  $L_c$ , cancels the reactance of the coupling capacitors to prevent any phase shift between the primary and the secondary side at the rated system frequency. But it causes phase shift at other frequencies. The step down transformer, PT, further decreases the voltage to the nominal output level. Finally, ferroresonance suppression circuit prevents any possible high voltages due to ferroresonance as told in Section 2.2.

By considering the components above, the equivalent circuit of the CVT can be derived as in Figure 2.3. Firstly, equivalent coupling capacitances can be shown by a single capacitance,  $C_e$ .  $L_c$  has some resistance and capacitance in addition to inductance as well, which are denoted by  $L_c$ ,  $C_c$  and  $R_c$ . The PT is represented through  $L_p$ ,  $C_p$  and  $R_p$  by referring all the parameters to the primary side. The configuration of the ferroresonance suppression circuit can be active or passive depending on the design and transient performance requirements. Here, active ferroresonance suppression circuit is modeled but both active and passive ferroresonance suppression circuits will be considered further in this section. So, the ferroresonance suppression circuit is

formed of  $L_f$ ,  $C_f$  and  $R_f$ . Finally the burden can be resistive only or resistive and inductive. The final circuit is shown in Figure 2.3 [14].

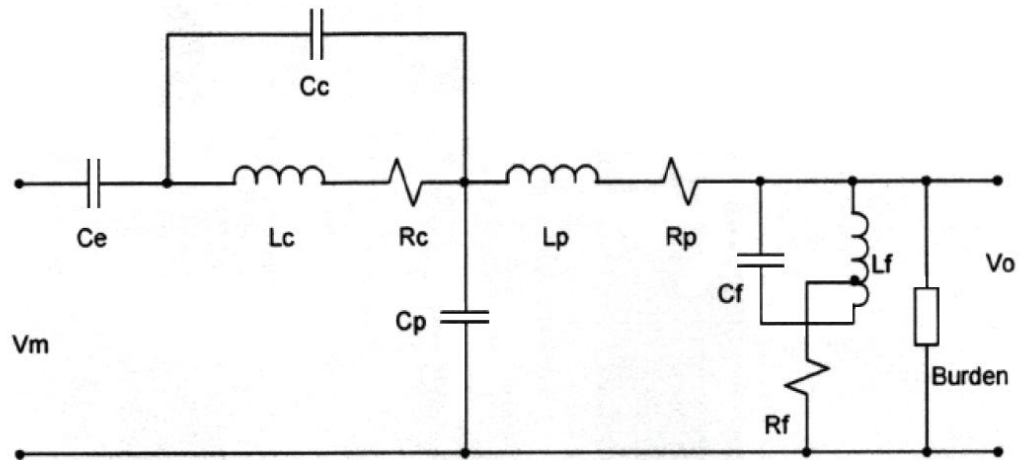


Figure 2.3: Equivalent circuit of a CVT

The disadvantages of CVTs can be seen from Figures 2.2 and 2.3. It is quite clear that there will be iron core losses because of PT and  $L_c$  which result in measuring error because of frequency dependence. Also, PT and  $L_c$  are the reasons of series ferroresonance as mentioned before in Section 2.2. Of course, to avoid damages of ferroresonance, FSC is included in the design but the cost of it is the inaccurate measurements of transients and harmonics, especially the 3<sup>rd</sup> harmonic which is very important. Another problem of the CVTs is the storage elements,  $C_e$  and  $L_c$ , because they affect the response of the CVT to a rapid change in the input; that is a transient event. As the capacitance of the coupling capacitors increases, transient performance of the CVT increases, too; but this also increases the cost of the CVT [13]. Because of the nature of the storage elements, transient performance of the CVT depends on the instant of the fault. The worst case is a fault occurred at the zero crossing of the voltage; where the best performance of the CVT exists at a fault occurred at the peak value of the voltage [13]. The step down transformer, PT, affects the transient performance, too. Because, the turns ratio of PT determines the loading of coupling capacitors by the burden. As the turns ratio increases, effect of burden on the coupling capacitances decreases. Finally, magnitude and power factor of the burden affects the transient performance of the CVT. Also, as mentioned before,  $L_c$  compensates the

phase shift of coupling capacitors at the rated system frequency. But there will be particular phase shifts at harmonic voltages. So; as seen, all parameters of a CVT affects its transient and harmonic measurement performance.

At this point of the thesis, it will be beneficial to explain ferroresonance suppression circuits in more detail. Two types of ferroresonance suppression circuits are used in CVTs: active and passive ferroresonance suppression circuits. Figure 2.4 shows the scheme of an active ferroresonance suppression circuit and Figure 2.5 shows the scheme of a passive ferroresonance suppression circuit.

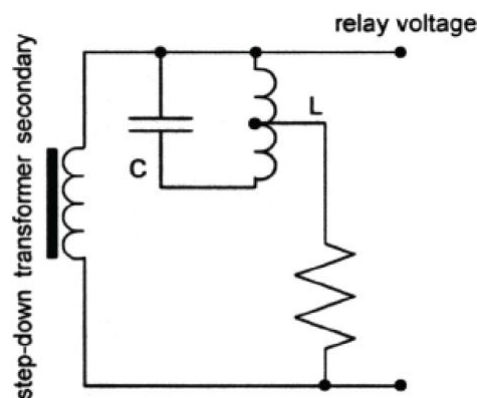


Figure 2.4: Active FSC

As seen from the Figure 2.4 above, the active ferroresonance suppression circuit is composed of an LC tuning circuit and a loading resistor. The LC circuit resonates at the rated frequency of the system and so presents a high impedance to the fundamental component of the voltage. The loading resistor, R, increases the resonant impedance at the system frequency and prevents the ferroresonance suppression circuit to behave like short-circuited at other frequencies; because the impedance of that LC circuit decreases gradually down to the resistance of the loading resistor, R. So; this circuit attenuates the components of the voltage other than the fundamental. Also, the attenuation level is changing according to the frequency. That is; the active ferroresonance suppression circuit behaves like a bandpass filter. Also, the storage elements makes the transient response of the CVT worse. So, a CVT including active ferroresonance suppression circuit is inadequate for harmonic and transient measurements.

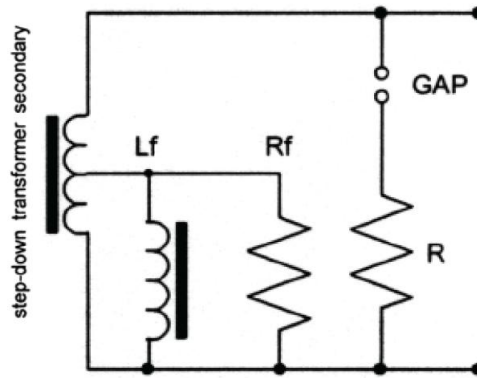


Figure 2.5: Passive FSC

As seen from the Figure 2.5 above, the passive ferroresonance suppression circuit is composed of permanently connected resistor,  $R_f$  and saturable inductor,  $L_f$  in addition to the loading resistor,  $R$ . The loading resistor is connected via an air-gap, so in normal operation, it has no effect on the circuit. But whenever the secondary voltage increases due to the induced voltage caused by ferroresonance oscillation, flash over occurs across the air-gap and the energy attenuates at the loading resistor,  $R$ .  $L_f$  is designed to saturate at about 150% of the nominal voltage to provide an extra protection against ferroresonance oscillation. This circuit results in better frequency response than the active ferroresonance suppression circuit. But an inaccurate measurement of the 3<sup>rd</sup> harmonic is still present but not as erroneous as the active one. The biggest disadvantage of this circuit is the permanently connected resistor,  $R_f$ . It increases the VA loading of the step down transformer, PT, and so; for the same burden specification, CVT including passive ferroresonance suppression circuit requires a bigger intermediate step down transformer than the one including active ferroresonance suppression circuit; which increases the cost of the CVT.

As explained above; CVT is not suitable for harmonic measurements due to the given reasons. The fundamental problem is the frequency response of the CVT which is a result of the defined issues, mainly the ferroresonance problem. Figure 2.6 shows the frequency response of a capacitive voltage transformer. But this curve is not valid for all CVTs. Even two different brand mark CVTs can have different frequency

response curves at the same voltage level. But the fundamental point is that; the frequency response of the CVT is far from being linear.

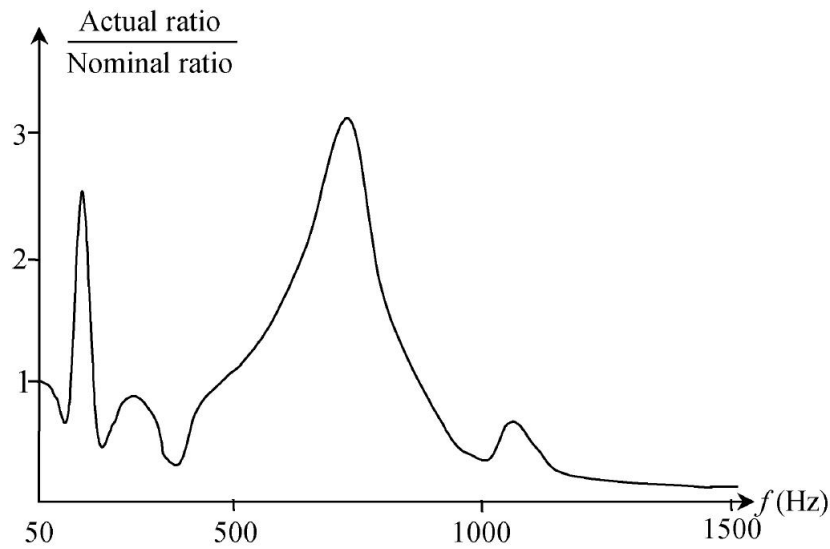


Figure 2.6: Frequency response of a typical CVT [11]

## 2.2.2 Inductive Voltage Transformers

Inductive voltage transformers (IVTs) are also named as voltage transformers or potential transformers in the literature. IVTs are magnetic potential transformers and they are bulky and expensive transformers compared to CVTs, especially in HV and EHV levels. That is why CVTs are preferred, as mentioned before. It is a conventional view that frequency response of inductive voltage transformers are better than the CVTs. This is true for some cases but there are also problems at harmonic voltage measurements.

Transient overvoltages or overcurrents can cause the iron core of one or two IVTs to saturate which may start the ferroresonance oscillation as shown in Figure 2.7. The voltage of one or two phases rises with respect to the ground as a result of the ferroresonance oscillation and this overvoltage may reach a destructive level on the secondary side, depending on the magnetizing inductance of IVT and the system capacitance,  $C_0$ .

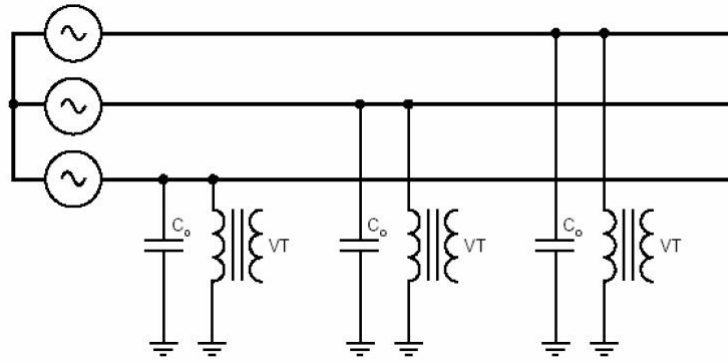


Figure 2.7: Three phase system including IVTs and capacitances

There are a few different ways of avoiding or damping ferroresonance in IVTs but they are different from the ferroresonance suppression circuits of CVTs. Also, remember that series ferroresonance exists in CVTs; where parallel ferroresonance occurs in IVTs, from the Section 2.2. One of the precautions is grounding the primary neutral point of the IVT through a resistor or nonlinear resistor as shown in the Figure 2.8 [11].

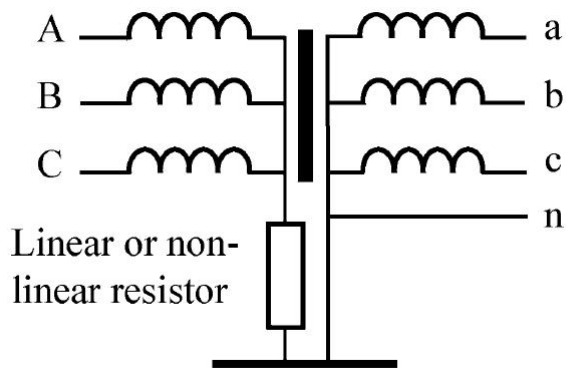


Figure 2.8: IVT with a resistor on the primary side for damping ferroresonance

This configuration provides a good protection against ferroresonance oscillations and overvoltages due to ferroresonance but the IVT then, suffers at harmonic measurements. Due to the neutral resistor,  $R$ , the harmonic measurement on the secondary side will not reflect the actual values because of the zero sequence component. As

is known, three phase systems are composed of positive, negative and zero sequence components. The positive and negative sequence components are symmetric and their sum is zero. So, these two components do not affect the inaccurate harmonic measurements. But when zero sequence component is present, it induces a voltage across the resistor,  $R$ , as shown in Figure 2.9.

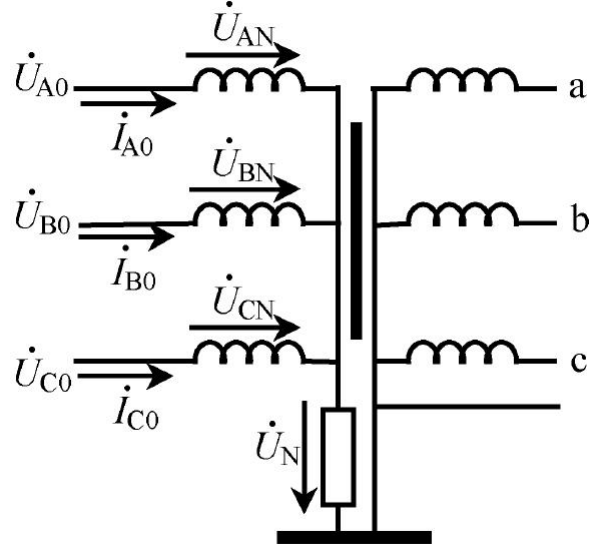


Figure 2.9: Zero sequence components at an IVT with a neutral resistor on the primary

Where;  $\dot{U}_{A0} = \dot{U}_{B0} = \dot{U}_{C0} = \dot{U}_0$  denotes the zero sequence harmonic voltage on the bus and  $\dot{I}_{A0} = \dot{I}_{B0} = \dot{I}_{C0} = \dot{I}_0$  denotes the zero sequence harmonic current components in the primary winding of the IVT. Then the voltage at the neutral point according to ground becomes

$$\dot{U}_N = 3\dot{I}_0R \quad (2.6)$$

So, the zero sequence harmonic voltage on the primary winding is

$$\dot{U}_{AN} = \dot{U}_{A0} - \dot{U}_N = \dot{U}_{A0} - 3\dot{I}_0R \quad (2.7)$$

by using the Equation 2.6. Depending on the design of the IVT, the resistor can be

very high, and/or the zero sequence harmonic current can be high too; thus affecting the accuracy of the measurement on the secondary. It is quite normal to have zero sequence harmonic currents on the voltage transformer due to its magnetization characteristics. The exciting current of the transformer is not purely sinusoidal and contains zero sequence component. Also the triplen harmonics in the magnetizing current is mainly zero sequence component, too.

Sometimes, the secondary side is grounded instead of the primary side. The grounding way is important here from the point of damping the oscillations and accuracy of the measurements. If the IVT has only one secondary output, then a resistor is connected to the secondary winding directly between the neutral point and the ground, as in the primary winding case. In this case, extra loading of the transformer occurs due to the connected resistor. In general, voltage transformers have at least two windings on the secondary; one for metering and one for protection purposes. The grounding of the neutral point is done through an air-gap for this type of transformers as shown in Figure 2.10.

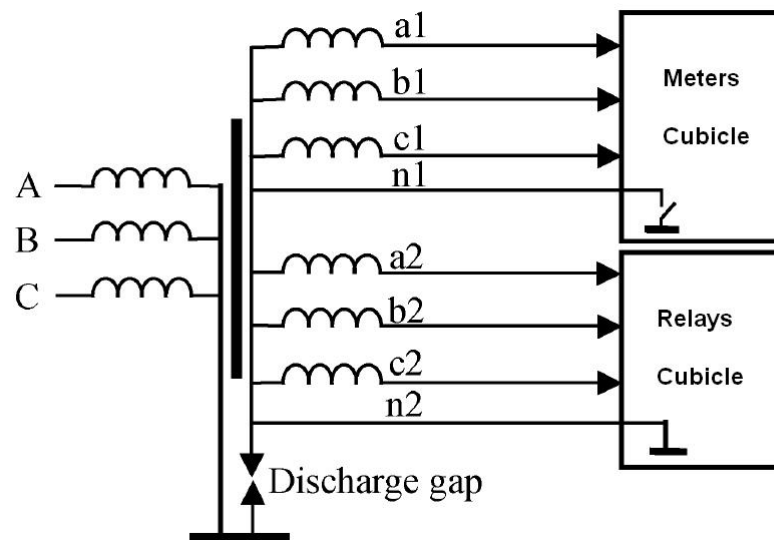


Figure 2.10: A discharge gap between the neutral point and ground on the secondary side [11]

As seen from the Figure 2.10, the actual grounding point is in one of the cubicles, generally in the relays cubicle, through a neutral line. But this configuration is in-

convenient for harmonic voltage measurements due to the mutual inductance and the stray capacitances. The best solution for this case is grounding the meters and relays separately through the neutral line of the IVT and connecting the neutral points of the secondary windings to the ground through separate discharge gaps, as shown in Figure 2.11.

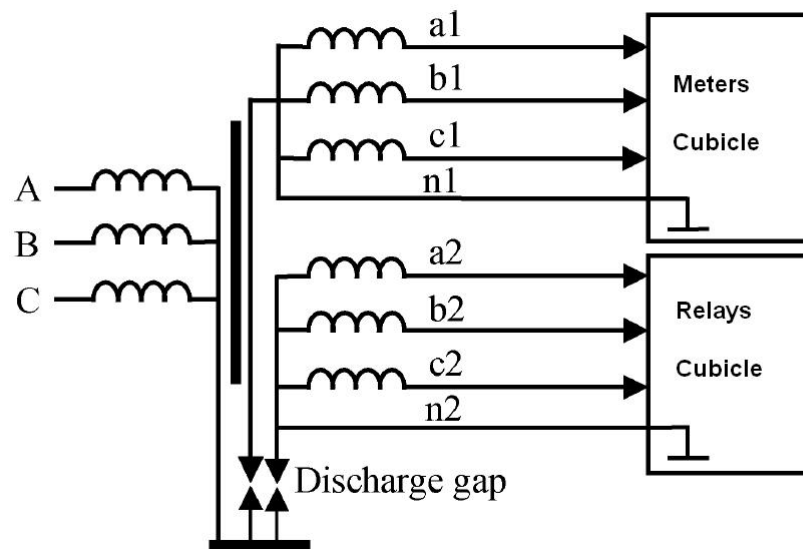


Figure 2.11: IVT having discharge gaps on each secondary windings [11]

The solution shown in Figure 2.11, reduces the total length of the neutral cable and so decreases the mutual inductance and stray capacitance. So; better harmonic measurements may be taken, but the result would not respond to today's requirements.

### 2.2.3 Capacitive Voltage Dividers

Capacitive Voltage Dividers are not used widely although they have no ferroresonance problem and have a satisfactory transient performance. The most important disadvantages of capacitive voltage dividers are, changing ratio and phase angle with burden in addition to need of high-input-impedance instrumentation amplifier. Also, for best results, input amplifier should be battery operated or should use a suitably shielded and isolated supply. And the leads from the low-voltage capacitor to the input amplifier should be as short as possible. In general, short leads from amplifier to

analyzer will reduce phase angle errors significantly, which is generally not possible in substations. Another disadvantage of CVDs is the limit on the burden they can supply without saturation due to the amplifier. The equivalent circuit of a capacitive voltage divider is shown in Figure 2.12.

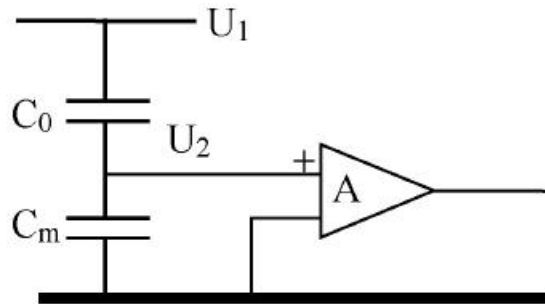


Figure 2.12: Equivalent circuit of a capacitive voltage divider (CVD)

### 2.3 Resistive - Capacitive Voltage Transformers (RCVTs)

RCVTs are manufactured by Trench Switzerland AG [19] in order to correspond to the needs in power systems since 1960. It is developed to overcome the deficiencies of CVTs and IVTs. RCVTs can be replaced directly with the conventional voltage transformers as well as can be used for specific applications up to 765 kV. General application areas of RCVTs are:

- HV DC transmission systems
- AC-DC-AC coupling stations
- Measurement of transient operations by switching operations
- Measurement of harmonics and subharmonics in the frequency range DC - 1 MHz
- Precision RC divider as actual sensor for close loop control HV DC system as voltage source of 300 kV and 600 kV to supply research electron microscope for the semiconductor industries.

As seen, one of the biggest advantages of RCVT is the measurement of DC voltages and also a wide frequency bandwidth for AC voltages up to 1 MHz. RCVTs may be used instead of conventional voltage transformers in substations especially when critical harmonic measurements are necessary in addition to the specific applications defined above.



Figure 2.13: 420kV RCVT in the substation of Temelli in Ankara

A real-life photo of the RCVT is shown in Figure 2.13, where the schematic view is available in Figure 2.14 in addition to the equivalent circuit shown in Figure 2.15.

The parts of the RCVT shown in Figure 2.15 are :

1. High voltage terminal of the primary voltage  $U_{PR}$
2. Low voltage terminal of the secondary voltage  $U_{SR1}$
3. Primary resistors  $\sum_{v=1}^{v=n} R_{pv}$

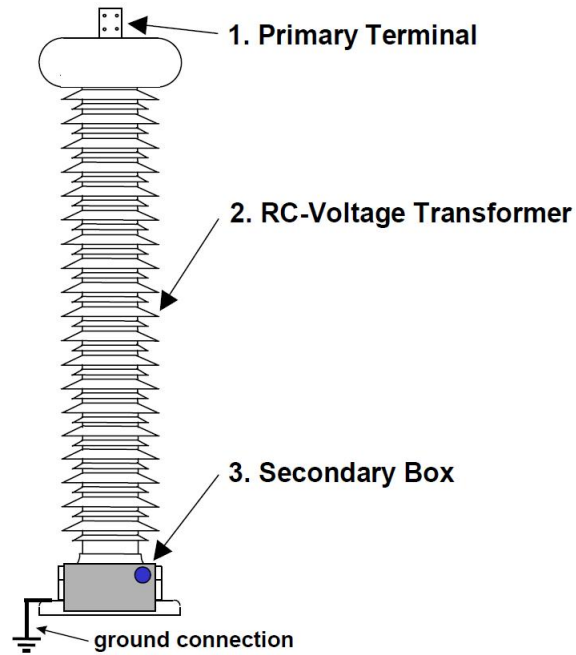


Figure 2.14: Schematic view of the RCVT

4. Secondary resistor  $R_s$  and secondary capacitor  $C_s$

5. Parallel capacitors  $\sum_{v=1}^{v=n} \frac{1}{C_{pv}}$

6. Stray capacitors  $C_{e1} \dots C_{en}$  between divider and ground

7. Ratio and phase displacement adjusting network (factory)

8. Double shielded connection cable with two twisted pair, length  $L_x$

9. Output voltage  $U_{SR2}$

As can be seen from Figure 2.15, there is no saturable core in RCVT which means that RCVT has no saturation problem. RCVT does not include any inductance in addition to a magnetic core. So; there is no ferroresonance problem in RCVT, too. The two fundamental problems of conventional voltage transformers (Please refer to Section 2.2) are removed at RCVT by ejecting the magnetic cores and inductances.

Another important characteristic of RCVT comes from the resistors in parallel to the capacitors. This configuration overcomes the trapped charges problem, which is also

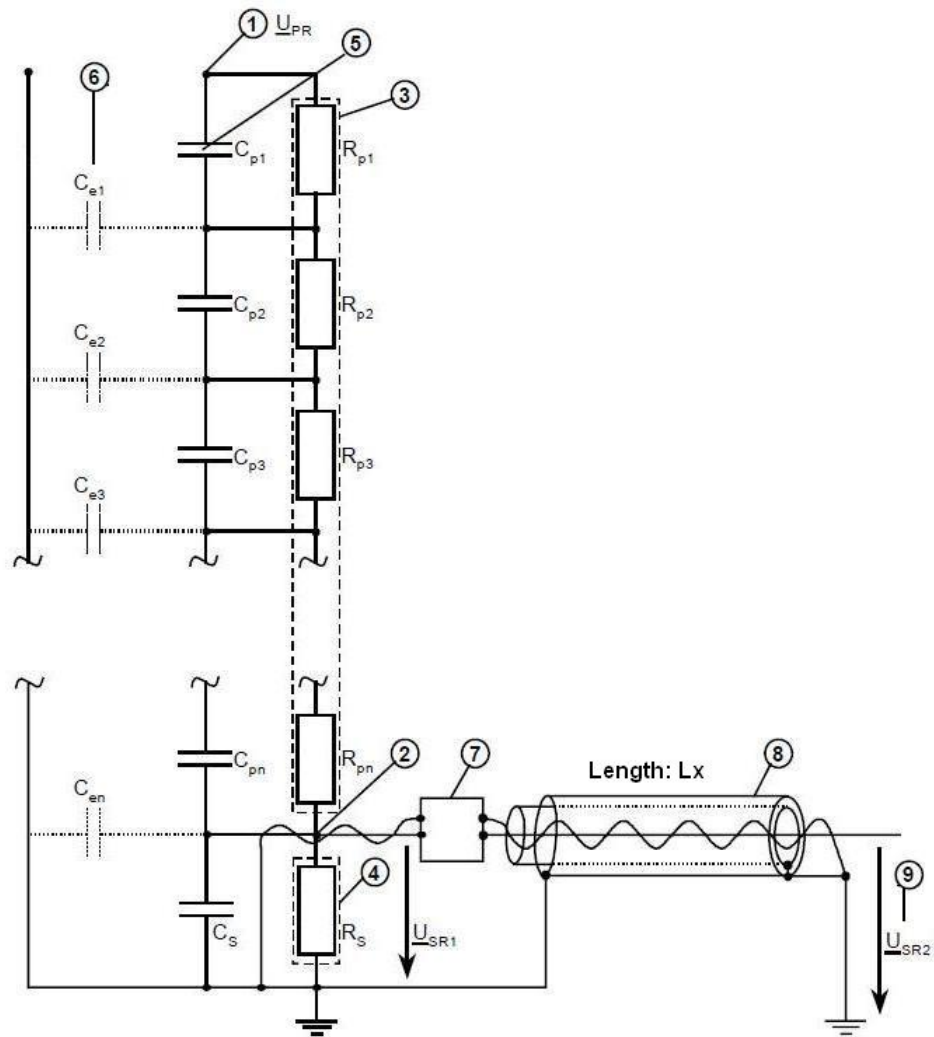


Figure 2.15: Equivalent Circuit of the RCVT

one of the main concerns at CVTs and capacitive voltage dividers. When a CVT or capacitive voltage divider removed from the line while the voltage is at its maximum by opening the circuit breakers for example, the capacitors at the primary side stay charged, while the secondary side is discharged through the burden it is connected. If the line is closed again before the primary capacitors are discharged, a transient state occurs due to the trapped charges. This phenomena both affects the power quality and causes inaccurate measurements until the capacitors become discharged. There is no such a problem for RCVT due to the resistors in the primary side, because the capacitors are discharged through the parallel resistors, at the same time with the

secondary side due to the time constant, which is determined by;

$$R_p \cdot C_p = R_s \cdot C_s \quad (2.8)$$

The resistors in parallel to the capacitors have been selected after several tests to guarantee an extremely low resistance variation with time, electrical stress and temperature. Of course, these resistors are quite low inductive resistors. The insulation system of the column is build up of oil, paper or  $SF_6$  inside and porcelain or composite insulators outside. The RCVTs used in this thesis are  $SF_6$  inside, composite insulator outside type for 420 kV measurements and oil inside, porcelain outside type for 36 kV measurements.

RCVTs satisfy the requirements of international standards for electronic voltage transformers like IEC 60044-7 [4]. The accuracy class of the RCVT is 0.2 or better (Please refer to Table 2.3).

By analyzing the equivalent circuit of RCVT shown in Figure 2.15, the transfer function can be found. Firstly, it should be noted that,  $R_{pv}$  and  $R_s$  are low inductive resistors and their inductance is negligible and their values do not change by dynamic stresses due to surge voltages or external physical effects.  $C_{pv}$  and  $C_s$  are also low inductive capacitors and their inductance is negligible, too. Then, the transfer function becomes,

$$\frac{U_{SR}}{U_{PR}} = \frac{R_s}{R_s + R_p \frac{1+R_s j\omega C_s}{1+R_p j\omega C_p}} = \frac{C_p}{C_p + C_s \frac{1+ \frac{1}{j\omega C_s R_s}}{1+ \frac{1}{j\omega C_p R_p}}} \quad (2.9)$$

by using Equation 2.8. The frequency independence can also be shown as;

$$\text{a) for } \omega \ll 1 \quad \Rightarrow \quad \frac{U_{SR}}{U_{PR}} = \frac{R_s}{R_p + R_s} \quad (2.10)$$

$$\text{b) for } \omega \gg 1 \quad \Rightarrow \quad \frac{U_{SR}}{U_{PR}} \approx \frac{C_p}{C_p + C_s} \quad (2.11)$$

Then, the temperature dependence can be formulated as;

$$\text{a) small } w \text{ and } R_p \gg R_s \quad \Rightarrow \quad \frac{U_{SR}}{U_{PR}} \approx \frac{R_{s20^\circ C} (1 + TK_{RS} \cdot \Delta T_{RS})}{R_{p20^\circ C} (1 + TK_{RP} \cdot \Delta T_{RP})} \quad (2.12)$$

$$\text{b) large } w \text{ and } C_s \gg C_p \quad \Rightarrow \quad \frac{U_{SR}}{U_{PR}} \approx \frac{C_{p20^\circ C} (1 + TK_{CP} \cdot \Delta T_{CP})}{C_{s20^\circ C} (1 + TK_{CS} \cdot \Delta T_{CS})} \quad (2.13)$$

For temperature independence, the temperature coefficients of  $R_p$  and  $R_s$  and the difference of the temperature variations,  $\Delta T_{RP}$  and  $\Delta T_{RS}$ , on the respective elements must be small, and the same requirements are valid for  $C_p$  and  $C_s$ , as can be seen from Equation 2.12 for resistors and Equation 2.13 for capacitors. The climate tests, done by Trench Group [19], have confirmed that the ratio,  $\frac{U_{SR}}{U_{PR}}$ , changes under the permissible limits according to the accuracy class of the RCVT.

Special care must be shown to the termination of the RCVT for accurate measurements. For steady state 50 Hz applications, the termination cable in Figure 2.15 can be used. For specific applications requiring a frequency response between DC - 1 MHz, a 50  $\Omega$  coaxial or triaxial cable must be used, and this should be connected to the interconnection of primary and secondary part of the divider via a low inductive 50  $\Omega$  resistor. The input impedance of the connected control equipment must be;  $|Z_i| \geq 1M\Omega$ , as shown in the Figure 2.16. But this can be adapted by the manufacturer, Trench Group [19], to satisfy customer requirement specifically. The termination of the RCVTs throughout this thesis is done by 50  $\Omega$  triaxial cable to be able to shield the cable on both sides. The input impedance of the measurement system is 108 k $\Omega$  resistor in parallel with 1 nF capacitor, which was suggested by the manufacturer, Trench Group [19].

The details of theory of RCVT are defined up to this point and it is easy to see that RCVT removes saturation, ferroresonance and trapped charges problems in addition to its wider bandwidth including DC. Throughout the rest of this section, comparison between RCVT and conventional voltage transformers takes place. Table 2.5 includes a detailed comparison between RCVT and conventional transformers.

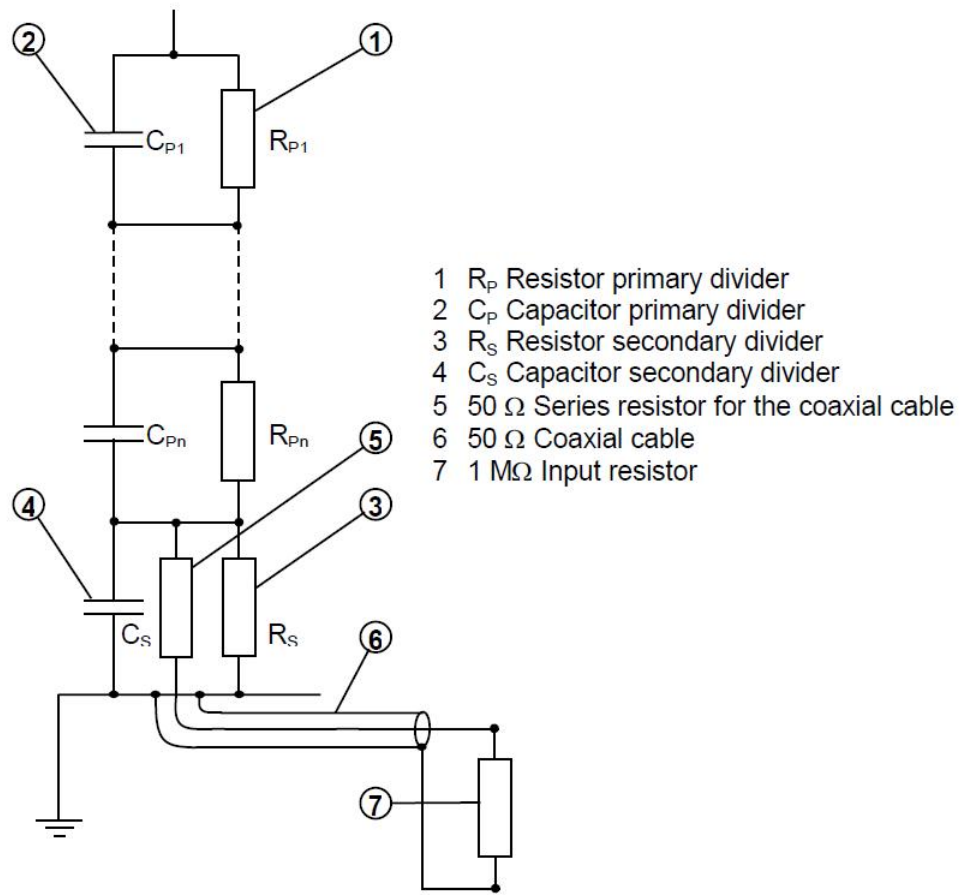


Figure 2.16: Termination of a 50  $\Omega$  coaxial cable on an RCVT

Investigating the Table 2.5, it is seen that RCVTs and IVTs have better steady state accuracy than the CVTs and CVDs where at transient state, RCVT has the best performance with its frequency response and phase response. Measuring DC component affects the transient performance of RCVT in positive way, especially at a re-close of a line with trapped charges caused by an improper action of protection relays maybe. Also burden range does not affect IVTs and RCVTs so much.

For comparing the transformers from the point of reliability, it is seen that RCVTs and CVDs are more reliable than CVTs and IVTs. Rows 3, 5 and 6 in Table 2.5 determines the reliability of the device. Ferroresonance problem is defined in detail in Section 2.2. RCVTs and CVDs can withstand a short circuit at the secondary side without any damage due to the divider characteristics. But this is not true for IVTs

and CVTs due to the magnetic potential transformer they include. A short circuited secondary results in transformer saturation and damage at CVTs and IVTs.

When RCVT is compared with conventional voltage transformers in terms of phase shifts and amplitude errors with respect to frequency, RCVT is even more better than the conventional transformers. The tests are made by Trench for general information and the results are seen in Figures 2.17, 2.18, 2.19 and 2.20. Investigating the results, peak errors are seen for IVTs and CVTs which correspond to the ferroresonance frequency. Of course, it should be noted that, the frequencies are not constant for all cases due to the nature of ferroresonance. As defined in Section 2.2, ferroresonance depends on system capacitance as well as transformer capacitance and inductance. So, as mentioned, it is impossible to know the ferroresonance frequency which depends on both the power system and the transformer type and brand. But this will not change the main result, just the peaks would occur in another frequency and amplitude of error would vary.

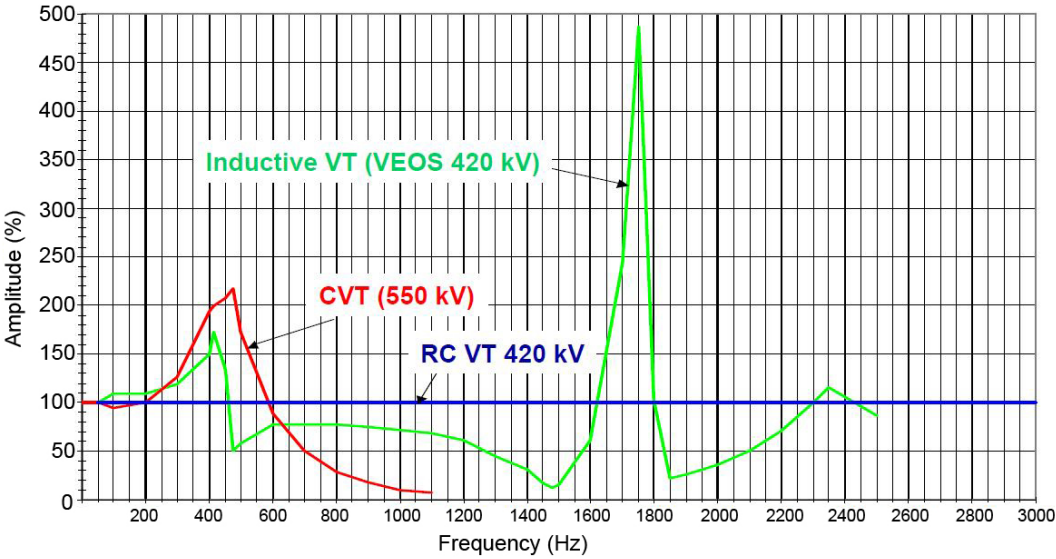


Figure 2.17: Comparison of amplitude errors of RCVT and conventional transformers [19]

Table 2.5: Voltage Transformer Technology Comparison [7]

No.	Technology ⇒	IVT	CVT	C-Divider	RCVT
	Performance				
1	Steady State Accuracy	(++) Excellent	(+) Good	(+) Good	(++) Excellent
2	High Voltage Line and Busbar Discharge	(- -) No	(- -) No	(- -) No	(+) Yes with long time constant
3	Ferroresonance with System or Itself	(- -) Yes	(- -) Yes	(++) No, no ferroresonance possible	(++) No, no ferroresonance possible
4	Transient Performance	(- -) 10Hz - 1 kHz Sufficient for slower protection functions	(- -) 45Hz - 55Hz Requires additional damping or relay correction	(+) 20Hz - 2MHz Sufficient for traditional protection functions	(++) 0Hz - 2MHz Excellent
5	Short Circuit Secondary	(- -) Requires fuses to prevent damage	(- -) Requires fuses to prevent damage	(++) Can be shorted for extended periods without damage	(++) Can be shorted for extended periods without damage
6	Dielectric Performance against surge	(+) Requires high skill level to design layer windings. The external voltage grading must be designed.	(++) Linear internal and external voltage distribution. The external voltage distribution is obtained by the internal voltage distribution of the active part.		
7	Burden Range	(++) Burden must be within spec. range	(-) Ferroresonance damping increases with burden	(-) Ratio and phase angle changes with burden	(+) Can be easy adapted
Grading Legend: (- -) unsatisfactory, (-) poor, (+) satisfactory, (++) excellent					

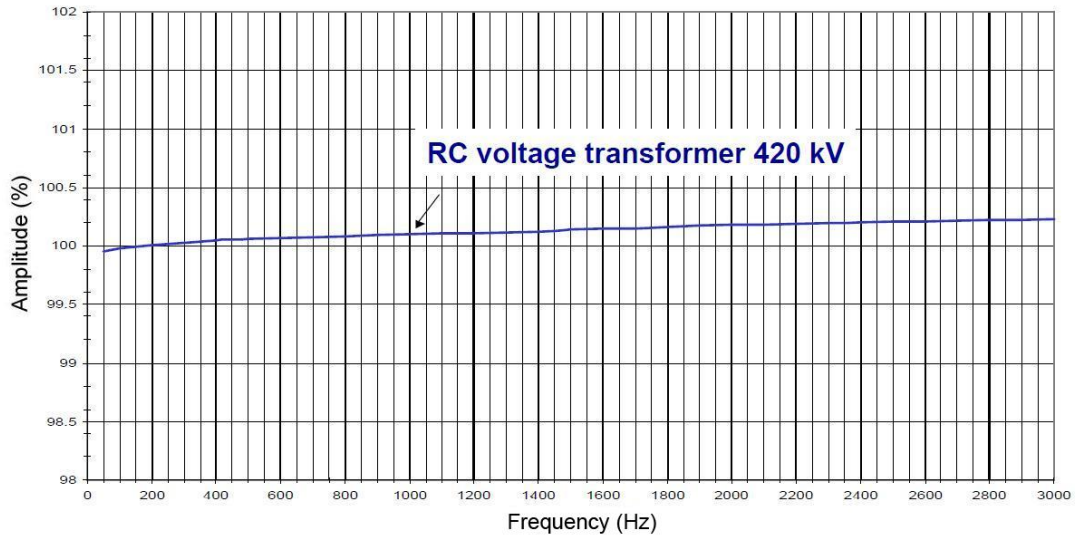


Figure 2.18: Accuracy of RCVT over frequency range [19]

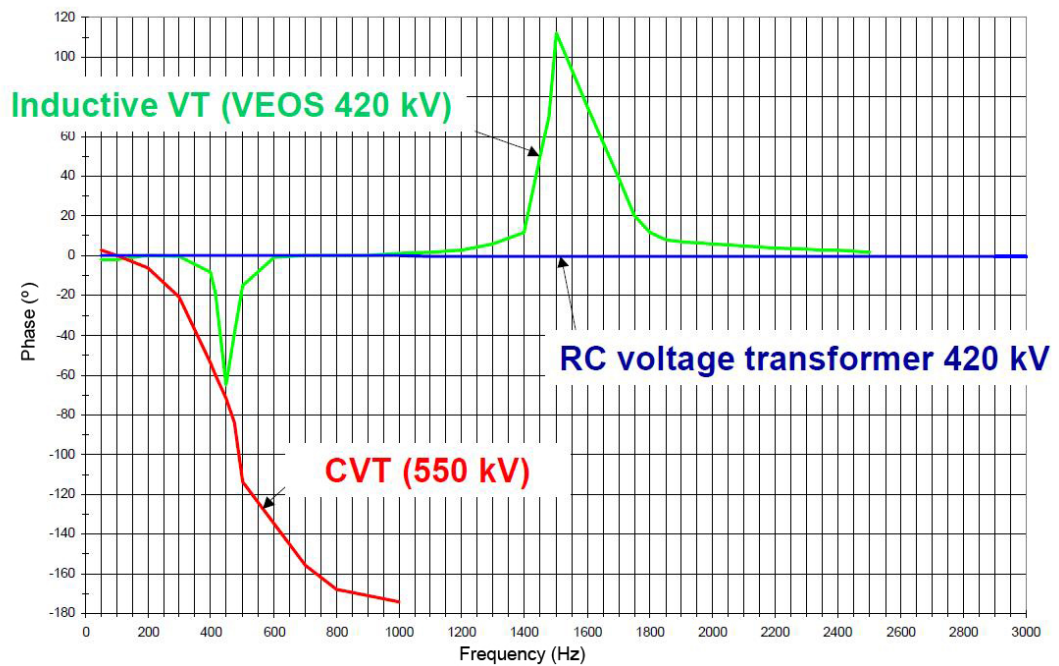


Figure 2.19: Comparison of phase shifts of RCVT and conventional transformers [19]

As is the scope of this thesis, conventional voltage transformers can not be used in harmonic voltage measurements as seen from the Figures 2.17 and 2.19. There are huge errors both in amplitude and phase deviation. Also, their frequency response is

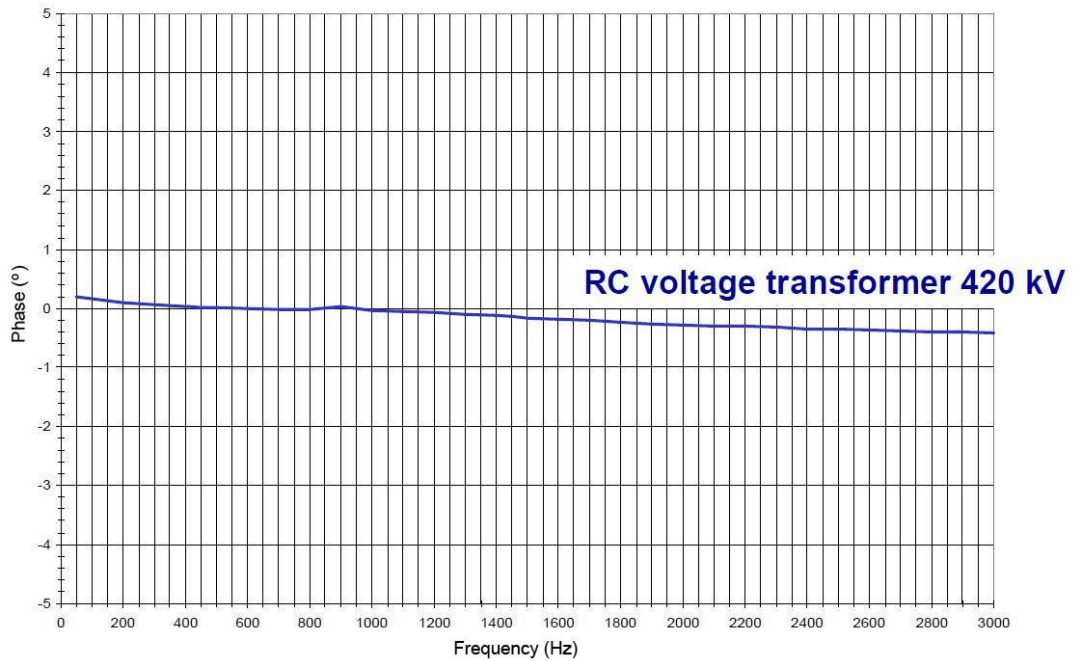


Figure 2.20: Phase deviation of RCVT over frequency range [19]

not linear. The sources of error have been defined in Section 2.2 but the main reason is ferroresonance, which is unpredictable. However, RCVT has almost zero error at both amplitude accuracy and phase deviation. Also, by investigating the Figures 2.18 and 2.20, it is seen that RCVT has approximately linear frequency response. Also, by taking care of calibration data of RCVT in the measurement software, almost absolute accuracy data can be taken by RCVT, especially in harmonic voltage measurements.

For this thesis and the project, one set of 420 kV and four sets of 36 kV RCVTs are purchased. Each set contains three columns for 3-phase measurements. The specific calibration data for 420 kV RCVTs used in this thesis are available in Appendix A. 36 kV RCVTs have similar specific calibration data, too.

## 2.4 Optical Voltage and Current Transducers (NXVCT and NXCT)

Optical voltage and current sensors are manufactured by NxtPhase T&D Corporation [20] to present a new solution for measurements in power systems. But today, NxtPhase has been bankrupt and bought by Areva T&D. Like RCVTs, NXVCTs were

produced to overcome the deficiencies of conventional voltage and current transformers. NXVCT is capable of measuring current in addition to voltage, which is an advantage over RCVT. NXVCT is a combined sensor, which means measuring both current and voltage. Only current and voltage sensors are available also, for cheaper solutions, named as NXCT and NXVT respectively. NXVCT and NXCT are used throughout this thesis and project. The theory of NXCT and NXVCT are, of course, the same for current measurement optically. So, throughout this chapter, NXVCT will be defined.

NXVCT satisfies the international standard requirements, IEC 0.2 [2] (refer to Table 2.3) for voltage measurements and IEC 0.2S [1] for current measurements. 0.2S and 0.5S are accuracy classes for specific applications. The limits are shown in Table 2.6 for measuring current transformers for special application.

Table 2.6: Limits of current error and phase displacement for measuring current transformers for special application [1]

Accuracy class	± Percentage current (ratio) error at percentage of rated current shown below					± Phase displacement at percentage of rated current shown below									
						Minutes					Centiradians				
	1	5	20	100	120	1	5	20	100	120	1	5	20	100	120
0.2S	0,75	0,35	0,2	0,2	0,2	30	15	10	10	10	0,9	0,45	0,3	0,3	0,3
0.5S	1,5	0,75	0,5	0,5	0,5	90	45	30	30	30	2,7	1,35	0,9	0,9	0,9

As mentioned, theory of NXVCT depends on optical sensors and signals. Indeed, current and voltage measurement theories and techniques are different, which will be defined in this section further. As benefits of optical technology, NXVCT removes the deficiencies of conventional voltage and current transformers. There is no saturation, ferroresonance, trapped charges and open or short-circuited secondary problems for the optical transducers, because it does not include any storage elements and transformers. The NXVCT provides a wide dynamic range over a wide bandwidth, DC to 20 kHz for current measurements and 0.5 Hz to 6 kHz for voltage measurements. The bandwidth may change at a special request depending on the application and it provides excellent phase and amplitude accuracy over the bandwidth. Also, the mea-

surement accuracy is not affected by temperature changes and vibration. The system includes a temperature sensor for the outdoor temperature and fixes its coefficients according to the temperature. The operating temperature of the column is  $-40\text{ }^{\circ}\text{C}$  to  $50\text{ }^{\circ}\text{C}$ , outdoor. The NXVCT uses dry nitrogen gas as insulating gas instead of oil, cellulose or  $SF_6$ , which is environmentally friendly and composite insulator is used as the outside insulator. As an achievement of this insulator scheme, weight of an NXVCT is just about 10% of a conventional device. Also, due to the optical signals it uses, galvanic isolation from the high voltage line is provided. As another advantage of NXVCT, it provides voltage and current transducer in a single device in addition to metering and protection outputs also in the same device, which yields gain in space. The schematic of an NXVCT column is shown in Figure 2.21 and used 420 kV NXVCTs are shown in Figure 2.22. The accuracy of a typical NXVCT is shown in Figure 2.23 for voltage measurements in comparison with the IEC 0.2 standard [2] and in Figure 2.24 for current measurements in comparison with the IEC 0.2S standard [1].

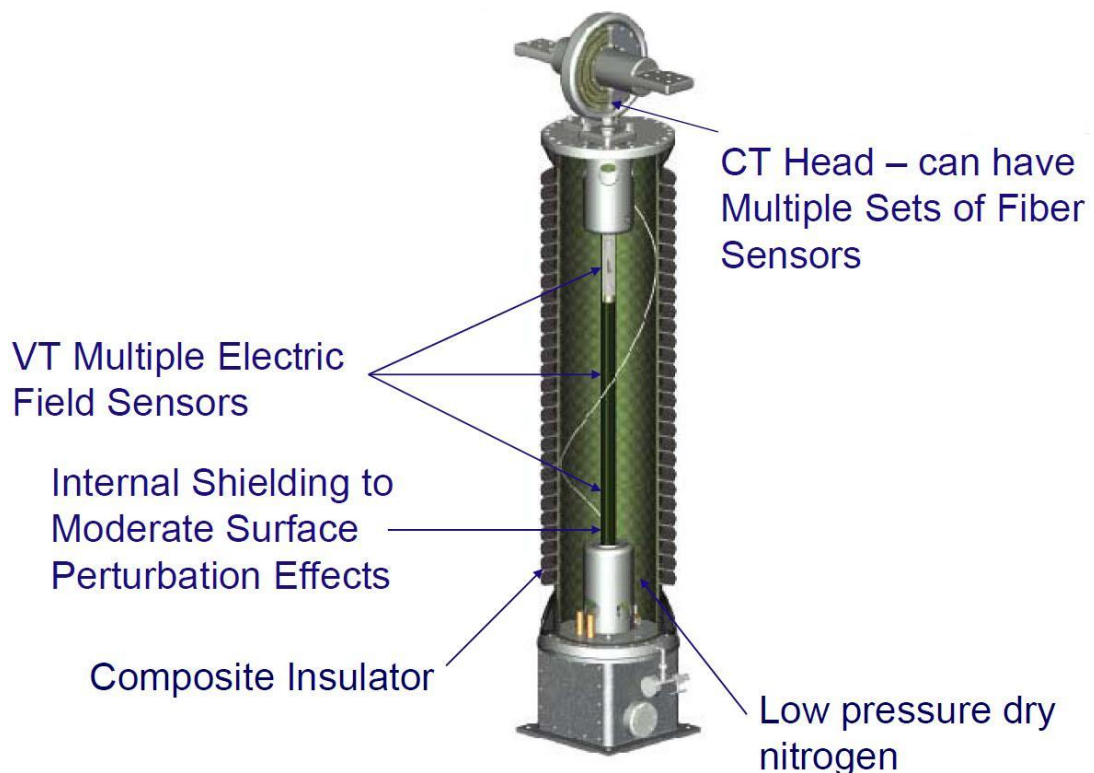


Figure 2.21: Schematic of an NXVCT column



Figure 2.22: 420 kV NXVCT at substation of Temelli in Ankara

The NXVCT system is mainly formed of three parts:

- Column assembly
- Fiber and electrical cable assembly
- Electronics assembly housed in 19” standard control rack

The simplified connection scheme of the NXVCT system is shown in Figure 2.25. The electronics, housed in cabinets in the control room operate as a transducer between optical and electrical signals. The system also includes a Graphical User Interface (GUI) software for monitoring system health, parameter modification and monitoring the output data of the columns, through the electronics. The most important benefit of this system is adjustable turn - ratio through the GUI.

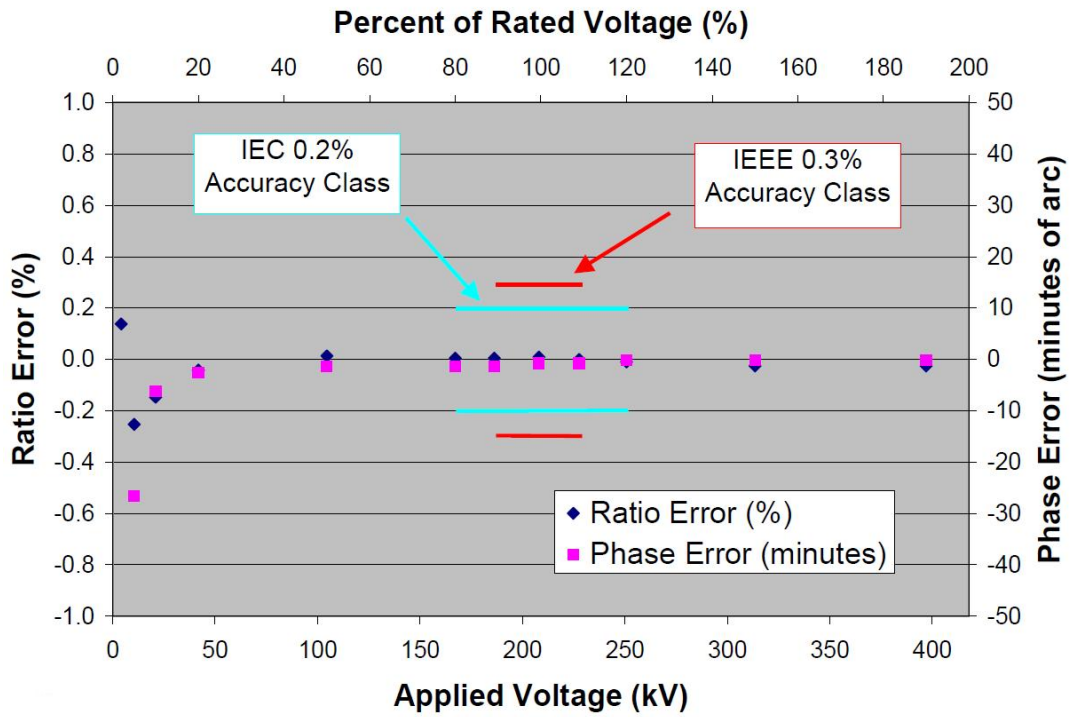


Figure 2.23: Accuracy of NXVT [22]

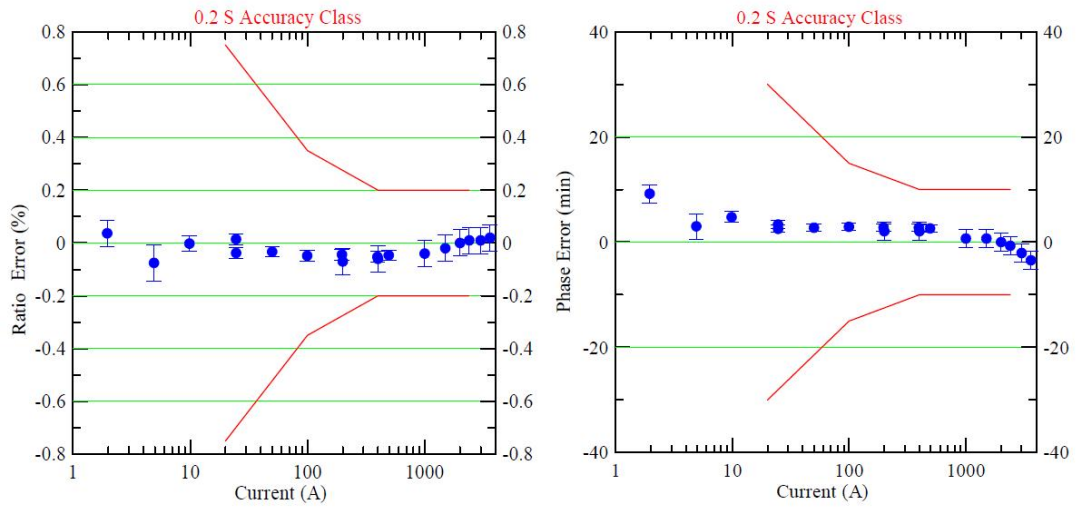


Figure 2.24: Accuracy of NXCT [21]

The electronics system is formed by three parts:

- Fiber Splice tray; for the connection of fiber cables

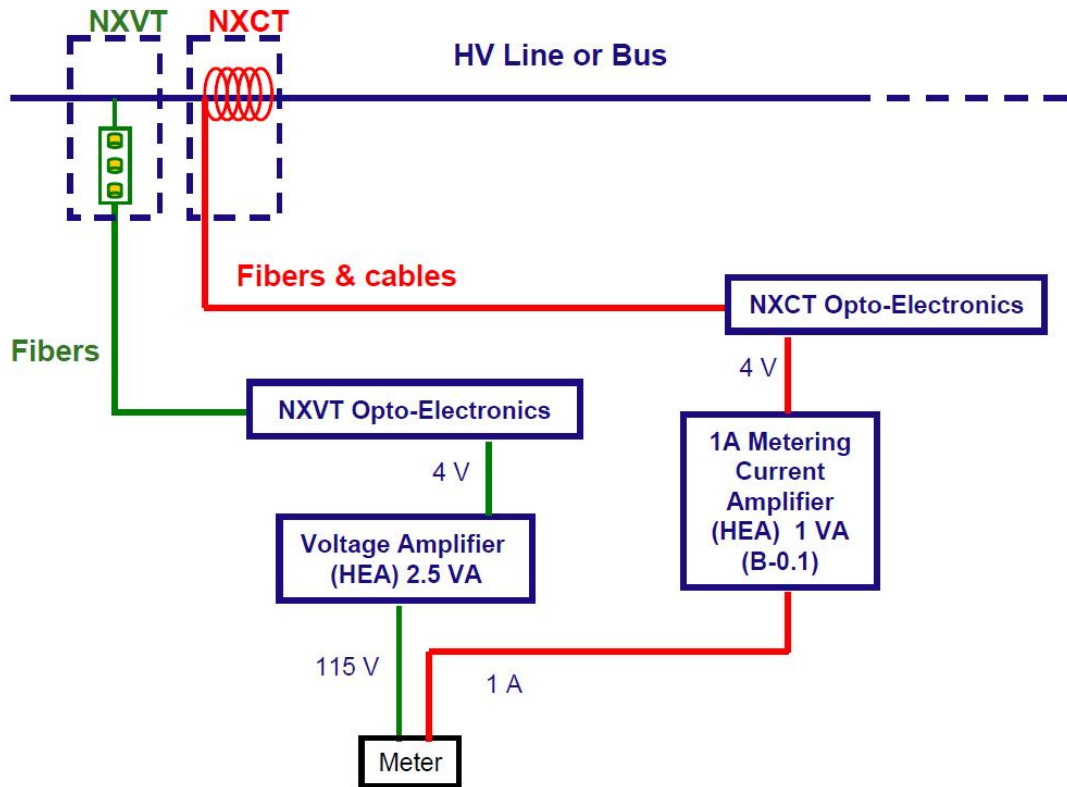


Figure 2.25: General Connection scheme of an NXVCT system [21]

- Electro - Optics Chassis (EOC); includes optical sensors and is used for signal processing, self - monitoring and sensor output interface which may be digital or low energy analog. Also, metering and protection outputs of NXVCT have separate EOCs.
- Power Supply Unit (PSU); for  $\pm 6 V$  and  $\pm 15 V$  outputs to supply the EOC. Required input voltage is  $70 V_{dc}$  to  $150 V_{dc}$  and input power is  $270 W$  but depends on the number of sensors.

The operating temperature for the electronics is  $-5^{\circ}C$  to  $40^{\circ}C$ , indoor and they are shown in Figure 2.26.

Nine systems are bought from NxtPhase T&D Corporation [20] for this thesis to satisfy different measurement scenarios:



Figure 2.26: The Electronic System - Back and Front View of the Cabinet

- NXVCT - 229 : 420 kV, 2000 A, both metering and protection current outputs
- NXVCT - 230 : 420 kV, 450 A, only metering current output
- NXVCT - 231 : 420 kV, 450 A, both metering and protection current outputs
- NXVCT - 237 : 170 kV, 2000 A, both metering and protection current outputs
- NXCT - 111 : 36 kV, 2500 A, both metering and protection current outputs
- NXCT - 112 : 36 kV, 2500 A, both metering and protection current outputs
- NXCT - 113 : 36 kV, 1000 A, both metering and protection current outputs
- NXCT - 114 : 36 kV, 1000 A, both metering and protection current outputs
- NXCT - 115 : 36 kV, 100 A, both metering and protection current outputs

The specific calibration data had been sent by NxtPhase for the columns bought for this work and one of them is available in Appendix B as an example.

At this point of the thesis, it will be beneficial to investigate the theory of voltage and current measurements by optical sensors in separate sections.

**2.4.1 Optical Current Transducer**

Optical current sensors are achieving increased acceptance and use in high voltage substations due to their superior accuracy, bandwidth, dynamic range and inherent isolation [23]. The biggest advantage of optical current sensors against conventional current transformers is that, there is no saturable magnetic core. So; they can measure high, distorted currents more accurately than the conventional ones. If an optimum system is designed, the optical current transducers can measure fault currents exceeding  $400\text{ kA}_{peak}$ , including DC.

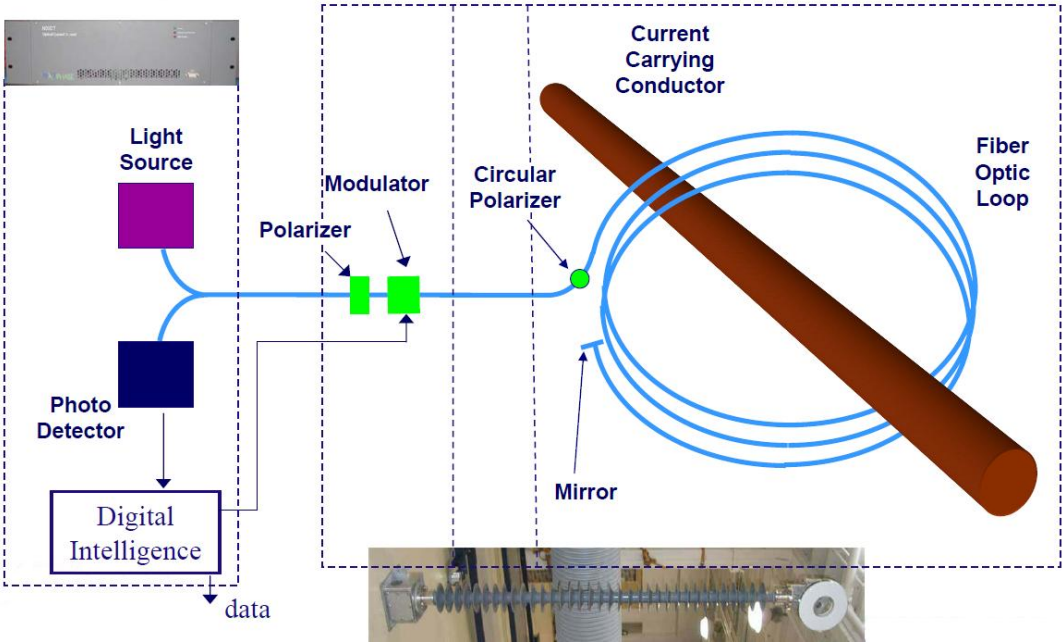


Figure 2.27: Fiber Optic Current Sensor Optical Block Diagram [21]

The block diagram of an optical current sensor is shown in Figure 2.27 in addition to the components it includes. The light source, located in the electronics in the control room, sends light to the linear polarizer and then to a polarization splitter, to create two linearly polarized waves. Then, these waves travel to an optical phase modulator. The linearly polarized waves travel to the sensor head through fiber optic cables and

reach to a circular polarizer. The linearly polarized waves became right and left hand circularly polarized waves at the output of this unit. Then, the circularly polarized waves traverse the optical sensing loop through the fiber optic cable at the sensor head of the optical CT. While encircling the loop, the magnetic field induced by the current flowing into the CT head, creates an optical phase shift between the two light waves due to the Faraday effect. At the end of the loop, the light waves are reflected back from a mirror and they return back to the control room through the same path. The phase shifted light waves are received by the photo detector and the electronics de-modulate the light waves to determine the phase shift which is proportional to the current flowing into the CT head. Finally, a digital or analog signal is produced by the electronics as output, representing an image of the primary current.

The optical sensor has a transfer function with a sine wave characteristics. In normal operation while the primary current is at rated or lower, the sensor operates at the linear portion of that transfer function. But, whenever the current increases substantially like in a fault condition, the transfer function jumps to the nonlinear portion of the sine wave. However, the electronic system can realize this situation, as the nonlinear portion of the sine wave had been well defined. And so; the system can continue to measure the current accurately up to a limit. When the operation jumps to  $\pm \pi$  radians of the sine wave and continues to increase, the electronics may interpret the current at the opposite end of the sine wave, which physically means jumping of the current sensor's output to a current of negative polarity with respect to its previous value. The number of jumping may be several depending on the situation. This case is directly related to the number of fiber turns at the sensor head which are used for current sensing. That is; as the number of fiber turns increases, the maximum current which can be measured by the optical sensor, decreases. But also, signal to noise ratio increases as the number of fiber turns increases. So, a choice has to be made between signal to noise ratio and the maximum measurable current, of course this choice depends on the application [23].

As mentioned, noise in current measurements depends on the number of fiber turns and so the maximum measurable current. Another parameter is the bandwidth of the sensor. The noise formulation for current measurement at the primary side of the NXVCT (and NXCT) is given in Equation 2.14.

$$N_{primary} = \frac{0.2}{\# \text{ of fiber turns}} \times \sqrt{f_{BW}} \quad , A_{rms} \quad (2.14)$$

For example, for the sensors which have been used throughout this thesis, having a bandwidth of 20 kHz and 44 fiber turns, the noise at the primary side can be calculated by using the Equation 2.14, as :

$$N_{primary} = \frac{0.2}{44} \times \sqrt{20000} = 0.64 A_{rms} \quad \text{primary current}$$

The noise defined here is superimposed on the true waveform and it is White Noise, which means zero mean Gaussian noise. So, this means that the average value of the noise is zero and for the applications which does not require instantaneous values, the average value of the measured data can be used to eject the noise completely, which can not be done for this thesis. But, noise is a consideration for only very low primary currents.

The optical current transducers were tested in Japan in field for their long-term reliability during 2 years. The sensors used in that work were bought from Toshiba Corporation, instead of NxtPhase T&D Corporation; but the used technology and the operating principle of both sensors are the same. As a conclusion, that research confirmed the reliability of the optical current sensors [24].

#### 2.4.2 Optical Voltage Transducer

Optical voltage transducers provide wider bandwidth, larger dynamic range, lighter weight, smaller space and stability over temperature changes and dielectric stresses when compared to the conventional voltage transformers. Also, due to the optical fibers, they obtain inherent electrical isolation and immunity to electromagnetic interference [25],[26].

As is known, the voltage difference between two points can be calculated by measuring at least one component of electrical field surrounding them. By using the cartesian coordinate system, the voltage difference between points a and b may be represented by the line integral;

$$V_{ba} = - \int_a^b E_x(x) dx \quad (2.15)$$

where  $E_x(x)$  is the x-component of the electric field along the x-axis. If the point a is the origin, then Equation 2.15 becomes;

$$V_b = - \int_0^b E_x(x) dx. \quad (2.16)$$

To be able to apply this theory at optical voltage transducers, it has to be discrete. So, the Equation 2.16 should be approximated by weighted sums of the samples of electric field component.

$$V_b \approx - \sum_{i=1}^N \alpha_i E_x(x_i) \quad (2.17)$$

where,  $\alpha_i$  are the weights and  $x_i$  are the abscissas,  $N$  is the number of samples and  $E_x(x_i)$  is the x component of the electric field at the  $x_i$ . Of course, the electric field along the path of integration may vary depending on the conductor geometries and the dielectric medium. So, it is desired to have a weighted sum which is not affected by the possible variations of  $E_x(x_i)$  when there is a constant voltage difference. That is, determining the number of samples, and so the number of electric field sensors is the main concern here. Also, the number of sensors depends on the required accuracy and the environmental conditions. There are various methods to approximate an integral into a weighted sum; like Cotes and Gaussian quadrature formulas. For a given number of samples, Gaussian quadrature formulation would give more accurate results than Cotes formulation. The NxtPhase T&D Corporation uses a different formulation at optical voltage transducers they manufactured, which is based on Gaussian quadrature formula and refers it as Quadrature Method [25]. The formulation is simulated and tested by NxtPhase T&D Corporation and it is seen that, this method gives the best results for quite accurate measurements and also by using minimum number of sensors [25],[26].

The problem is finding  $\alpha_i$  and  $x_i$  in Equation 2.17 in addition to the number of sensors. By experimental tests, it is found that, three electric field sensors are sufficient to

satisfy the requirements of accuracy class IEC 0.2 [2], [26]. Then, the problem is finding three  $x_i$  and  $\alpha_i$  values by using the quadrature method. An unperturbed system is considered for a customized Gaussian quadrature formula which accounts for the basic shape of  $E_x$  and referred as  $E_x^{unp}$  along the path of integration. Then  $E_x$  becomes;

$$E_x = \rho(x)E_x^{unp} \quad (2.18)$$

where  $\rho$  is any polynomial of degree  $2N - 1$  or less. At this method,  $E_x^{unp}$  must be known and it may be found analytically or experimentally.  $\rho$  can be determined by considering the worst case condition that may occur at a substation according to standards, for example clearances [25].

Further tests are made by NxtPhase T&D Corporation to check the accuracy of optical voltage transducers and the test results satisfy the IEC 0.2 [2] requirements even for various cases of electric field perturbations caused by nearby metallic objects and a neighboring optical voltage transducer.

In conclusion, the voltage and current transducers used in this thesis remove the deficiencies of conventional instrument transformers. The used transducers are much more suitable to measure harmonic components than the conventional ones due to their wider bandwidth. Also, there are no ferroresonance and isolation problems and hence, these transducers can be connected directly to high voltage lines. Another point is that, most instrument transformers installed in substations are class 0.5 for metering and even for some points, there is only protection type transformers with an accuracy class of 5P. The used transducers have an accuracy class of 0.2 for voltage measurements and an accuracy class of 0.2S for current measurements. That is why, the fundamental component will be measured more accurately throughout this thesis. These transducers are installed on trailers to develop a mobile measurement system in order to measure as many feeders as possible to calibrate various types of conventional transformers. Also, the measurements shall be taken at as many substations as possible which include high order harmonics in order to compare a wider bandwidth. The developed mobile measurement system is described in next chapter, Chapter 3.

## **CHAPTER 3**

### **MOBILE MEASUREMENT INFRASTRUCTURE**

Number of measurements plays an important role for the variety and consistency of the thesis; especially measurements should be taken from different types of instrument transformers for the calibration purposes. To correspond to these requirements, mobile measurement systems are designed. A measurement system consists of two trailers; one for the columns and one for the electronic systems. Electronic system is designed to sample data as accurate as possible. It processes the analog data output of columns and converts it into a format which is suitable for data acquisition cards. High-speed computers are used for sampling and processing data at a rate of 102.4 kHz. Also, high capacity hard disks are used for data storage. A software is developed to sample, process and store the processed data and the raw data. Throughout this chapter, developed mobile measurement system will be explained in detail. It will be convenient to divide this chapter into three sections: trailer of the columns, trailer of the electronic system and the software.

#### **3.1 Trailer of the Columns**

These trailers carry the RCVT and NXVCT columns for 420 kV and 170 kV and each trailer carries 3 columns. The dimensions of the trailer is 2.5x14.5 m (WxL); designed to fit the openings in the substations. Also, the columns are mobile on the trailer to fit the openings of transmission lines exactly. One of the columns on the trailer occupies one side of the trailer and can move along the whole trailer. Other 2 columns are at the same side, opposite side of the other column, and have a tolerance of 70 cm on the horizontal axis, totally. The same trailer can be used at both 420 kV

and 170 kV measurements as an advantage of the column moving along the whole trailer. The columns are installed on lifts to adjust the height of the column and for the column to touch the transmission line. The lifts can carry up to 2000 kgs and its height is 70 cm when it is closed. The maximum height of the lift is 4.5 m from its bottom and 6.3 m from the ground. The column height for 420 kV RCVT is 4.0 m; where it is 4.1 m for 420 kV NXVCT and 3.4 m for 170 kV NXVCT.

Figure 3.1 shows the trailer at the transportation position, while it is approaching to a measurement point at the substation. When the trailer is at the measurement point, it is balanced via the hydraulic stands. Balancing is needed not to damage the columns while tilting them up. Then, the columns are tilted up by the hydraulic jacks as shown in Figure 3.2 and Figure 3.3. If the transmission lines are higher, then the lifts are raised by other hydraulic jacks as shown in Figure 3.4. The hydraulic jacks are shown in Figure 3.5.



Figure 3.1: 420 kV NXVCT columns are at transportation position



Figure 3.2: 420 kV NXVCT column while tilting up for connection



Figure 3.3: 420 kV NXVCT column is tilted up



Figure 3.4: 420 kV RCVT columns are raised by the lift

One of the most important points in the design of the mobile trailers is the cable management. Each RCVT column has just one triaxial cable for the secondary output as explained in Section 2.3; but the situation is more complicated for NXVCT. Each column has 5 fiber-optic cables; 3 of them are for voltage measurement, 1 of them is for metering current output and the last one is for protection current output. Also, each NXVCT column has 4 electrical signal cables to drive the modulator unit as defined in Section 2.4; 2 cables for metering and 2 cables for protection current output. Of course, if NXVCT has only metering current output like NXVCT-230, then, both fiber-optic and electrical cables for protection current output will not be present. Because the columns on the trailer are mobile both vertically and horizontally; the cables must be mobile, too. So, movable cable ducts are used as shown in Figure 3.5.

All of these cables are connected between trailer of the columns and trailer of the electronics. The triaxial cable of RCVT is on a reel and attached to secondary output connector of the column at one side and to the electronic system on the other side. The

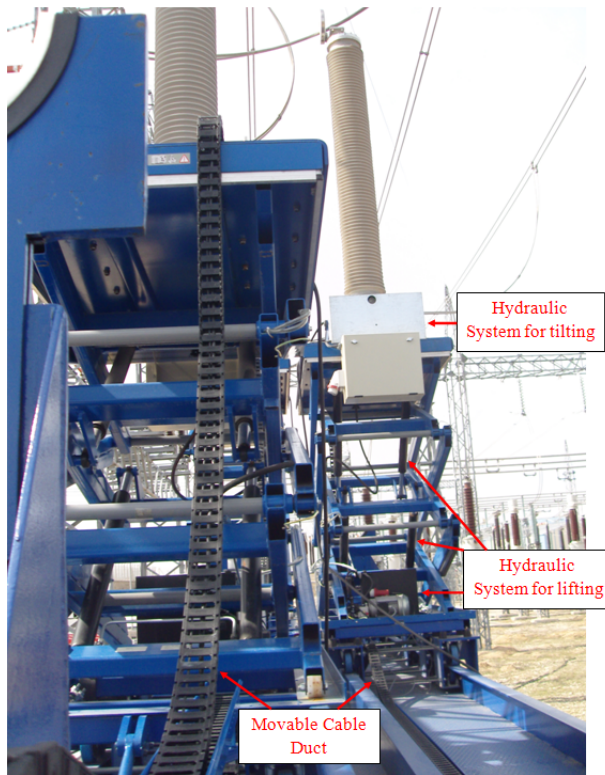


Figure 3.5: Movable Cable Duct and Hydraulic System

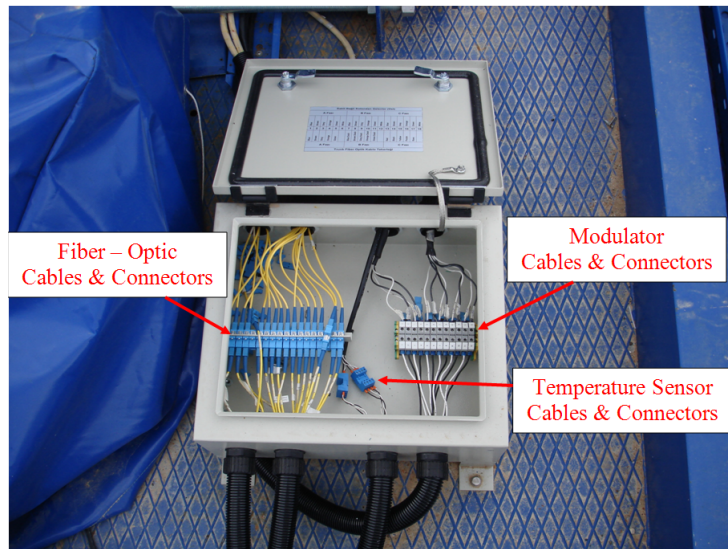


Figure 3.6: Connection Cabinet on the Trailer

cables of NXVCT are combined with the column and have a length of 35 m, which is not enough for this work. So, there are two reels, one for fiber-optic cable and the other one for the modulator cable. These cables are connected to the ones coming out of the column on the trailer via connectors and are attached to the electronic system on the other side. Connection must be solid for fiber-optic connectors against loss of connection and should be protected against external effects, like rain. That's why, the connection is done inside a cabinet which is mounted on the trailer, as shown in Figure 3.6.

Also, the cables coming out of NXVCT columns are too long for the connection on the trailer, 35 m as mentioned. So, these cables are coiled up inside another cabinet and adjusted for the connection cabinet. The cabinet also includes the temperature sensor of the NXVCT system which had been mentioned in Section 2.4 and shown in Figure 3.7. The temperature sensor cable is attached to another cable in the connection cabinet and connected to the electronic system via that cable.



Figure 3.7: Temperature Sensors and Coiled up Cables

This system is used at 380 kV and 154 kV measurements. The trailer used at 36 kV measurements is different but cable management is the same. 3 RCVT columns are used for voltage measurement and 3 NXCT columns are used for current measurement at 36 kV. The trailer is shown in Figure 3.8.



Figure 3.8: Trailer which is used at 36 kV measurements

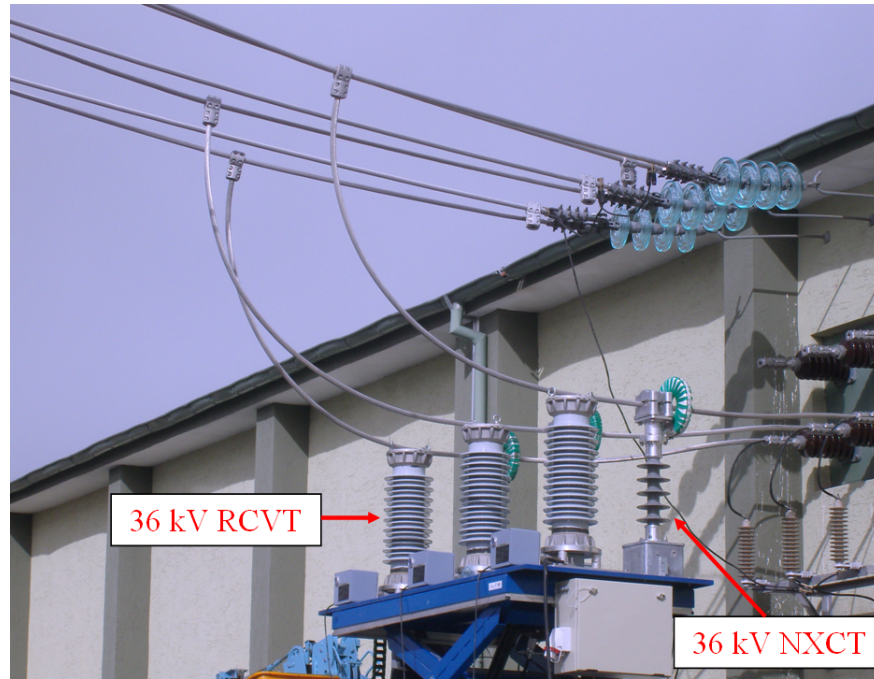


Figure 3.9: 36 kV RCVT and NXCT Columns at field measurement

### 3.2 Trailer of the Electronic System

Electronic interface units required to take measurements by RCVT and NXVCT are mounted in enclosed trailers which is shown in Figure 3.10.

The trailer includes electro - optic interface units of NXVCT and NXCT system as explained in Section 2.4, interface module of analog signals and the computer which includes the data acquisition cards. The electronic system is supplied from 110  $V_{dc}$  in the substation and converts it to other required dc voltages; 24V,  $\pm 15V$ ,  $\pm 12V$ , and 3.3V. The cabinets are shown in Figure 3.11.

The electro - optic interface had been explained in Section 2.4. Output of electro - optic interface, secondary output of RCVT and conventional voltage and current transformer secondary outputs are input to the interface module. The interface unit is mainly formed by a pcb which converts analog signal levels suitable for data acquisition card; conventional voltage transformer and RCVT outputs are divided by 56, conventional current transformer outputs are divided by 20 and NXVCT outputs are



Figure 3.10: Trailer of the Electronic System

divided by 2.5, approximately. Each pcb is tested separately to find exact division ratio, phase shift and dc offset values against harmonics up to 50<sup>th</sup> harmonic. These values are taken into account at measurements by the software so there shall remain no error related to the interface module. The pcbs are shown in Figure 3.12.

Another input to the interface unit is the GPS antenna which is used for synchronous measurements between the systems and shown in Figure 3.13. The incoming signal is 9.9328 MHz and this signal is transferred to the data acquisition card. Then, data acquisition card counts 97 pulses and samples its input channels. So, a sampling frequency of 102.4 kHz is obtained, which equals to  $50 \text{ Hz} \times 2^{11}$ . This sampling frequency is chosen so that the FFT algorithm runs faster when the sampling rate is 2<sup>n</sup> multiple of the fundamental frequency. As a result, sampling is done synchronously and at a constant rate.

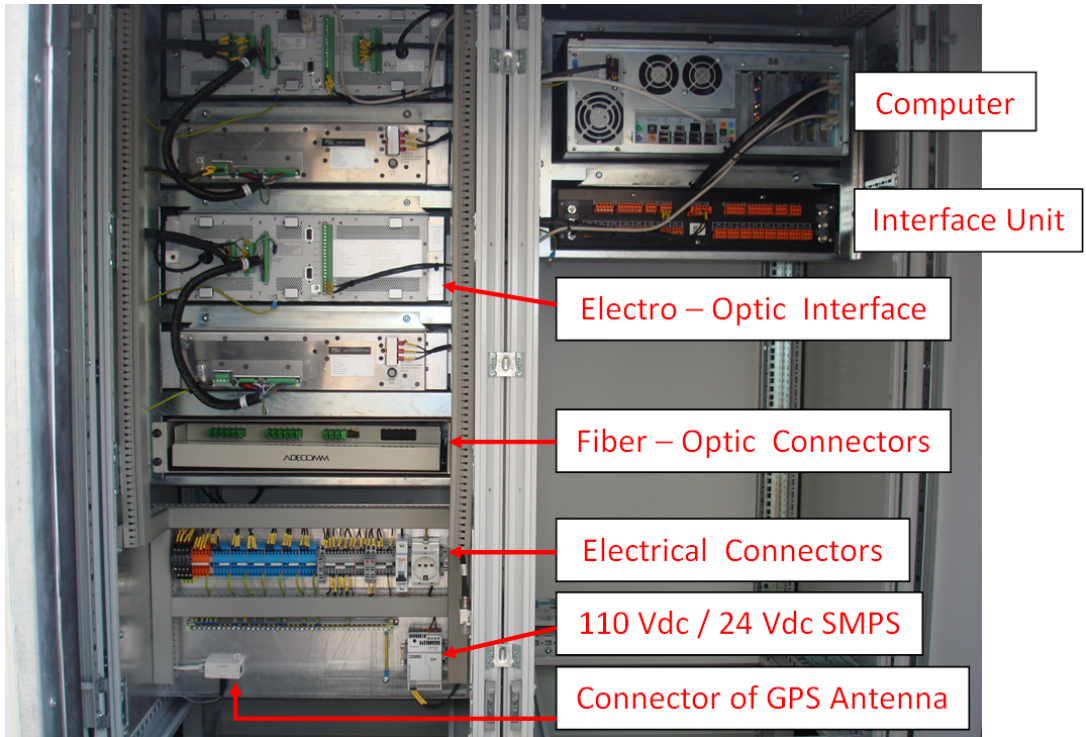


Figure 3.11: Cabinets in the trailer

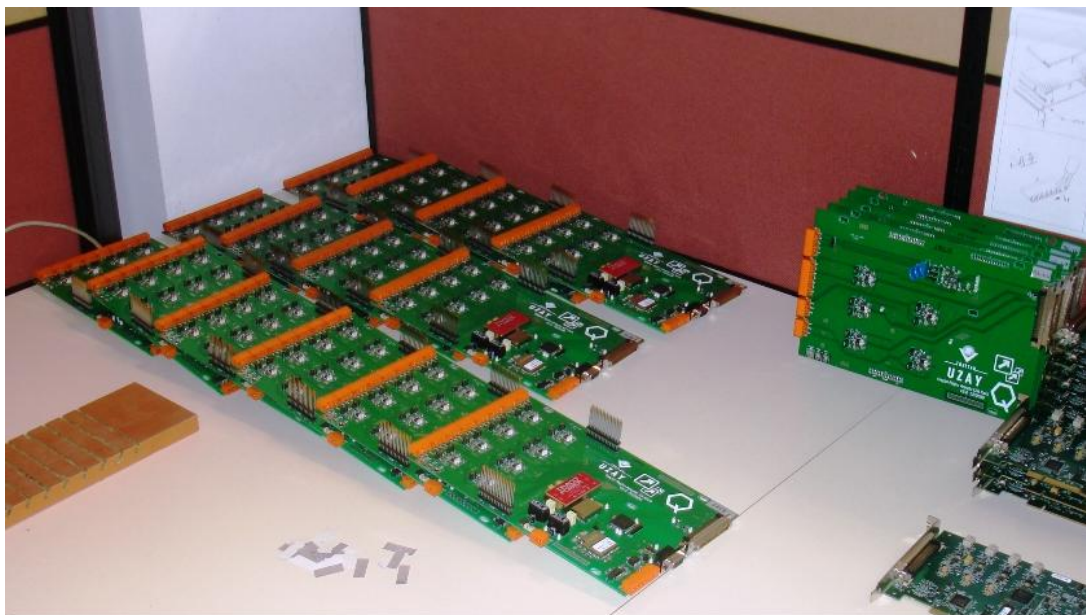


Figure 3.12: Interface PCBs



Figure 3.13: GPS and Wireless Antennas

Data acquisition card (DAQ card) is mounted in the computer chassis. It is a product of National Instruments [31], named PCI-6123 and is shown in Figure 3.14. The DAQ card can sample its 8 differential analog inputs simultaneously at a maximum sampling rate of 500 kS/sec/ch. Two DAQ cards are used per a measurement system, because 15 channels are needed.

The computer in the trailer runs the software of the measurement and samples data via data acquisition cards mounted on its PCI busses. It also stores the raw data and processed data in its hard disc. No monitor, keyboard and mouse is available in the trailer because the computer is controlled via remote desktop property, generally. But, of course, these human interface equipments are connected sometimes, instead of remote desktop property. The computer is connected to the local area network via the wireless antenna shown in Figure 3.13. All trailers have the mentioned wireless antenna so a measurement system can be controlled from another measurement system by remote desktop property. A wireless antenna is also connected to an ADSL



Figure 3.14: DAQ Card

modem in the control room, so the measurement system can be controlled by using internet also. As mentioned before, the electronic system is supplied by  $110 V_{dc}$ , so the power supply of the computer is a special ATX type which is supplied by  $110 V_{dc}$ .

### 3.3 Measurement Software

A high level software is developed during this thesis based on C and LabWindows/CVI [31]. The main source code is in C language and embedded in LabWindows/CVI which is used for graphical display and object-oriented human interface. The fundamental property of the software is that it takes all calibration coefficients of RCVT, NXVCT, NXCT and interface pcb into account and processes the measured raw data according to these coefficients, so there shall remain no error related to them. Also, the information of which transducer and which phase is connected to which channel is another input to the software and the software uses this input while processing data according to the coefficients and naming data while saving. The inputs must be entered properly before starting the measurement. The settings screen is shown in Figure 3.15 and display screen is shown in Figure 3.16.

**Geçici Rejim Ayar Ekranı**

**Genel Ayarlar**

Ham veri yazılın  Frekans hesapla  Harmonikler hesapla  
 RMS hesapla  Güç hesapla  İnterharmonikler hesapla  
 Olaylar kaydedilsin  Transient'lar kaydedilsin  Çözünürlük (Hz) 5  
 Karpışma hesapla  Dengesizlik hesapla  Optik ayar yapılı

Buffer Size: 1843200.00 Nsamples: 307200.00 1. Kart Kanal Listesi: Dev1/ai0:5  
Sampling Rate: 102400.00 External Clock: /Dev1/PP17 2. Kart Kanal Listesi: Dev2/ai7:7  
Bağlantı Türü: Düz (3 Faz) Ham Veri Yazma Sıklığı (sn): 9 Referans Seçimi: Ia0\_m

DAQ Kart: Dev1 a0 Ia0\_p a1 Ic0\_p a2 Ib0\_p a3 Ia0\_m a4 Ic0\_m a5 Ib0\_m a6 a7

**Öfset ve Min-Max Ayarları**

a0 ofset: 1.20 a1 ofset: -1.00 a2 ofset: 1.90 a3 ofset: 1.20 a4 ofset: -1.10 a5 ofset: -0.40 a6 ofset: 0.20 a7 ofset: 0.30  
a0 min: -2.50 a1 min: -2.50 a2 min: -2.50 a3 min: -2.50 a4 min: -2.50 a5 min: -2.50 a6 min: -10.00 a7 min: -10.00  
a0 max: 2.50 a1 max: 2.50 a2 max: 2.50 a3 max: 2.50 a4 max: 2.50 a5 max: 2.50 a6 max: 10.00 a7 max: 10.00

**Çarpın Genelik Kanal No. ai0** Kopyalama Kısavolu: Genlik Türü Ölçüm Trafosu Değerleri Frekans Aralığı: 550 2500 Kopyalanacak Değer: -32.0000 Kopyala

**Ölçüm Sistemi Değerleri**

50 Hz	2.5015	100	2.5015	150	2.5015	200	2.5015	250	2.5015	300	2.5015	350	2.5015	400	2.5015	450	2.5015	500	2.5015
550 Hz	2.5015	600	2.5015	650	2.5015	700	2.5015	750	2.5015	800	2.5015	850	2.5015	900	2.5015	950	2.5015	1000	2.5015
1050 Hz	2.5016	1100	2.5025	1150	2.5025	1200	2.5025	1250	2.5025	1300	2.5025	1350	2.5025	1400	2.5025	1450	2.5025	1500	2.5025
1550 Hz	2.5025	1600	2.5025	1650	2.5025	1700	2.5025	1750	2.5025	1800	2.5025	1850	2.5025	1900	2.5025	1950	2.5025	2000	2.5025
2050 Hz	2.5025	2100	2.5025	2150	2.5025	2200	2.5025	2250	2.5025	2300	2.5025	2350	2.5025	2400	2.5025	2450	2.5025	2500	2.5032

**Ölçüm Trafosu Değerleri**

50 Hz	10001.00	100	9989.250	150	9976.110	200	9926.030	250	9899.559	300	9895.000	350	9893.719	400	9860.000	450	9860.000	500	9860.000
550 Hz	9829.469	600	9815.000	650	9815.000	700	9815.000	750	9803.160	800	10100.00	850	10100.00	900	10100.00	950	10100.00	1000	10391.91
1050 Hz	10200.00	1100	10200.00	1150	10200.00	1200	10200.00	1250	10200.00	1300	10200.00	1350	10200.00	1400	10200.00	1450	10200.00	1500	10018.50
1550 Hz	9970.000	1600	9970.000	1650	9970.000	1700	9970.000	1750	9970.000	1800	9970.000	1850	9970.000	1900	9970.000	1950	9970.000	2000	9929.620
2050 Hz	9880.000	2100	9880.000	2150	9880.000	2200	9880.000	2250	9880.000	2300	9880.000	2350	9880.000	2400	9880.000	2450	9880.000	2500	9831.410

**Genilim Transient Ayarları**

Karşılaştırma Sınır: 1.50 Örnek Sayısı: 3  
 Eğim Sınır: 3.00 Örnek Sayısı: 3

**Akım Transient Ayarları**

Karşılaştırma Sınır: 1.50 Örnek Sayısı: 3  
 Eğim Sınır: 3.00 Örnek Sayısı: 3

**Genilim Olay Ayarları**

Tepe Hist: 0.02 Sınır1: 1.10 Sınır2: 1.10  
Çukur Hist: 0.02 Sınır1: 0.90 Sınır2: 0.90  
Kesinti Hist: 0.02 Sınır1: 0.10 Sınır2: 0.10  
Nom (kV) 0: 230.00 K: 230.00 R: 230.00

**Akım Olay Ayarları**

Tepe Hist: 0.02 Sınır1: 1.50 Sınır2: 1.50  
Çukur Hist: 0.02 Sınır1: 0.50 Sınır2: 0.50  
Kesinti Hist: 0.02 Sınır1: 0.10 Sınır2: 0.10  
Nom (A) 0m: 200.00 Op: 200.00 K: 200.00

**Güç Bileşenleri Seçimi**

Akım: Konvansiyonel A. Akım: Optik-m A. Genilim: Optik G.  
Genilim: Konvansiyonel A. Genilim: Konvansiyonel A.

ÖLÇÜM VERİLERİNİ SİL ÖLÇÜMÜ BAŞLAT GÖRÜNTÜLEMİYİ BAŞLAT KAYDET

Figure 3.15: Setting Screen of the Software

The purpose of the software is not only the steady-state measurements for conventional instrument transformer calibration. As mentioned before, switching transient measurements are taken throughout this work. So, the software can detect and save events occurred during the measurement if wanted according to IEC 61000-4-30 standard. Also, frequency, RMS values of measured channels are calculated for 10 cycles and stored in the hard disc. Another output of the software is power, which is calculated for every second and stored as active, reactive and apparent power, in addition to power factor. Flicker is calculated and stored by the software according to IEC 61000-4-15 standard for 10 minutes. Finally, the software calculates and stores unbalance percentage according to IEC 61000-4-30 for 3 phases of the same type of transducer for 3 seconds. As a result, the developed software is capable of calculating all power quality components, but this thesis is not interested in these parameters.

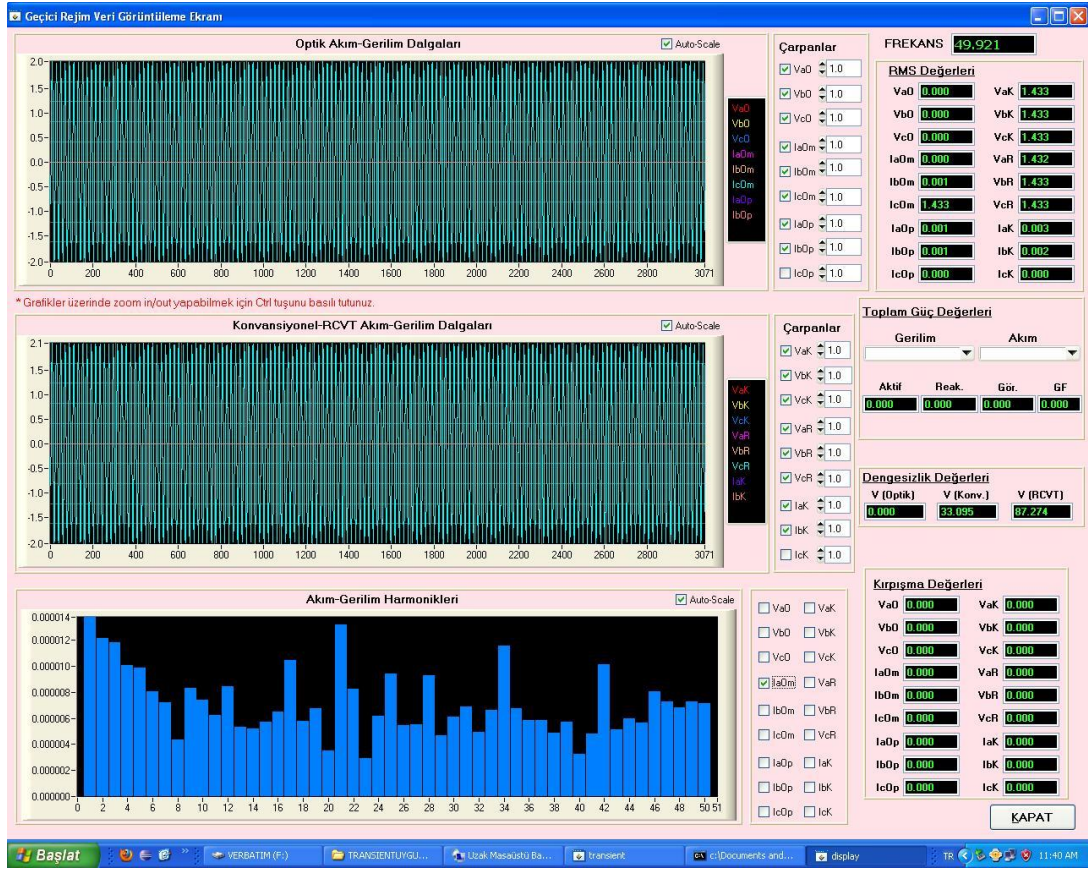


Figure 3.16: Display Screen of the Software

The key property of the software for the thesis is the FFT engine, which takes the FFT of the input and store the output data. Also, the graphic at the bottom of Figure 3.16 is an example of display of harmonics. The software takes the FFT in three different methods; line harmonic, group harmonic and subgroup harmonic, which are defined in IEC 61000-4-7 [5] as follows:

**Group Harmonic:** In this method, to calculate the RMS value of an harmonic component, half of the components between the adjacent harmonics are taken into consideration. But, only intermediate components above the second order harmonic shall be used [5]. For example; to calculate the RMS value of third harmonic component at a 50 Hz system, the components between 125 - 175 Hz are taken into calculation. The RMS value is calculated according to Equation 3.1 [5]. And illustration of harmonic and interharmonic groups are shown in Figure 3.17 for a 50 Hz supply.

$$Y_{g,h}^2 = \frac{1}{2} \cdot Y_{C,(N \times h) - N/2}^2 + \sum_{k=(-N/2)+1}^{(N/2)-1} Y_{C,(N \times h)+k}^2 + \frac{1}{2} \cdot Y_{C,(N \times h)+N/2}^2 \quad (3.1)$$

Where;

Y is the variable replaceable by I, U;

$Y_{g,h}$  is the rms value of the harmonic group;

$Y_{C,k}$  is the rms value of the spectral component of order k;

h is the running integer number for harmonic orders;

k is the running integer number for spectral components;

N is the number of power supply periods within the window width.

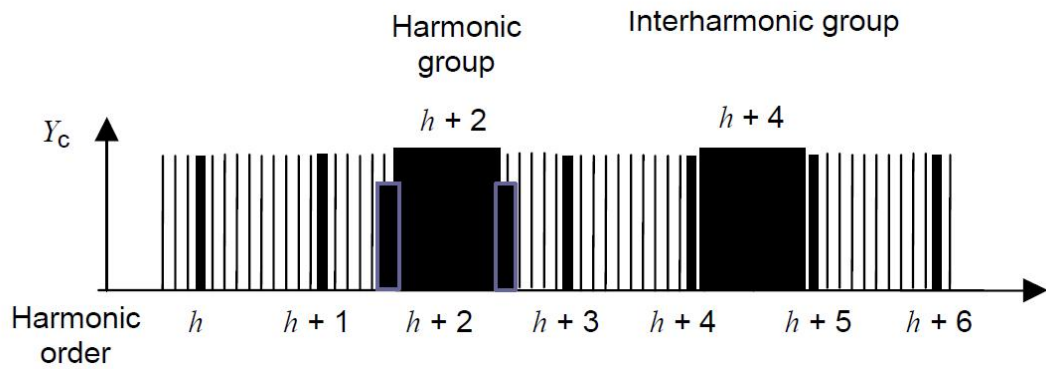


Figure 3.17: Illustration of harmonic and interharmonic groups for a 50 Hz supply [5]

**Subgroup Harmonic:** At this method, to calculate the RMS value of an harmonic component, two adjacent components are taken into account according to Equation 3.2 [5]. This method considers the transfer of harmonic component energy to adjacent spectral components due to fluctuation of voltage. The illustration of harmonic and interharmonic subgroups are shown in Figure 3.18 for a 50 Hz supply.

$$Y_{sg,h}^2 = \sum_{k=-1}^1 Y_{C,(N \times h)+k}^2 \quad (3.2)$$

Where;

$Y_{sg,h}^2$  is the rms value of the harmonic subgroup.

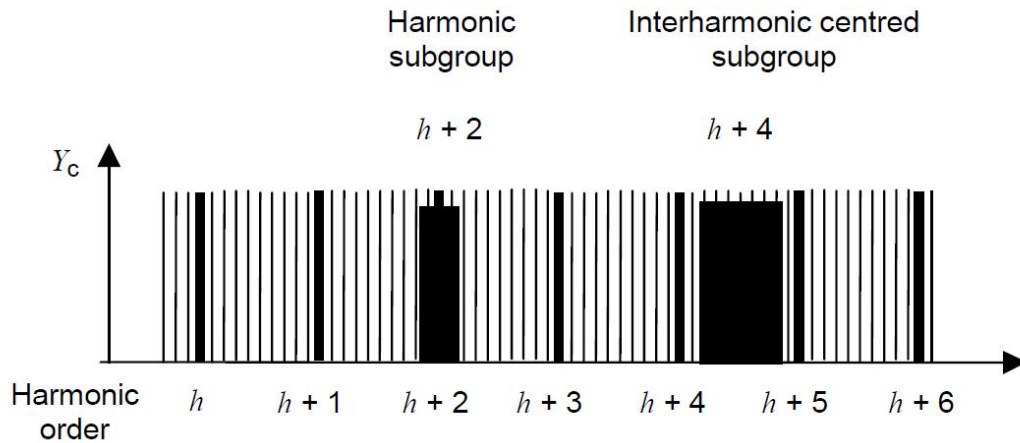


Figure 3.18: Illustration of harmonic and interharmonic subgroups for a 50 Hz supply [5]

**Line Harmonic:** This is the conventional method which considers only the spectral component which is at the considered harmonic frequency. It should be noted that, there is no phase output of group and subgroup harmonic methods, which is an important difference of line harmonic method. Throughout the thesis, Line Harmonic method is used to compare and calibrate conventional instrument transformers against phase shift errors in addition to amplitude errors. The FFT is calculated over 10 cycles, which corresponds to a resolution of 5 Hz for fundamental frequency of 50 Hz; as is the case in the IEC 61000-4-7 [5].

## CHAPTER 4

### SIMULATION MODEL OF A CVT

Throughout this chapter, a capacitive voltage transformer (CVT) will be modeled and simulated. The frequency response and effects of its components, which are defined in Figure 2.2, will be shown. Effect of ferroresonance will not be shown in this model, because line impedance, burdens connected to the line and other parameters like switching instants are not available. The modeled transformer parameters belong to a capacitive voltage transformer, named KGT-170, which is manufactured by EMEK Electrical Industry Inc. [32], in Turkey. Also, measurement results of the same capacitive voltage transformer are available in Chapter 5.

#### 4.1 General Model of the CVT

Throughout this section, general model and frequency response of CVT will be presented. The model is simulated in PSCAD and the schematic of the simulation is shown in Figure 4.1.

Investigating Figure 4.1; the line voltage is equal to  $154/\sqrt{3} = 88.91 \text{ kV}$ . The coupling capacitor is 5062 pF at the HV side and 40500 pF at the MV side, yielding a division ratio of 9. That means  $V_{div}$  will be 9879 V. The compensating reactor,  $L_c$ , is used for compensating the phase shift of the coupling capacitors at 50 Hz, as explained in Subsection 2.2.1 in detail. The step down transformer has a turns ratio of 171, resulting an output voltage of 57.7 V. So, the overall division ratio of the CVT is;  $171 \times 9 = 1539$  and for comparing waveforms,  $V_{sec}$  is multiplied by this coefficient throughout the chapter. Finally, the CVT includes an active ferroresonance circuit,

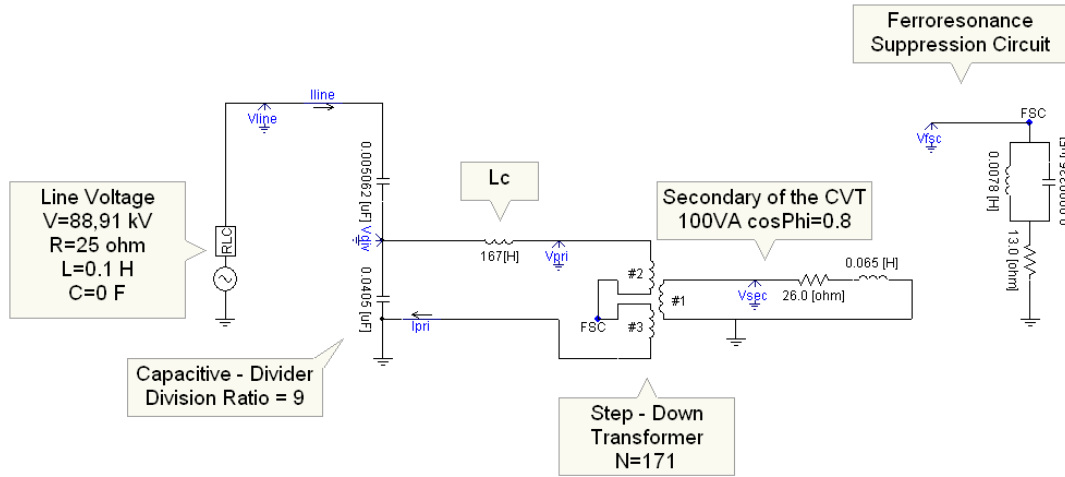


Figure 4.1: Schematic of the CVT used for the simulation

connected to the primary winding of the step down transformer. The third winding shown in Figure 4.1, has a potential of 100 V and so does the ferroresonance circuit. So, the second winding has the rest; 9779 V. Also, the CVT is a class 0.5 instrument transformer.

The simulation is run for 50, 150, 250, 350, 550 and 1000 Hz. It is seen from Table 4.1 that phase error is decreasing and amplitude error is increasing, as the frequency increases. The results are as expected;  $L_c$  and FSC are the main reasons of error. Because  $L_c$  is tuned to 50 Hz, it causes phase shift and induces voltage at other frequencies. And the FSC behaves like a bandpass filter with center frequency of 50 Hz, so attenuating the harmonics.

Table 4.1: Frequency Response of the CVT

Frequency (Hz)	Percentage Amplitude Error (%)	Phase Error (Degree)
50	0.4	0.01
150	50.1	21.6
250	59.3	18.0
350	62.2	12.6
550	64.1	9.8
1000	65.1	6.3

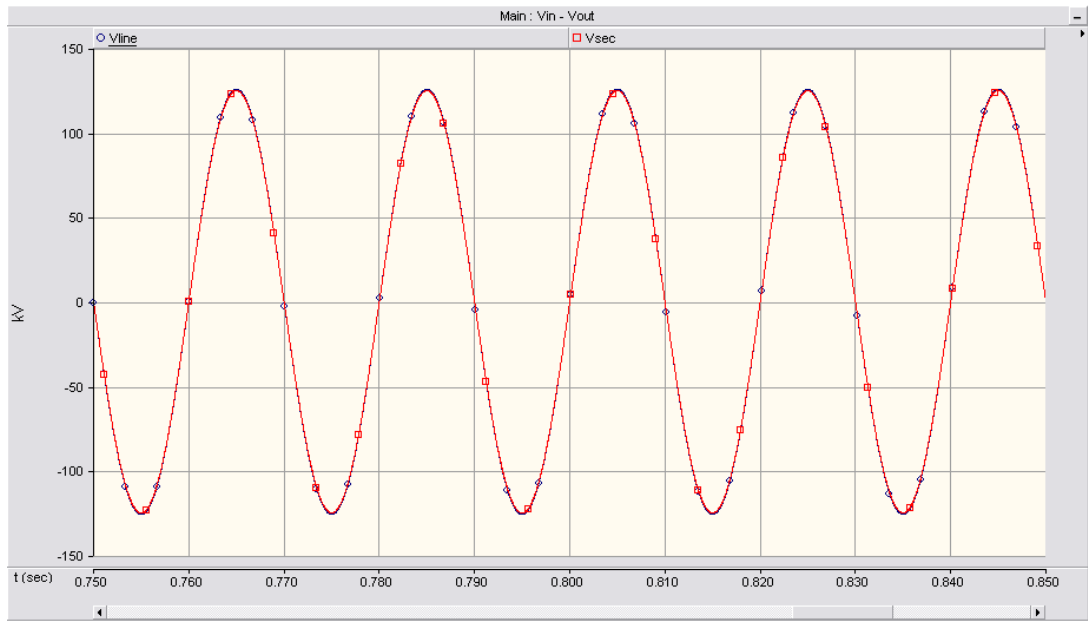


Figure 4.2: Response of CVT to 50 Hz input

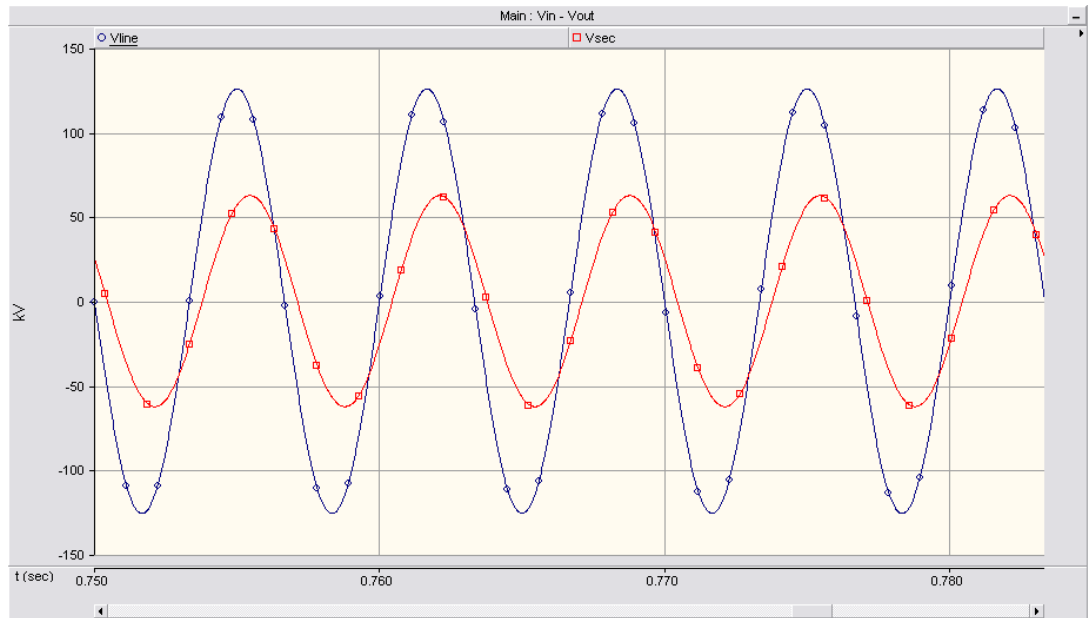


Figure 4.3: Response of CVT to 150 Hz input

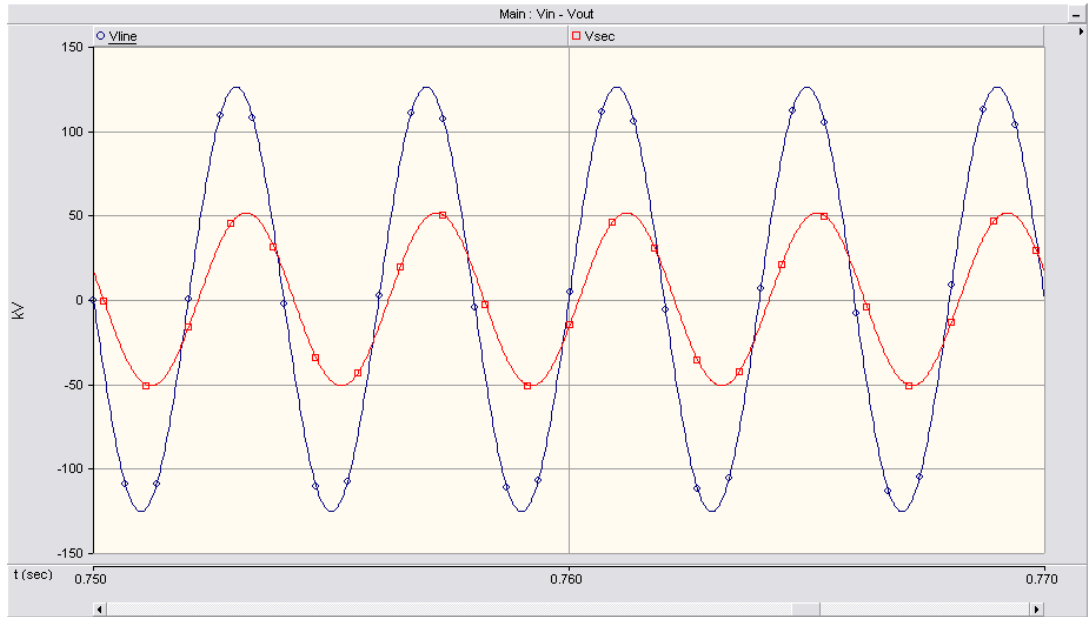


Figure 4.4: Response of CVT to 250 Hz input

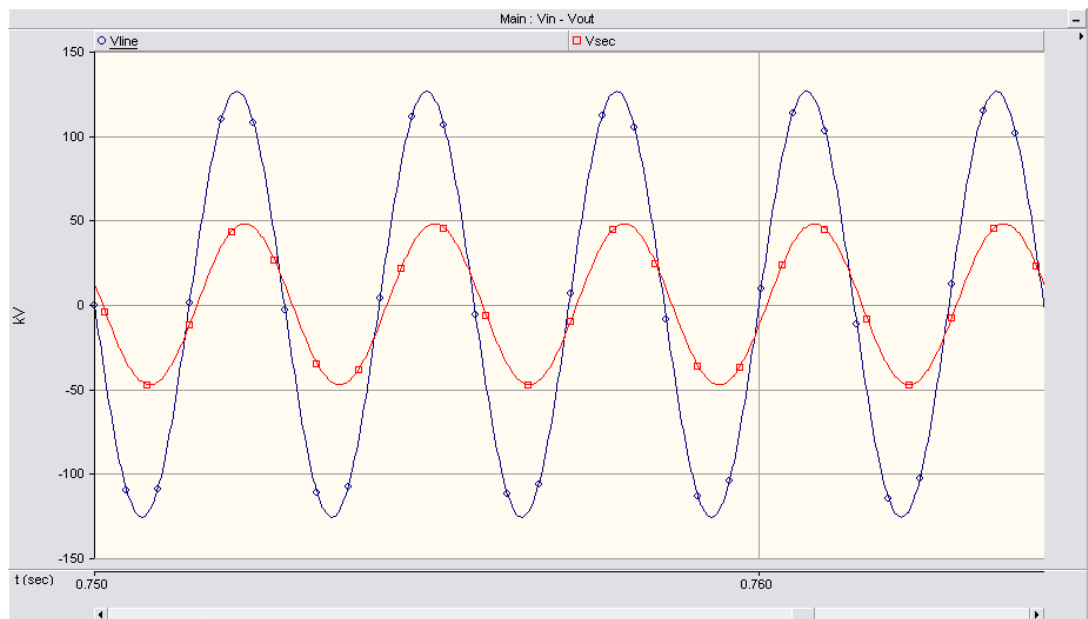


Figure 4.5: Response of CVT to 350 Hz input

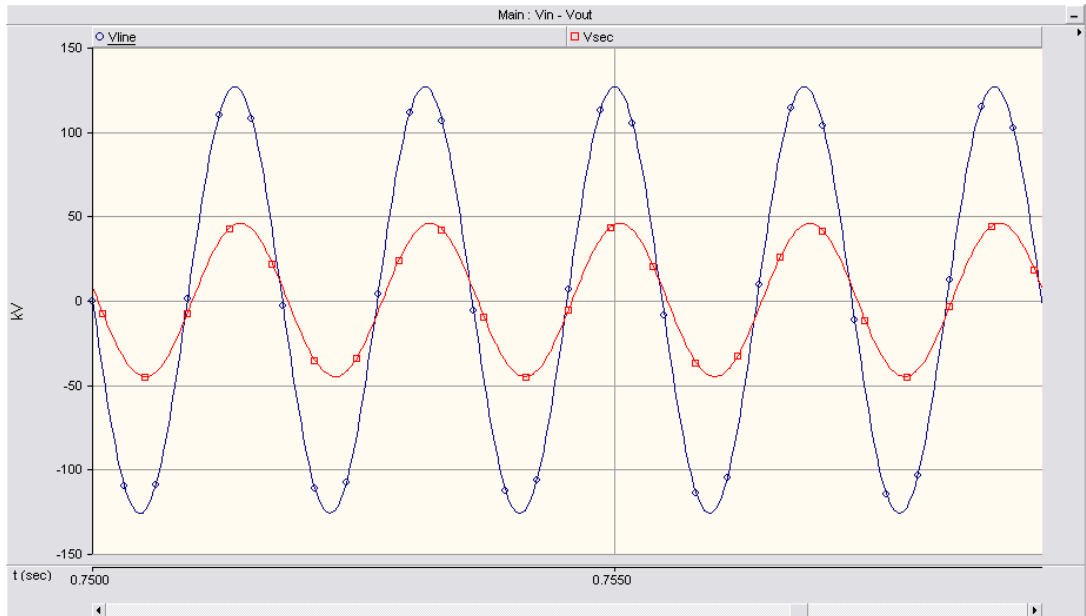


Figure 4.6: Response of CVT to 550 Hz input

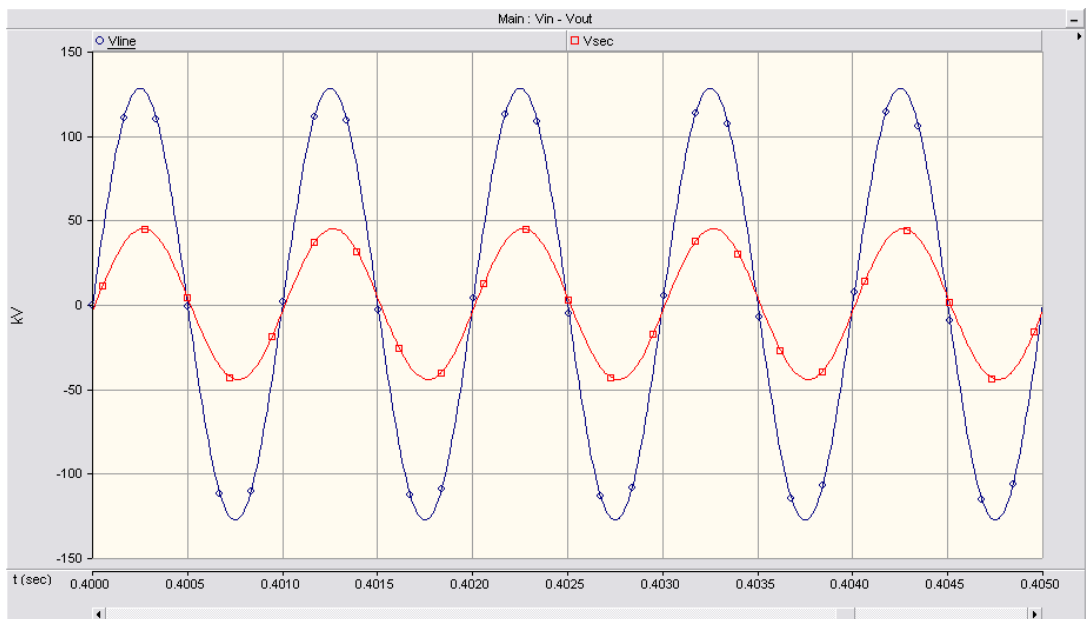


Figure 4.7: Response of CVT to 1 kHz input

## 4.2 Effect of $L_c$

As mentioned before,  $L_c$  is the compensating inductance due to the phase shift error of the coupling capacitors. In this section,  $L_c$  is extracted (i.e.; short-circuited) from the circuit and response of the CVT to 50 Hz is investigated. Extracting  $L_c$  results 27° phase shift leading; in addition to a percentage amplitude error of 4.6%, as shown in Figure 4.8. Also, by investigating the effects on harmonics, it is seen that existence of  $L_c$  affects harmonic measurement in a bad way as seen from the Table 4.2 and by comparing it with Table 4.1.

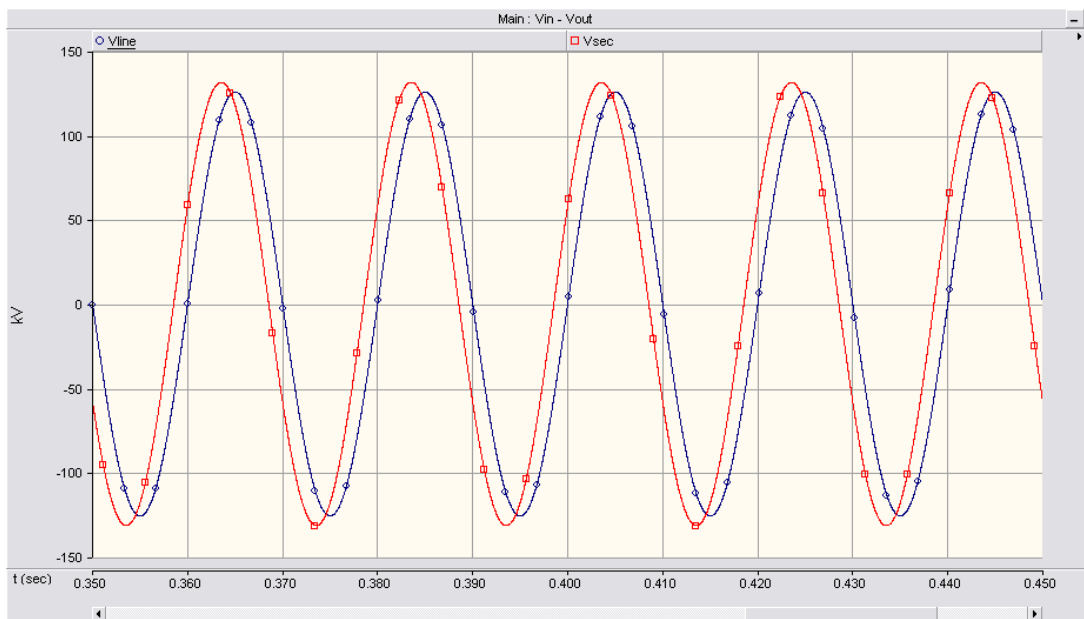


Figure 4.8: Response of CVT to 50 Hz input without  $L_c$

Table 4.2: Frequency Response of the CVT without  $L_c$

Frequency (Hz)	Percentage Amplitude Error (%)	Phase Error (Degree)
50	4.6	27
150	12.0	5.4
250	22.8	9.0
350	26.7	6.0
550	29.5	4.2
1000	30.9	2.6

### 4.3 Effect of Ferroresonance Suppression Circuit

In this section, the ferroresonance suppression circuit is extracted from the circuit and the frequency response of the CVT is investigated and the results are given in Table 4.3. It is seen that, existence of ferroresonance suppression circuit affects the harmonic measurement in a bad way, as expected. Another point is that performance of the CVT at fundamental frequency becomes worse because, the tuning frequency is changed.

Table 4.3: Frequency Response of the CVT without FSC

Frequency (Hz)	Percentage Amplitude Error (%)	Phase Error (Degree)
50	0.9	0.6
150	10.1	2.3
250	11.5	1.8
350	12.0	1.2
550	12.3	0.8
1000	12.5	0.1

In conclusion, the results of the simulation are consistent with the theory explained in Subsection 2.2.1 and it is seen that capacitive voltage transformer is not suitable for harmonic measurement. The compensating inductor  $L_c$  is needed for the fundamental frequency performance of the CVT but it decreases the performance of CVT for harmonic measurements. Another parameter, ferroresonance suppression circuit is needed to protect the CVT and the equipment connected to its secondary, like relays and meters. But when used, the capability of harmonic measurement decreases.

## CHAPTER 5

### FIELD TEST RESULTS

Field measurements are performed at 34.5, 154 and 380 kV voltage levels for both current and voltage measurements. Inductive voltage transformer is calibrated at 34.5 kV and capacitive voltage transformer is calibrated at 154 kV and 380 kV voltage levels. Also, NXVCT and RCVT voltage measurements are compared at 380 kV voltage level. Throughout this chapter, results of field measurements will be presented.

#### 5.1 RCVT versus NXVCT

Outputs of RCVT and NXVCT are compared to see the accuracy of the transducers at 380 kV by simultaneous measurements. Also, the accuracies of current measurement of NXVCT and NXCT are tested at laboratory by comparing output of NXCT with the calibration equipment and they are reliable.

Table 5.1: Comparison of NXVCT and RCVT at 380 kV

Frequency (Hz)	$V_{NXVCT}/V_{RCVT}$
50	1.0017
150	0.9137
250	1.0099
350	0.9962

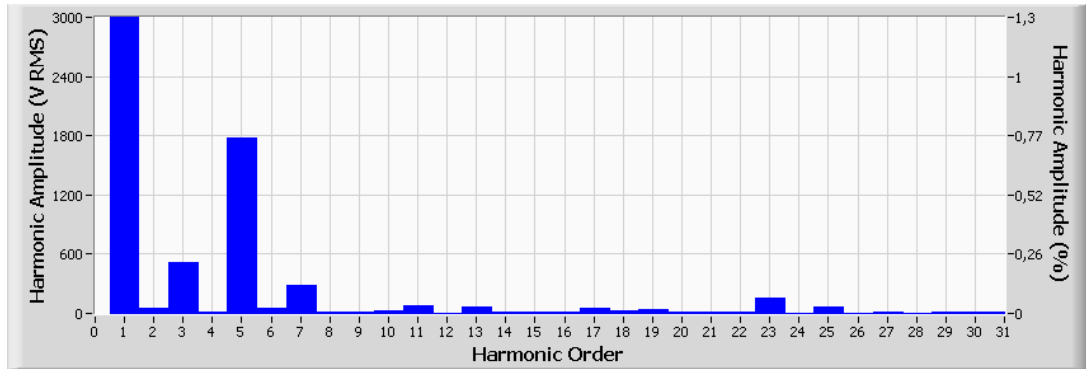


Figure 5.1: An output of NXVCT at 380 kV

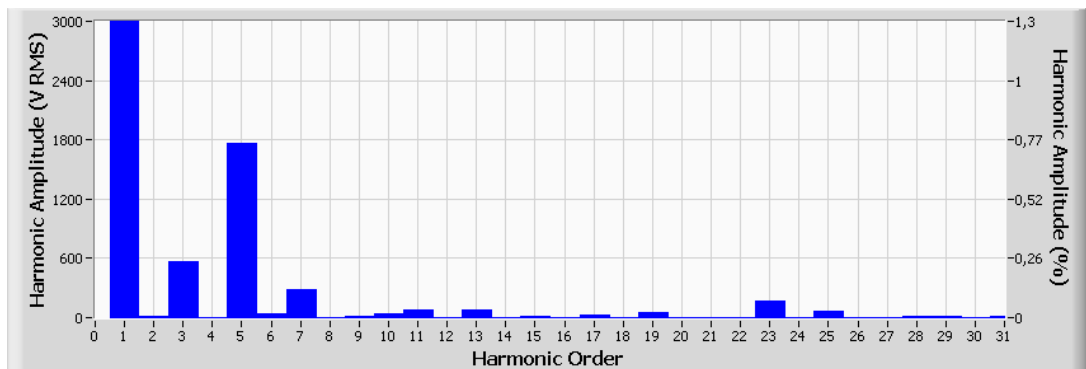


Figure 5.2: An output of RCVT at 380 kV

## 5.2 Voltage Measurements

### 5.2.1 Voltage Measurements at 34.5 kV

The conventional voltage transformer is; Bortrans GTR2-30 (IVT), 150VA, IEC 0.5,  $\frac{33}{\sqrt{3}}/\frac{0.1}{\sqrt{3}}$ . And the used transducer is 36 kV RCVT. The photo of the measurement system is shown in Figure 5.3 and two measurement data are shown in Figure 5.4 to 5.8; where Figure 5.4 and 5.5 are simultaneous measurements as Figure 5.7 and 5.8. Also, sample data of fundamental component and harmonic components are given in Table 5.2 through Table 5.6. Minus sign at phase differences means lagging.



Figure 5.3: Trailers used in measurements at 34.5 kV

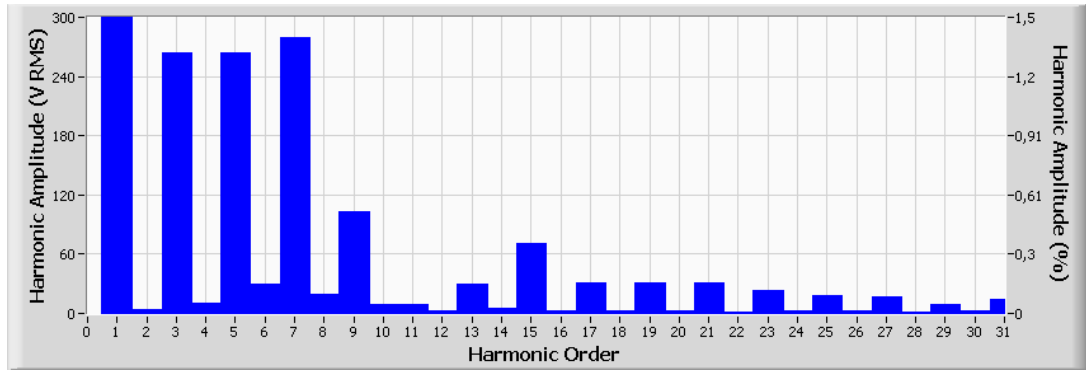


Figure 5.4: A sample data of conventional transformer at 34.5 kV

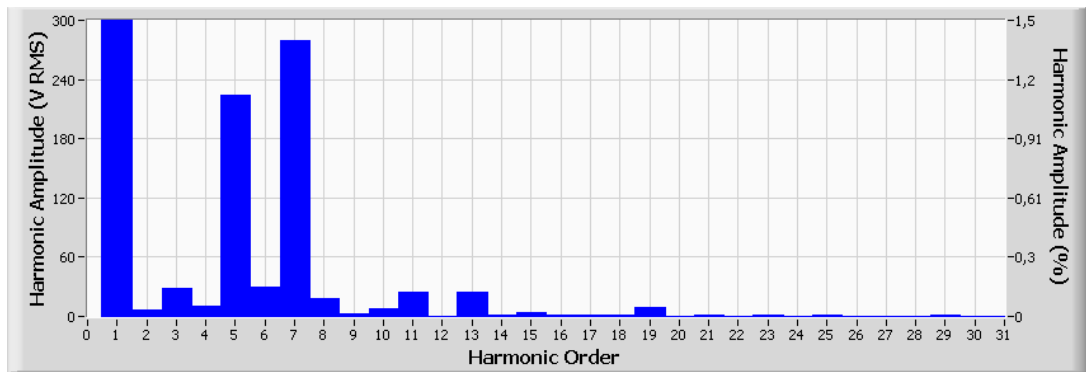


Figure 5.5: A sample data of RCVT at 34.5 kV

By investigating two bar plots above, it is seen that conventional voltage transformer measures the triplen harmonics much higher than the real value and amplifying the 5<sup>th</sup> harmonic about 1.2 times while measuring the 7<sup>th</sup> harmonic almost the same with the RCVT. The problem at triplen harmonics is not due to conventional transformer directly, rather related to the grounding scheme in the substation. The secondary line terminal of the conventional transformer is connected to the control room and it is connected to the trailer of electronic system through the control room. The other terminal of the conventional transformer, which is ground, is connected to ground cable of the substation which loops all substation. In the control room, the output of conventional transformer is measured according to the looped ground cable instead of direct connection to the conventional transformer secondary terminal. Also, a ground cable from the control room is supplied to the trailer of the electronic system for con-

ventional voltage transformer measurements by the personnel of TEIAS [28]. The simplified connection scheme is shown in Figure 5.6. So, due to unbalanced loads, a zero - sequence triplen harmonic current flows from the neutral point to the ground, which induces a voltage on the ground cable due to the impedance of the cable. The induced voltage is at triplen harmonic frequencies which is added to the output of the conventional voltage transformer, like an offset voltage, which depends on the cable impedance and so the cable length, in addition to the value of zero-sequence current. The effect of the offset like voltage can be seen when  $3^{rd}$  harmonic is present in the system as shown in Figure 5.7 and 5.8. To see the effect of cable length, the ground cable of the trailer is connected to the measurement system instead of the one coming from the control room which results a shorter ground cable and the amount of measured  $3^{rd}$  harmonic is decreased by 2.1 as shown in Figure 5.9 and 5.10. Changing the ground cable affects only the triplen harmonics components [11].

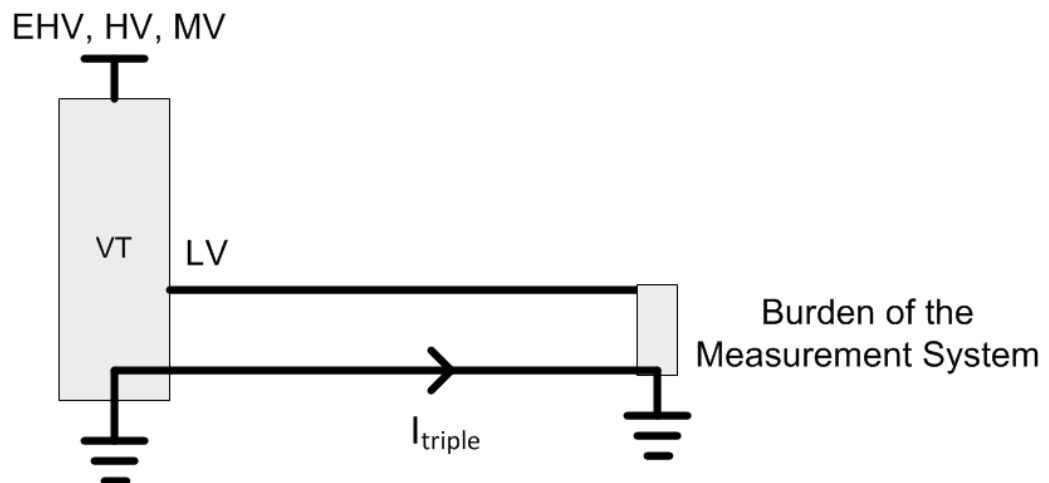


Figure 5.6: Simplified connection diagram of conventional voltage transformers.

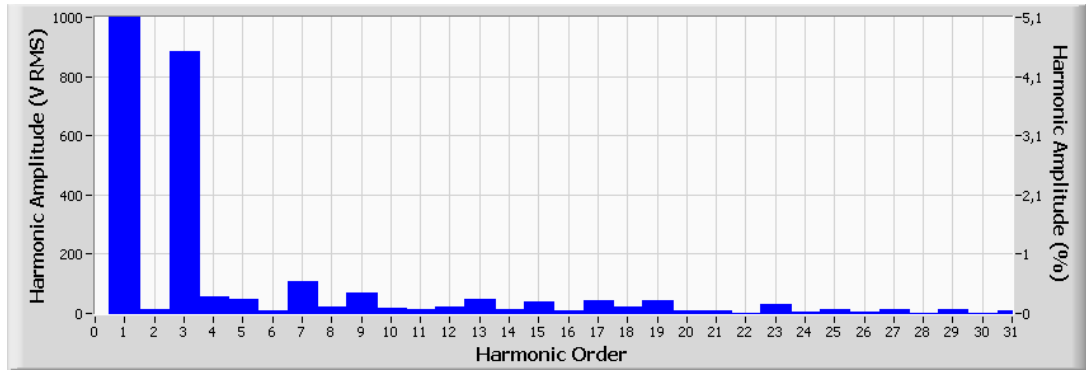


Figure 5.7: A sample data of conventional transformer at 34.5 kV

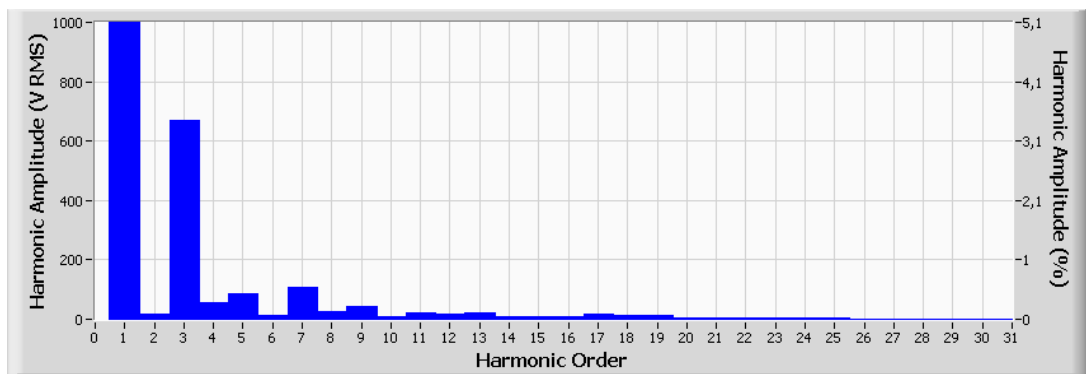


Figure 5.8: A sample data of RCVT at 34.5 kV

Table 5.2: Sample data of RCVT and IVT against fundamental component at 34.5 kV

Sample	$V_{RCVT}$ (V)	$V_{IVT}$ (V)	$V_{IVT}/V_{RCVT}$	$\phi_{IVT} - \phi_{RCVT}$ (Degree)
1	19765.7	19794.3	1.0015	-0.40
2	19771.4	19799.8	1.0014	-0.40
3	19463.1	19483.2	1.0010	-0.48

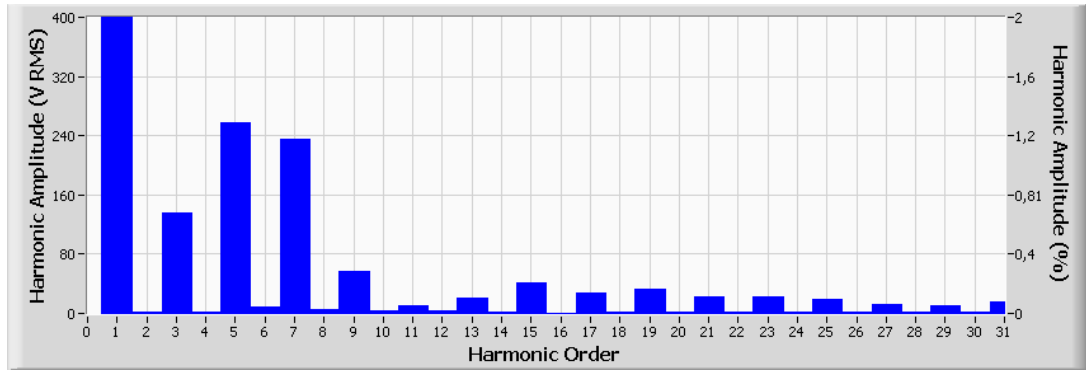


Figure 5.9: A sample data of conventional transformer at 34.5 kV when ground is connected to the trailer

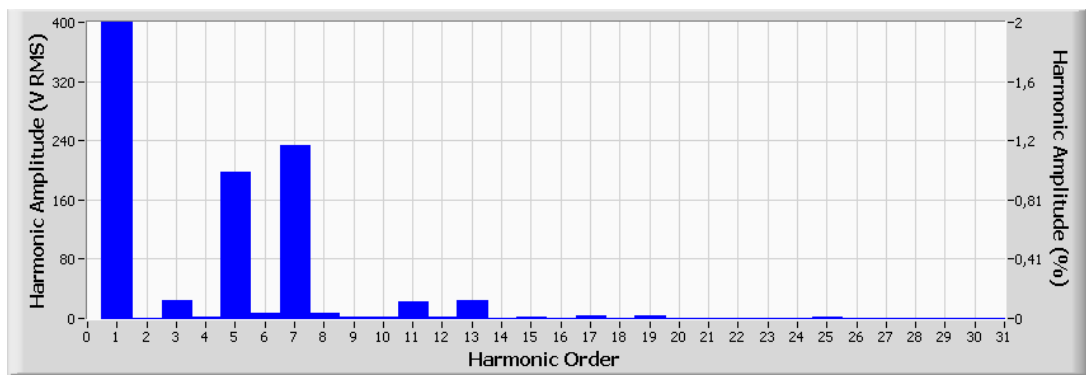


Figure 5.10: A sample data of RCVT at 34.5 kV when ground is connected to the trailer

Table 5.3: Sample data of RCVT and IVT against 3<sup>rd</sup> harmonic at 34.5 kV when ground cable is connected to the control room

Sample	$V_{h,RCVT}$ (V)	$V_{h,IVT}$ (V)	$V_{h,RCVT}$ (%)	$V_{h,IVT}$ (%)	$V_{IVT}/V_{RCVT}$	$\phi_{IVT} - \phi_{RCVT}$ (Degree)
1	28.984	265.340	0.1	1.3	9.1548	9.96
2	202.193	430.044	1.0	2.2	2.1269	4.76
3	670.957	886.172	3.4	4.5	1.3208	-0.49
4	700.065	915.234	3.5	4.6	1.3074	-0.38

Please also note that in Table 5.3;

$$265.340 - 28.984 = 236.356 \approx 227.851 = 430.044 - 202.193 \quad (5.1)$$

The offset like effect of triplen harmonic voltages is shown in Equation 5.1. The small difference may be due to measuring errors and/or change in the zero-sequence current.

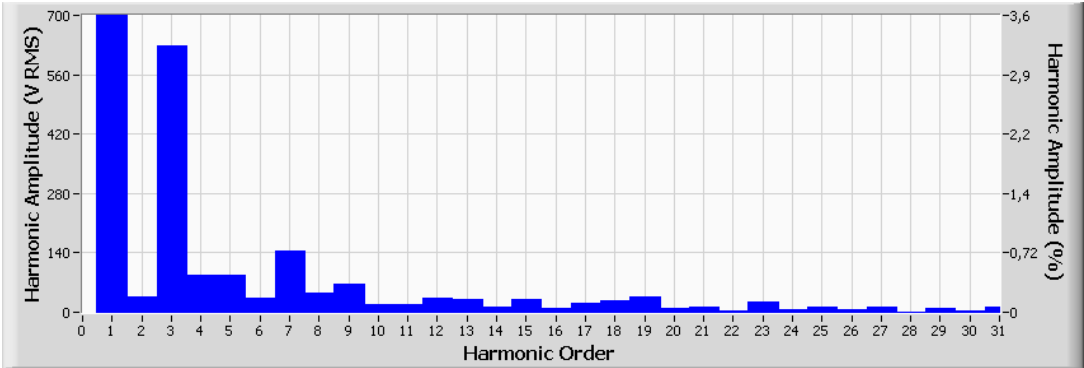


Figure 5.11: A sample data of conventional transformer at 34.5 kV when ground is connected to the trailer

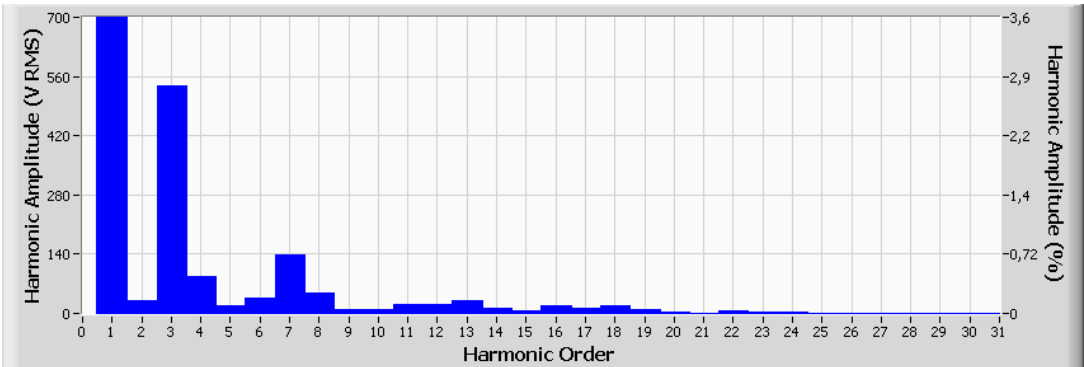


Figure 5.12: A sample data of RCVT at 34.5 kV when ground is connected to the trailer

Table 5.4: Sample data of RCVT and IVT against 3<sup>rd</sup> harmonic at 34.5 kV when ground cable is connected to the trailer of the electronic system

Sample	$V_{h,RCVT}$ (V)	$V_{h,IVT}$ (V)	$V_{h,RCVT}$ (%)	$V_{h,IVT}$ (%)	$V_{IVT}/V_{RCVT}$	$\phi_{IVT} - \phi_{RCVT}$ (Degree)
1	24.904	133.099	0.1	0.7	5.3445	24.01
2	537.769	627.997	2.7	3.2	1.1678	0.03
3	494.493	581.603	2.5	2.9	1.1762	1.79
4	705.976	794.213	3.6	4.0	1.1250	-0.80

As seen from Table 5.3 and 5.4, the offset voltage of 3<sup>rd</sup> harmonic due to zero-

sequence current is decreased to 108V from 236V.

Table 5.5: Sample data of RCVT and IVT against 5<sup>th</sup> harmonic at 34.5 kV

Sample	$V_{h,RCVT}$ (V)	$V_{h,IVT}$ (V)	$V_{h,RCVT}$ (%)	$V_{h,IVT}$ (%)	$V_{IVT}/V_{RCVT}$	$\phi_{IVT} - \phi_{RCVT}$ (Degree)
1	250.439	308.938	1.3	1.6	1.2336	7.53
2	226.119	265.752	1.1	1.3	1.1753	11.47
3	209.471	258.452	1.1	1.3	1.2338	12.91
4	130.267	163.846	0.6	0.8	1.2578	22.06

Table 5.6: Sample data of RCVT and IVT against 7<sup>th</sup> harmonic at 34.5 kV

Sample	$V_{h,RCVT}$ (V)	$V_{h,IVT}$ (V)	$V_{h,RCVT}$ (%)	$V_{h,IVT}$ (%)	$V_{IVT}/V_{RCVT}$	$\phi_{IVT} - \phi_{RCVT}$ (Degree)
1	277.406	276.151	1.4	1.4	0.9955	-9.10
2	287.734	287.882	1.5	1.5	1.0005	-8.94
3	105.346	109.221	0.5	0.6	1.0368	-12.32
4	322.876	323.204	1.6	1.6	1.0010	-9.09

## 5.2.2 Voltage Measurements at 154 kV

The conventional voltage transformer is; Emek KGT-170, 150VA, IEC 0.5,  $\frac{154}{\sqrt{3}}/\frac{0.1}{\sqrt{3}}$ ; which is the CVT modeled in Chapter 4. The used transducer is 170 kV NXVCT, which measures both voltage and current.

The measurement system is shown in Figure 5.13 and simultaneous data is shown in Figure 5.14 and 5.15. As seen from the figures, the triplen harmonics problem mentioned in Subsection 5.2.1 is present at this measurement, too. Sample data of fundamental component and harmonic components are given in Table 5.7 through Table 5.10. By investigating the data, it is seen that the CVT amplifies 3<sup>rd</sup> harmonic significantly. This is not only due to zero-sequence currents but also due to ferroresonance caused by switching of the loads connected to the transmission line, third harmonic is generally injected by switchings which may lead to ferroresonance. 5<sup>th</sup> harmonic is attenuated by about 0.9 which was higher in the simulation and 7<sup>th</sup> harmonic is

attenuated by 0.47, which was lower in simulation (refer to Table 4.1). The difference is due to the effect of ferroresonance and external parameters, like line impedance, and also difference between the model and real CVT parameters due to aging, which all affect the accuracy of the CVT.



Figure 5.13: Trailers used in measurements at 154 kV

Table 5.7: Sample data of NXVCT and CVT against fundamental component at 154 kV

Sample	$V_{NXVCT}$ (V)	$V_{CVT}$ (V)	$V_{CVT}/V_{NXVCT}$	$\phi_{CVT} - \phi_{NXVCT}$ (Degree)
1	91146.5	91640.2	1.0054	-0.02
2	91170.5	91664.9	1.0054	-0.02
3	91231.8	91728.4	1.0054	-0.02

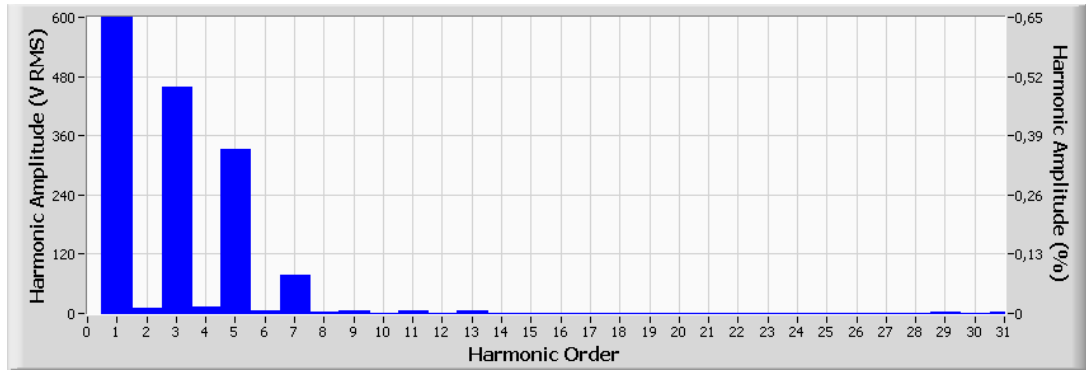


Figure 5.14: A sample data of conventional transformer at 154 kV

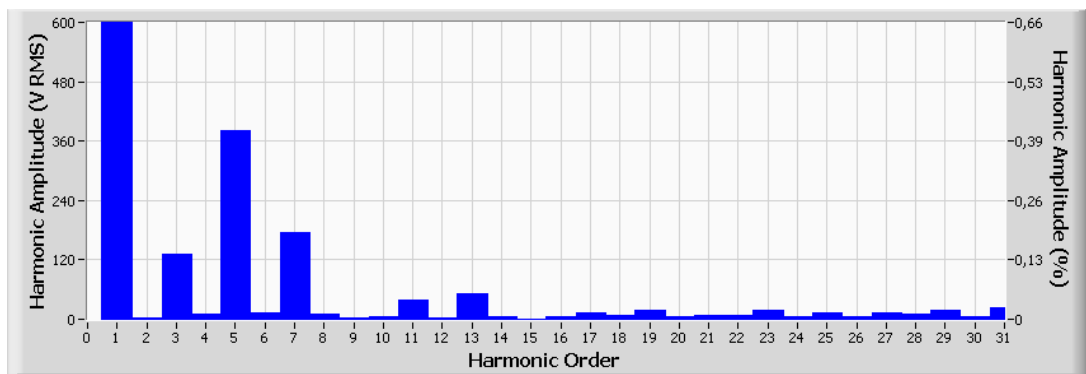


Figure 5.15: A sample data of NXVCT at 154 kV

Table 5.8: Sample data of NXVCT and CVT against 3<sup>rd</sup> harmonic at 154 kV

Sample	$V_{h,NXVCT}$ (V)	$V_{h,CVT}$ (V)	$V_{h,NXVCT}$ (%)	$V_{h,CVT}$ (%)	$V_{CVT}/V_{NXVCT}$	$\phi_{CVT} - \phi_{NXVCT}$ (Degree)
1	113.405	452.328	0.1	0.5	3.9886	18.01
2	151.772	505.374	0.2	0.6	3.3298	13.98
3	181.227	517.738	0.2	0.6	2.8569	5.75

Table 5.9: Sample data of NXVCT and CVT against 5<sup>th</sup> harmonic at 154 kV

Sample	$V_{h,NXVCT}$ (V)	$V_{h,CVT}$ (V)	$V_{h,NXVCT}$ (%)	$V_{h,CVT}$ (%)	$V_{CVT}/V_{NXVCT}$	$\phi_{CVT} - \phi_{NXVCT}$ (Degree)
1	379.860	331.991	0.4	0.4	0.8740	64.18
2	352.611	323.771	0.4	0.4	0.9182	119.20
3	332.619	301.684	0.4	0.3	0.9070	120.11

Table 5.10: Sample data of NXVCT and CVT against 7<sup>th</sup> harmonic at 154 kV

Sample	$V_{h,NXVCT}$ (V)	$V_{h,CVT}$ (V)	$V_{h,NXVCT}$ (%)	$V_{h,CVT}$ (%)	$V_{CVT}/V_{NXVCT}$	$\phi_{CVT} - \phi_{NXVCT}$ (Degree)
1	176.538	83.165	0.2	0.1	0.4711	65.28
2	164.139	77.259	0.2	0.1	0.4707	63.88
3	147.165	69.598	0.2	0.1	0.4729	60.00

### 5.2.3 Voltage Measurements at 380 kV

The conventional transformer is; Emek KGT-420, 150VA, IEC 0.5,  $\frac{380}{\sqrt{3}}/\frac{0.1}{\sqrt{3}}$ . The measurement system is shown in Figure 5.16 and simultaneous sample data are shown in Figure 5.17 and 5.18. The sample data of fundamental component and harmonic components are given in Table 5.11 through Table 5.14. By investigating the data, a significant amplification at 3<sup>rd</sup> harmonic is seen, due to zero-sequence currents and ferroresonance. Amplification at 5<sup>th</sup> and 7<sup>th</sup> harmonic components is present, too. As the percentage of 7<sup>th</sup> harmonic is very low, the measurement of CVT is not very reliable. But at 5<sup>th</sup> harmonic, it makes significant amplification and measure it as it is out of permissible limits, but in fact it is not.



Figure 5.16: Trailers used in measurements at 380 kV

Table 5.11: Sample data of NXVCT and CVT against fundamental component at 380 kV

Sample	$V_{NXVCT}$ (V)	$V_{CVT}$ (V)	$V_{CVT}/V_{NXVCT}$	$\phi_{CVT} - \phi_{NXVCT}$ (Degree)
1	234454	234090	0.9984	-0.17
2	234584	234223	0.9985	-0.17
3	234243	233877	0.9984	-0.18

Table 5.12: Sample data of NXVCT and CVT against 3<sup>rd</sup> harmonic at 380 kV

Sample	$V_{h,NXVCT}$ (V)	$V_{h,CVT}$ (V)	$V_{h,NXVCT}$ (%)	$V_{h,CVT}$ (%)	$V_{CVT}/V_{NXVCT}$	$\phi_{CVT} - \phi_{NXVCT}$ (Degree)
1	479.371	4220.980	0.2	1.8	8.8052	-82.87
2	518.923	4250.660	0.2	1.8	8.1913	-79.29
3	452.876	4117.830	0.2	1.8	9.0926	-98.70

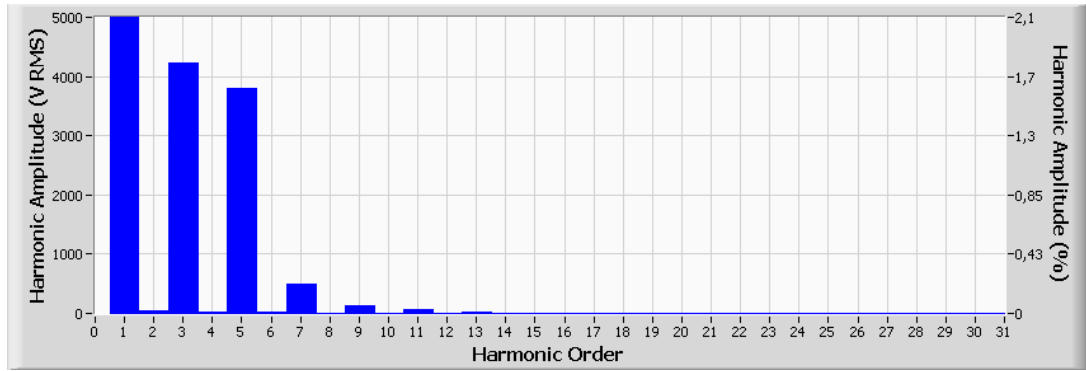


Figure 5.17: A sample data of conventional transformer at 380 kV

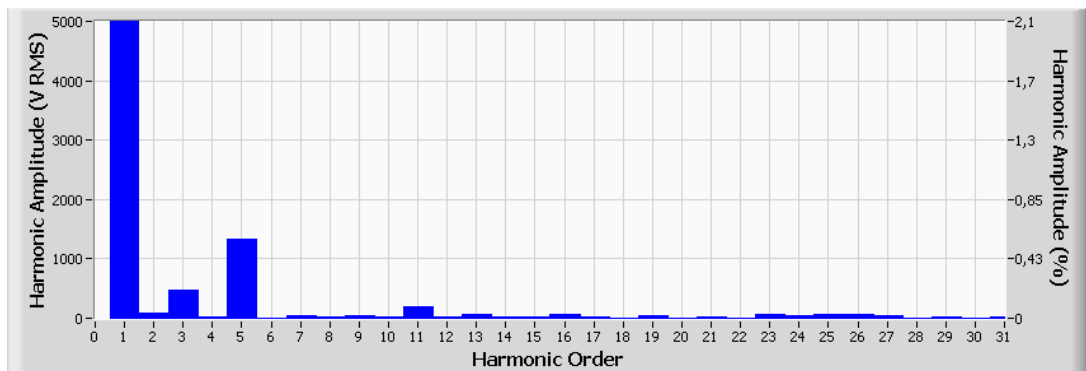


Figure 5.18: A sample data of NXVCT at 380 kV

Table 5.13: Sample data of NXVCT and CVT against 5<sup>th</sup> harmonic at 380 kV

Sample	$V_{h,NXVCT}$ (V)	$V_{h,CVT}$ (V)	$V_{h,NXVCT}$ (%)	$V_{h,CVT}$ (%)	$V_{CVT}/V_{NXVCT}$	$\phi_{CVT} - \phi_{NXVCT}$ (Degree)
1	1334.62	3806.92	0.6	1.6	2.8524	67.19
2	1315.51	3769.70	0.6	1.6	2.8656	67.83
3	1260.34	3636.01	0.5	1.6	2.8849	66.09

Table 5.14: Sample data of NXVCT and CVT against 7<sup>th</sup> harmonic at 380 kV

Sample	$V_{h,NXVCT}$ (V)	$V_{h,CVT}$ (V)	$V_{h,NXVCT}$ (%)	$V_{h,CVT}$ (%)	$V_{CVT}/V_{NXVCT}$	$\phi_{CVT} - \phi_{NXVCT}$ (Degree)
1	95.257	478.173	0.04	0.2	5.0198	136.23
2	73.105	429.635	0.03	0.2	5.8770	70.19
3	49.413	444.536	0.02	0.2	8.9964	65.30

As a conclusion, the conventional voltage transformers are not suitable for harmonic measurement. They have significant amplitude and phase errors. They may measure a harmonic component higher than the permissible limit although it is not and vice versa. The found calibration coefficient is specific to the transformer which the measurements are taken. There is also significant phase error, which is impossible to calibrate because of load dependence. But, harmonic phase is not as important as amplitude in real life because there is no limit of it and harmonic power is not considered.

### 5.3 Current Measurements

The important parameter is the ratio of both fundamental and harmonic current, to the rated current, for the accuracy of measurement. There is not such a case for voltage transformers, because the fundamental voltage is constant, neglecting the fluctuations. So, the present currents, both fundamental and harmonic components, are grouped and the results are investigated according to these groups.

### 5.3.1 Current Measurements at 34.5 kV

The conventional transformer is Emek KAC-45, 30 VA, IEC 1.0, 600/5 and the transducer used is 36 kV NXCT. Sample data are shown in Figure 5.19 and Figure 5.20. The deviation of the ratio is illustrated according to amplitude of fundamental component, amplitude of harmonic component and percentage of harmonic component through Figure 5.21 to 5.35. Also, phase error of the conventional CT is grouped according to amplitude of current and shown in Table 5.15 to 5.17.

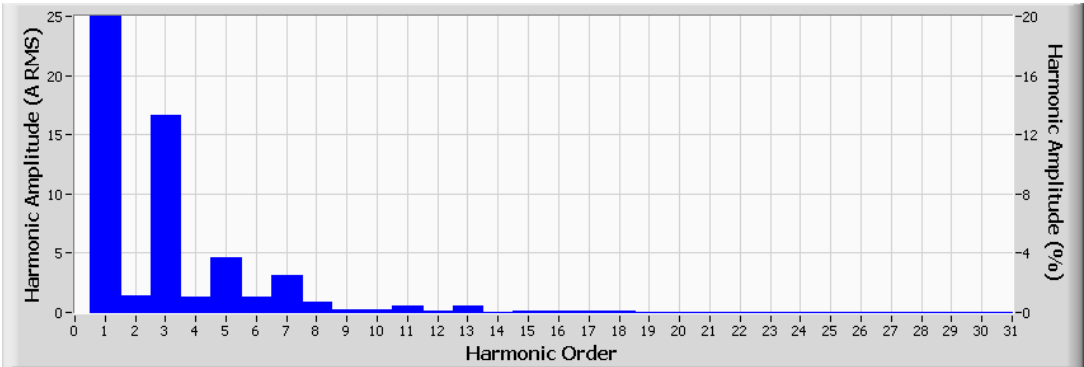


Figure 5.19: A sample data of conventional transformer at 34.5 kV

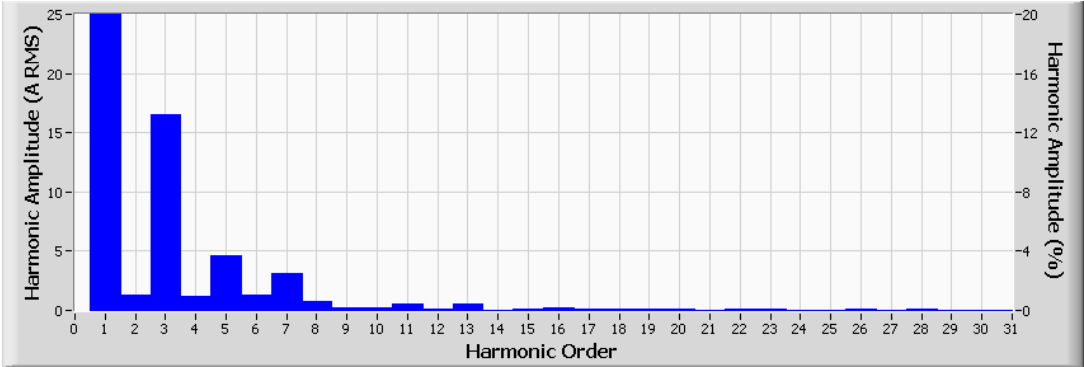


Figure 5.20: A sample data of NXCT at 34.5 kV

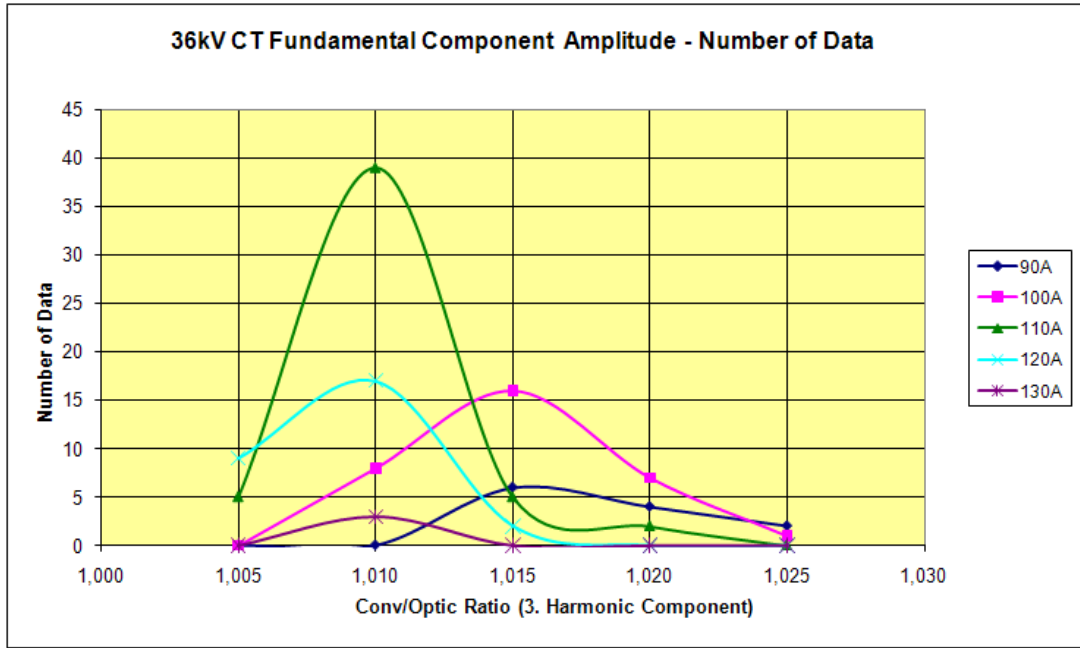


Figure 5.21: Deviation of  $I_{conv}/I_{NXCT}$  against amplitude of fundamental component for 3<sup>rd</sup> harmonic component

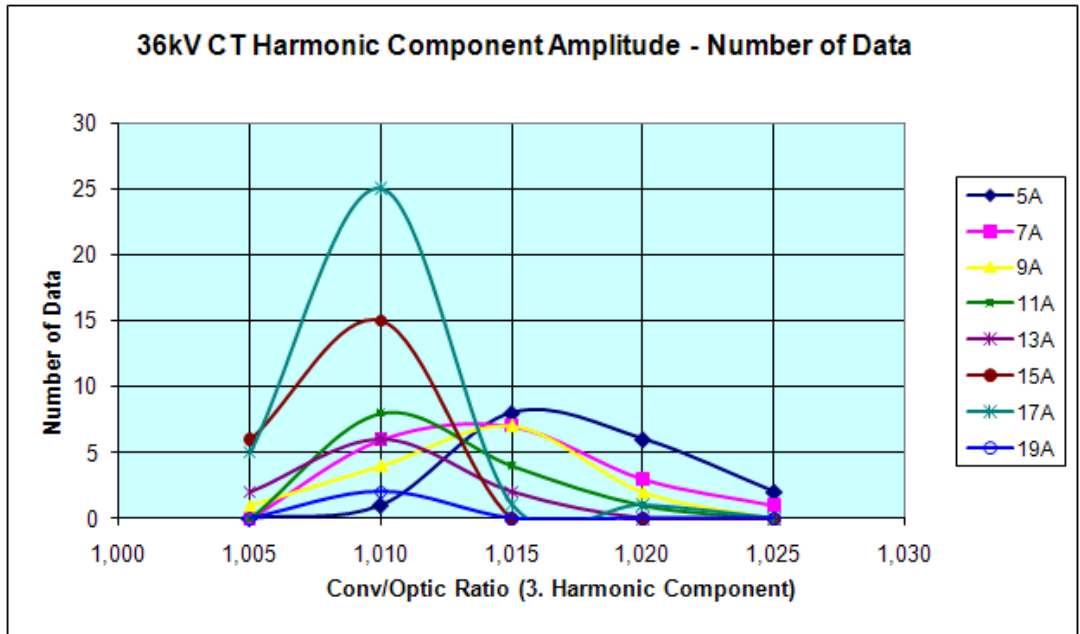


Figure 5.22: Deviation of  $I_{conv}/I_{NXCT}$  against amplitude of harmonic component for 3<sup>rd</sup> harmonic component

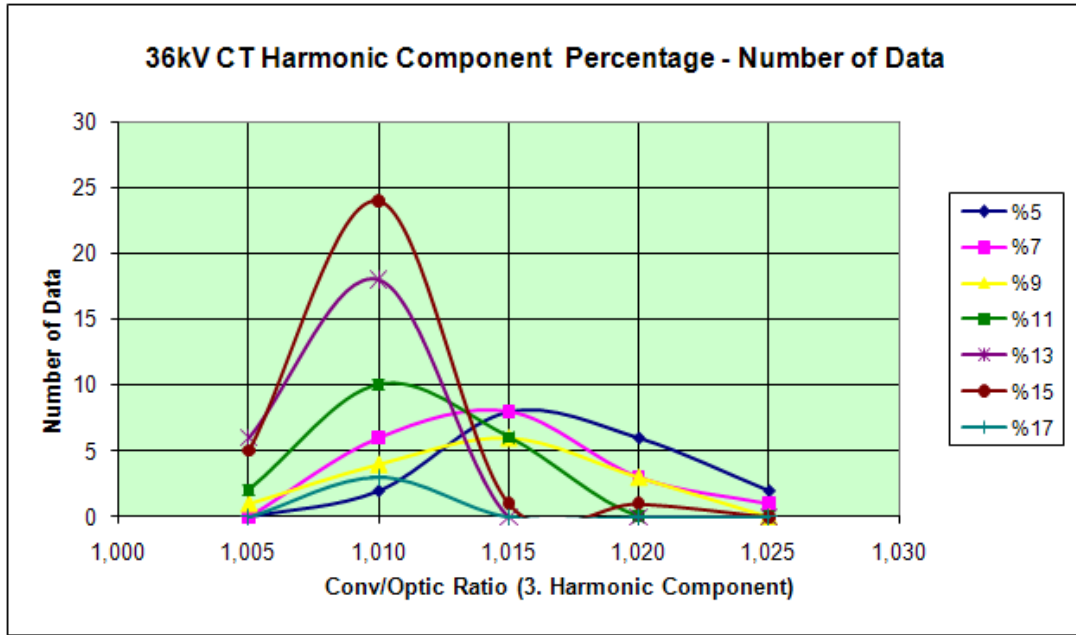


Figure 5.23: Deviation of  $I_{conv}/I_{NXCT}$  against percentage of harmonic component for 3<sup>rd</sup> harmonic component

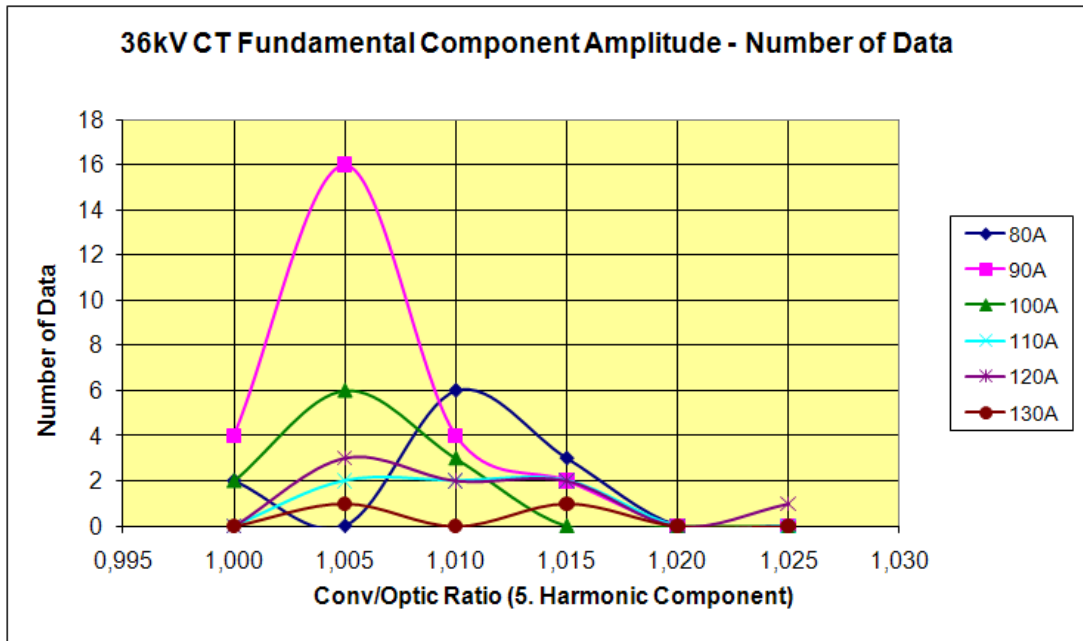


Figure 5.24: Deviation of  $I_{conv}/I_{NXCT}$  against amplitude of fundamental component for 5<sup>th</sup> harmonic component

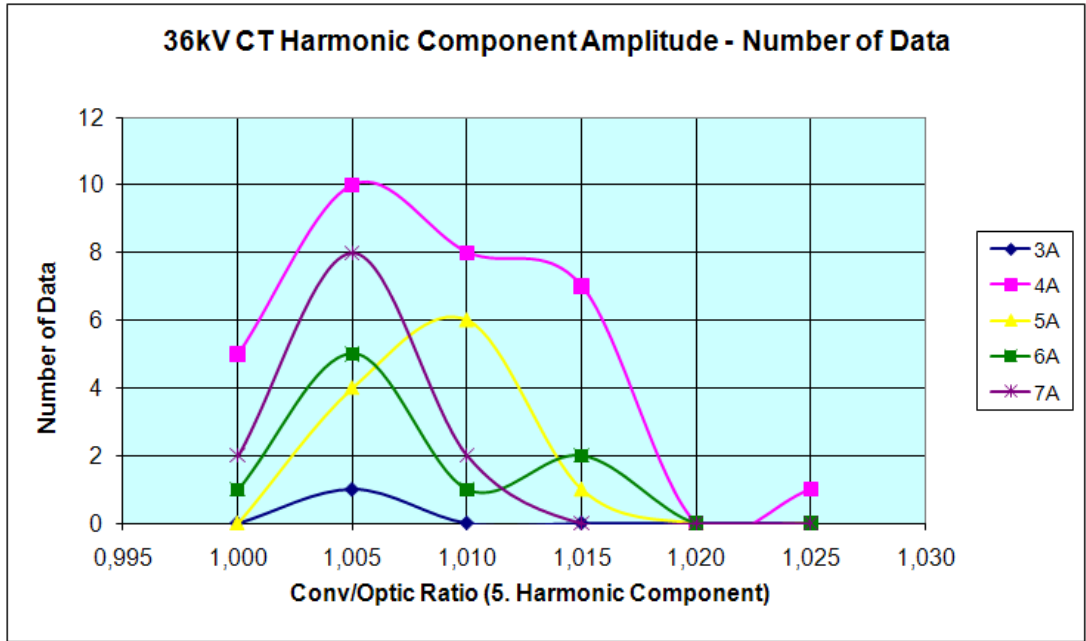


Figure 5.25: Deviation of  $I_{conv}/I_{NXCT}$  against amplitude of harmonic component for 5<sup>th</sup> harmonic component

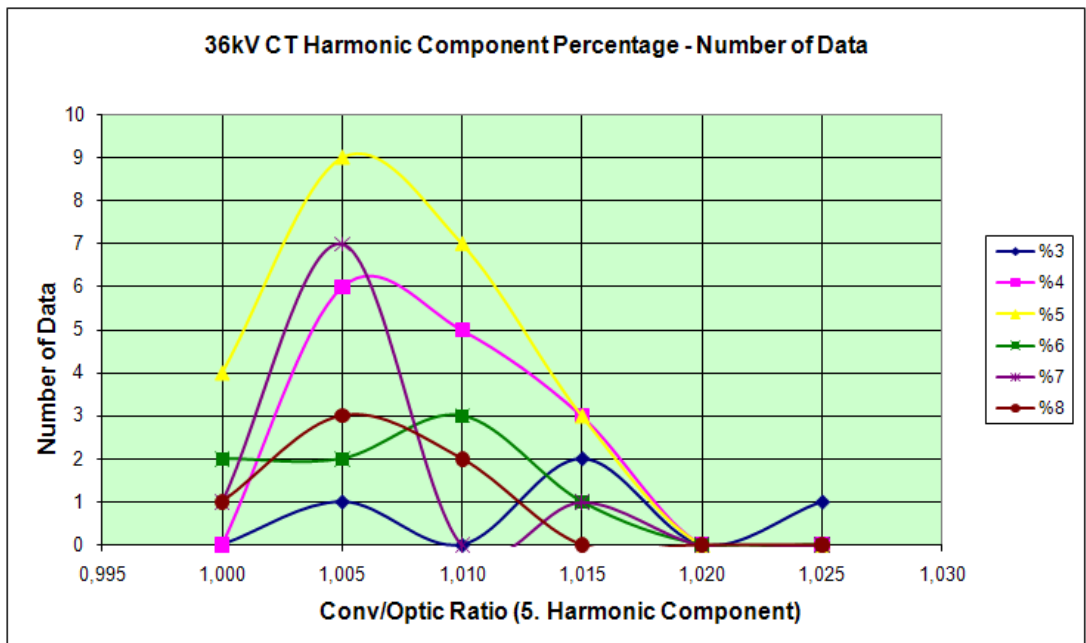


Figure 5.26: Deviation of  $I_{conv}/I_{NXCT}$  against percentage of harmonic component for 5<sup>th</sup> harmonic component

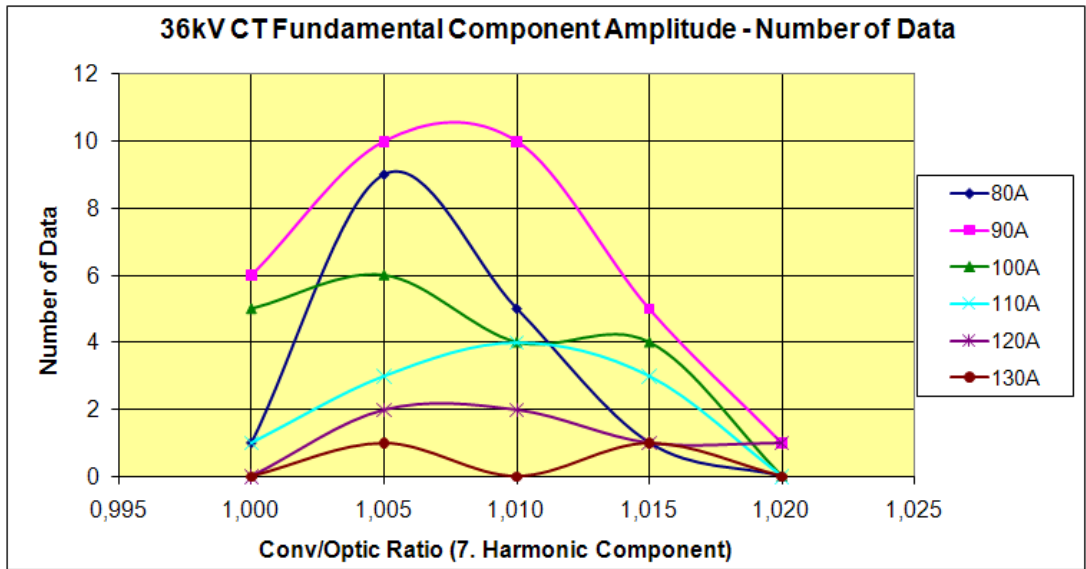


Figure 5.27: Deviation of  $I_{conv}/I_{NXCT}$  against amplitude of fundamental component for 7<sup>th</sup> harmonic component

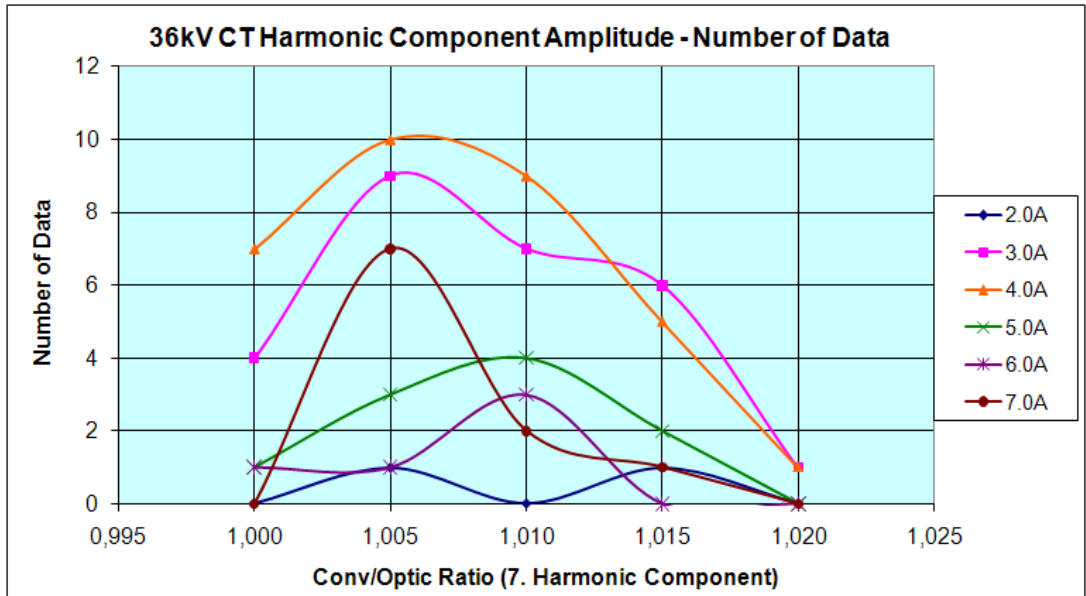


Figure 5.28: Deviation of  $I_{conv}/I_{NXCT}$  against amplitude of harmonic component for 7<sup>th</sup> harmonic component

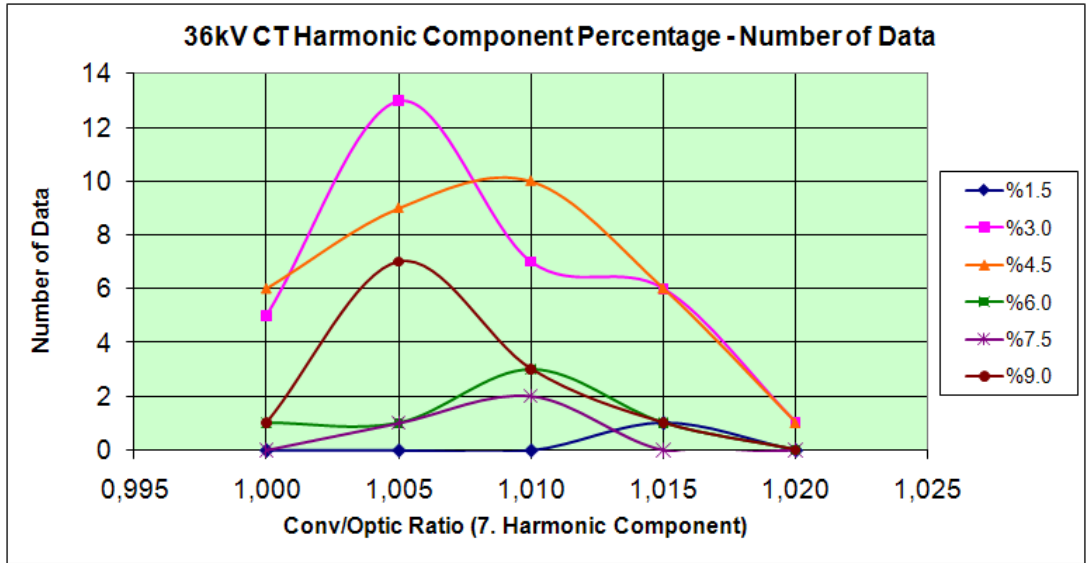


Figure 5.29: Deviation of  $I_{conv}/I_{NXCT}$  against percentage of harmonic component for 7<sup>th</sup> harmonic component

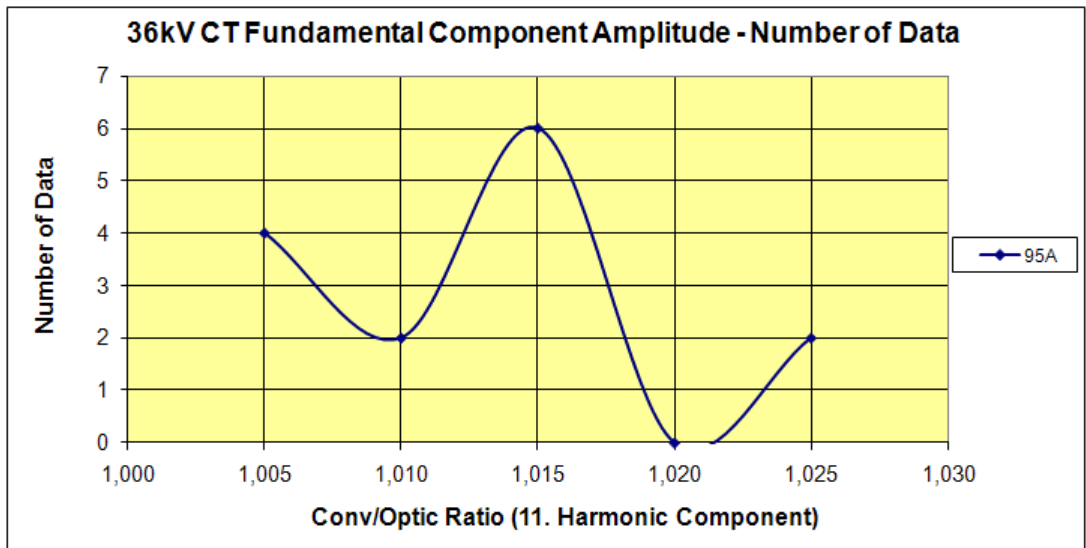


Figure 5.30: Deviation of  $I_{conv}/I_{NXCT}$  against amplitude of fundamental component for 11<sup>th</sup> harmonic component

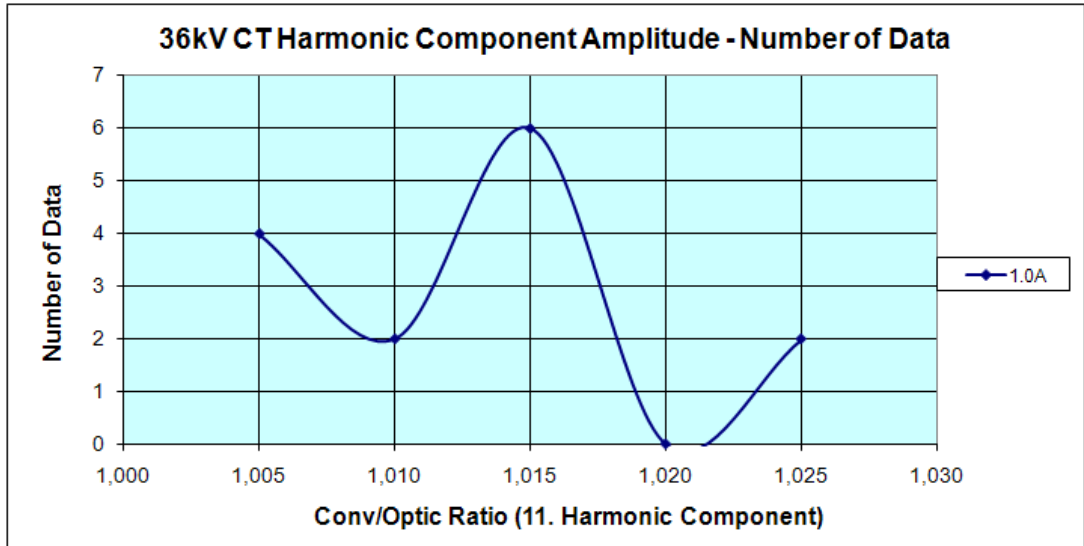


Figure 5.31: Deviation of  $I_{conv}/I_{NXCT}$  against amplitude of harmonic component for 11<sup>th</sup> harmonic component

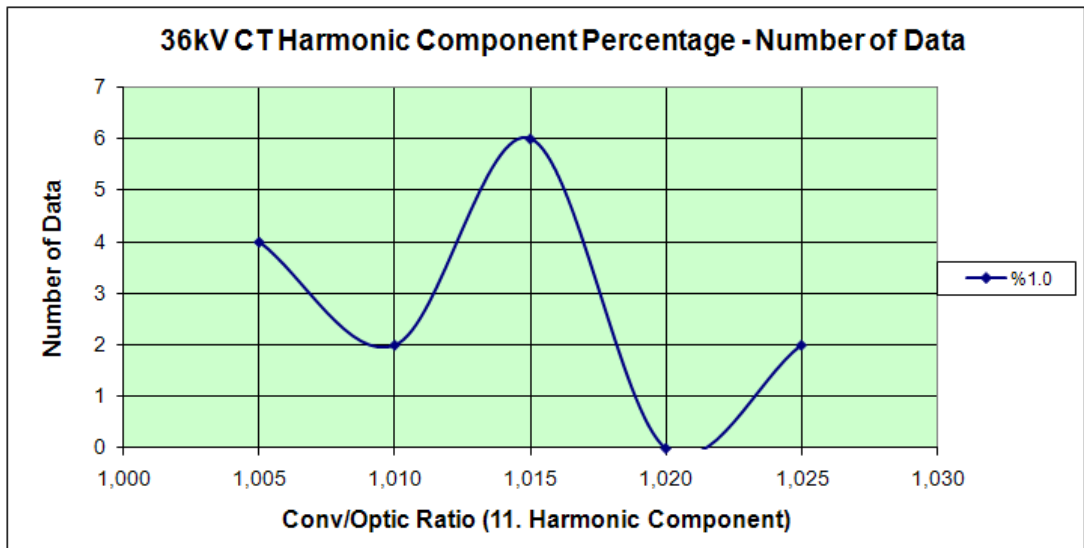


Figure 5.32: Deviation of  $I_{conv}/I_{NXCT}$  against percentage of harmonic component for 11<sup>th</sup> harmonic component

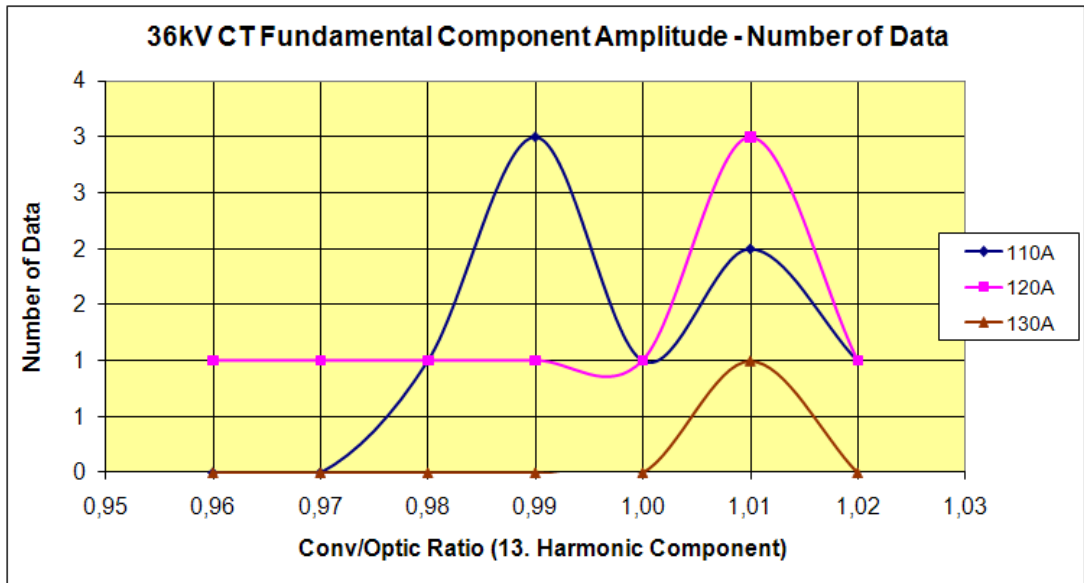


Figure 5.33: Deviation of  $I_{conv}/I_{NXCT}$  against amplitude of fundamental component for 13<sup>th</sup> harmonic component

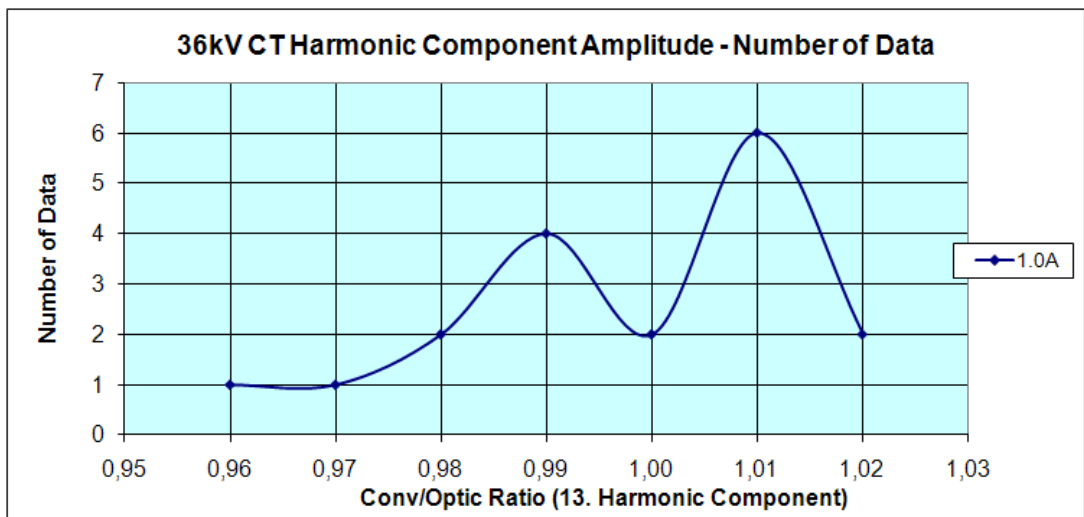


Figure 5.34: Deviation of  $I_{conv}/I_{NXCT}$  against amplitude of harmonic component for 13<sup>th</sup> harmonic component

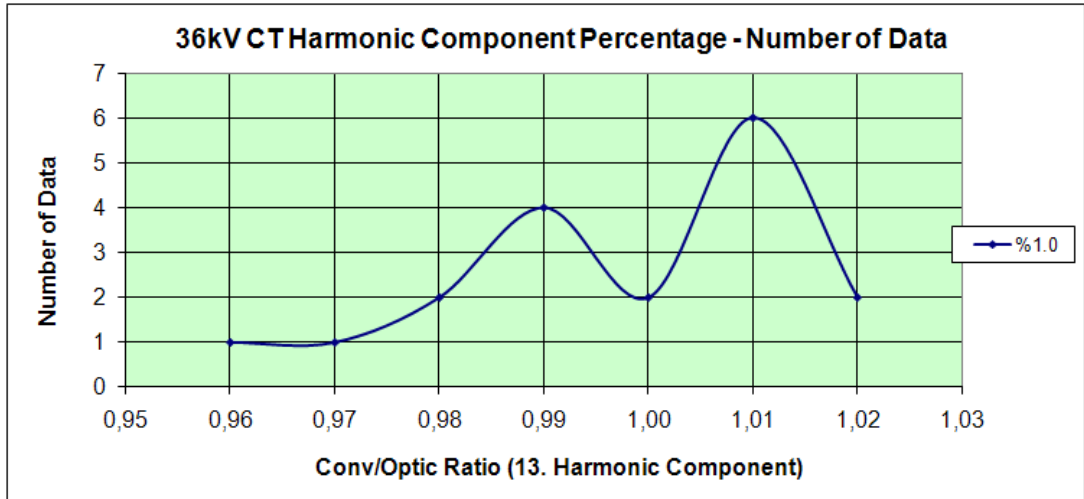


Figure 5.35: Deviation of  $I_{conv}/I_{NXCT}$  against percentage of harmonic component for 13<sup>th</sup> harmonic component

Table 5.15: Phase shift error of conventional CT at fundamental component at 34.5 kV

$I_1(A_{rms})$	$\phi_{conv} - \phi_{NXCT}$ (Degree)
90	1.29
100	1.23
110	1.18
120	1.14

Table 5.16: Phase shift error of conventional CT at 3<sup>rd</sup> harmonic component at 34.5 kV

$I_3(A_{rms})$	$\phi_{conv} - \phi_{NXCT}$ (Degree)
5	0.65
7	0.22
9	0.14
11	0.20
13	0.24
15	0.21
17	0.24
19	0.27

Table 5.17: Phase shift error of conventional CT at other harmonic component at 34.5 kV

Harmonic Order	$I_h(A_{rms})$	$\phi_{conv} - \phi_{NXCT}$ (Degree)
5	3.5 - 7.5	0.28
7	2.5 - 7.5	0.27
11	1.0	1.41
13	1.0	1.61

### 5.3.2 Current Measurements at 154 kV

The conventional transformer is; Emek ATK3-170, 30 VA, IEC 0.5, 2000/5 and the transducer used is 170 kV NXVCT. The harmonic current components and amplitudes were less than the ones at 34.5 kV voltage level and almost constant throughout the measurement. There was only third and fifth harmonic components. So, only the deviation against fundamental current is plotted for third and fifth harmonic components in Figure 5.36 and 5.37. Also, phase errors of the conventional CT is shown in Table 5.18.

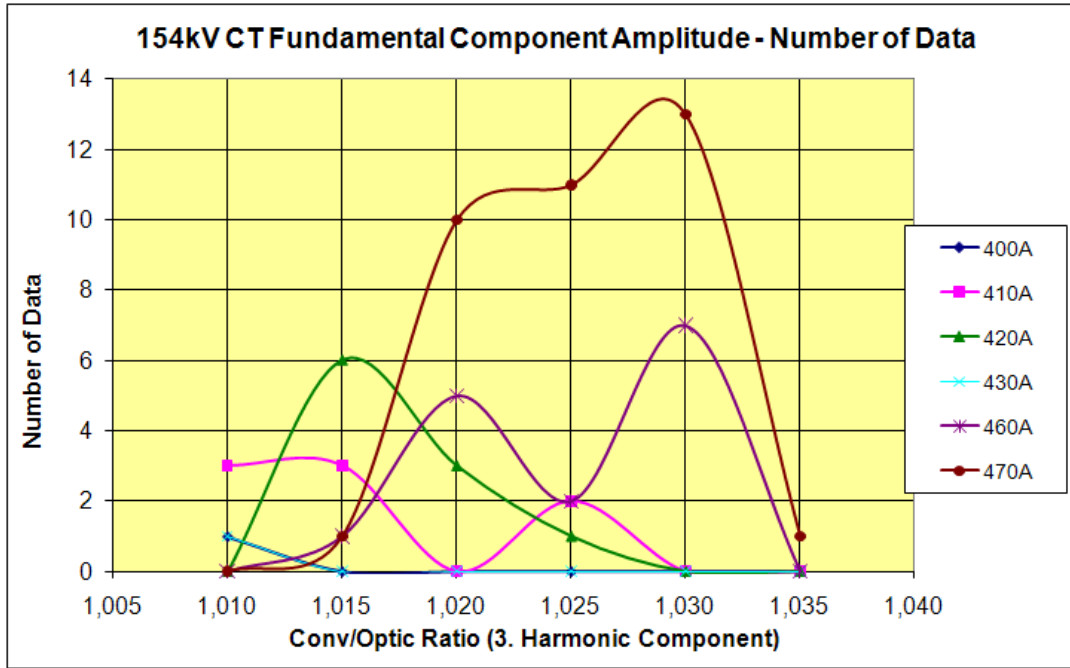


Figure 5.36: Deviation of  $I_{conv}/I_{NXVCT}$  against amplitude of fundamental component for 3<sup>rd</sup> harmonic component

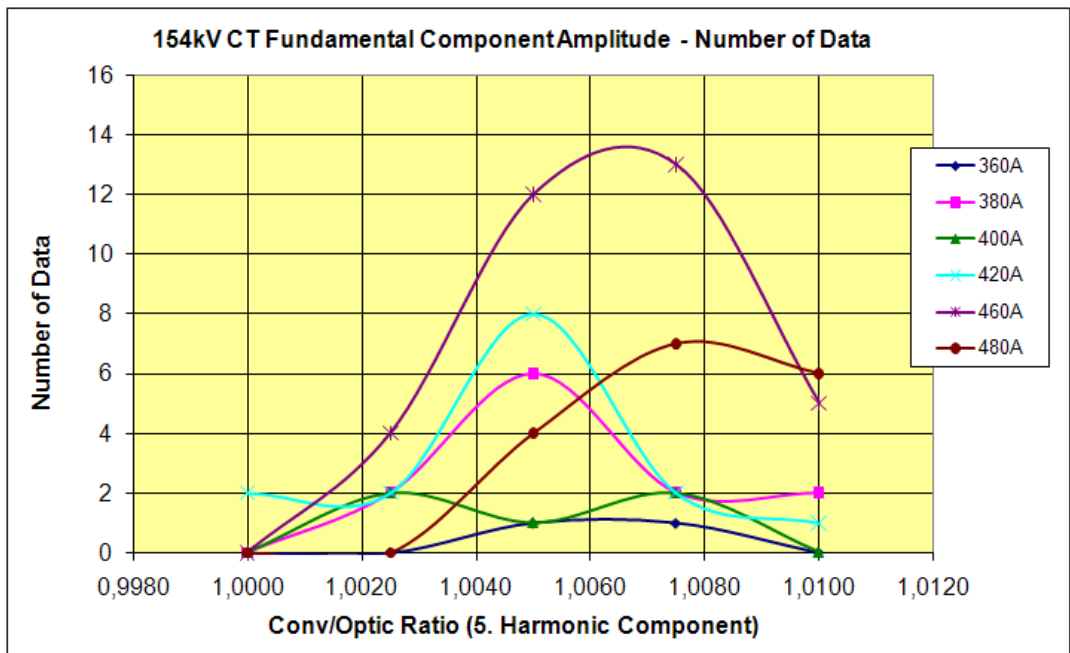


Figure 5.37: Deviation of  $I_{conv}/I_{NXVCT}$  against amplitude of fundamental component for 5<sup>th</sup> harmonic component

Table 5.18: Phase shift error of conventional CT at 154 kV

Harmonic Order	$I_h(A_{rms})$	$\phi_{conv} - \phi_{NXCT}$ (Degree)
1	380	1.13
1	410	0.57
1	420	0.56
1	465	0.56
3	2.5 - 3.0	-5.91
5	11.5 - 14.0	0.43

### 5.3.3 Current Measurements at 380 kV

The conventional transformer is; Areva, 30 VA, IEC 0.5, 500/1 and the transducer used is 420 kV NXVCT. The harmonic current components and amplitudes were less than the ones at 34.5 kV voltage level and almost constant throughout the measurement. There was only fifth harmonic component. So, only the deviation against fundamental current is plotted for fifth harmonic component in Figure 5.38. Also, phase errors of the conventional CT is shown in Table 5.19.

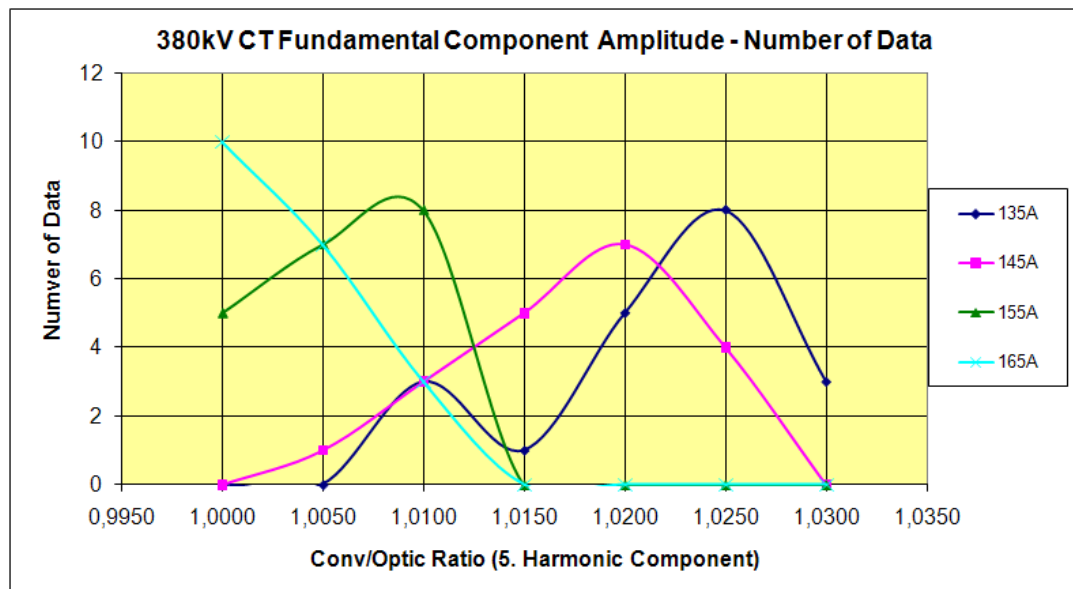


Figure 5.38: Deviation of  $I_{conv}/I_{NXVCT}$  against amplitude of fundamental component for 5<sup>th</sup> harmonic component

Table 5.19: Phase shift error of conventional CT at 380 kV

Harmonic Order	$I_h(A_{rms})$	$\phi_{conv} - \phi_{NXCT}$ (Degree)
1	135	0.16
1	145	0.17
1	155	0.15
1	165	0.14
3	1	1.62
5	3 - 5	0.86

As a conclusion of current measurements; it is seen that the conventional current transformers have satisfactory performance at harmonic measurements at both amplitude and phase measurements as mentioned by IEEE [6]. The accuracy of measurement is dependent on the ratio of the present current to rated current as expected. Also, the accuracy limits of current transformers are defined according to the ratio of flowing current to the rated current (refer to Table 2.1). It is seen from the plots that, as the current value increased, the accuracy of the current transformer increases and also the deviation of the error decreases. The phase error is also dependent on the current value but does not change significantly.

## CHAPTER 6

### CONCLUSION

A new calibration method of conventional instrument transformers is proposed in this thesis depending on simultaneous field measurements of the conventional instrument transformers and new technology transducers. The proposed method is applicable at medium voltage, high voltage and extra-high voltage levels. The fundamental advantage of the method is that it depends on field measurements from the primary terminals of conventional instrument transformers and so all external effects are taken into consideration, which can not be provided by theoretical approach, like ratio correction factor (RCF) approach. Also, taking measurements by high accuracy harmonic analyzers directly from the extra high voltage is impossible unless a coupling is used.

Optical transducers and resistive-capacitive voltage transformer (RCVT) have a lot of advantages over the conventional instrument transformers which results in accurate harmonic and transient-state measurements. Also, combined sensors (for example NXVCT) provide gain in space and simplicity in design. As a disadvantage, this is a new technology and so there are only a few manufacturers, which also makes these transducers expensive. But this disadvantage shall be eliminated in the future. The advantages may be listed as follows:

#### Advantages of Optical Voltage Transducers:

- Wider bandwidth (0.5 Hz - 6 kHz)
- Inherent electrical isolation and immunity to electromagnetic interference
- No ground loop problem

- No saturation problem
- No ferroresonance and trapped charges problems
- No short-circuited secondary problem
- Lighter weight and smaller space than the conventional ones
- Stability over temperature changes and dielectric stresses

#### **Advantages of Optical Current Transducers:**

- Wider bandwidth (DC - 20 kHz)
- Inherent electrical isolation and immunity to electromagnetic interference
- No saturation problem
- No open-secondary problem
- Lighter weight and smaller space than the conventional ones
- Stability over temperature changes and dielectric stresses

#### **Advantages of RCVT:**

- Wider bandwidth (DC - 1 MHz)
- No ground loop problem
- No saturation problem
- No ferroresonance and trapped charges problems
- No short-circuited secondary problem
- Lighter weight and smaller space than the conventional ones

The outputs of the thesis are consistent with the theory of the instrument transformers and the information in the literature, which also proves the accuracy of the used transducers; RCVT, NXCT and NXVCT. The conclusions derived from the outputs of the thesis are as follows:

- Conventional voltage transformers are not suitable for harmonic voltage measurement. They have significant amplitude and phase errors. The harmonic voltage may be amplified or attenuated depending on the external parameters. Due to dependency of substation it is installed, calibration must be done for each voltage instrument transformer uniquely.
- Inductive voltage transformers have better performance than capacitive voltage transformers at harmonic voltage measurement but the accuracy is not enough.
- Punitive sanctions for harmonics exceeding the determined limits will result in incorrect applications if the voltage instrument transformer is not calibrated. They can amplify the harmonic voltage upon or attenuate under the determined limit.
- The grounding scheme results in significant amplification at triplen harmonics; especially at 3<sup>rd</sup> harmonic component. The induced voltage on the ground cable is added on the measured triplen harmonics voltages like an offset voltage, which prevents finding a calibration coefficient. Since the induced voltage is not constant due to unbalanced loads, it makes the exact calibration impossible. To minimize this error, secondary terminals of the voltage instrument transformers should be connected to control room directly via a separate cable and grounded at only one side.
- Conventional current transformers can be used in harmonic current measurement due to their sufficient performance if the application in which they are used, is not a critical special application.
- Calibration of conventional current transformers depending on the method used throughout this thesis is quite easy as they are not affected from the external parameters.
- Accuracy of conventional current transformers can be increased by selecting proper nominal current rating for metering purposes rather than protection. The current values measured throughout this thesis were much lower than the rated values, which affects the overall accuracy of the conventional current transformer in a bad way.

As future-work, more measurements can be taken from different substations as the calibration coefficients are unique and each transformer may respond differently. This would diversify the content of the thesis. Especially measurements at the points where harmonic percentage is higher and/or higher order harmonics are present would be beneficial. By cooperating with TEIAS, measurements can be taken from all substations of Turkey and by using these coefficients in metering, accurate harmonic measurements can be achieved and hence punitive sanctions can be made applicable.

## REFERENCES

- [1] IEC 60044-1, *International Standard, Instrument Transformers - Current Transformers, Edition 1.2 2003-02*
- [2] IEC 60044-2, *International Standard, Instrument Transformers - Inductive Voltage Transformers, Edition 1.2 2003-02*
- [3] IEC 60044-5, *International Standard, Instrument Transformers - Capacitor Voltage Transformers, Edition 1.2 2003-02*
- [4] IEC 60044-7, *International Standard, Instrument Transformers - Electronic Voltage Transformers, First Edition 1999-12*
- [5] IEC 61000-4-7, *International Standard, EMC - Testing and Measurement Techniques - General guide on harmonics and interharmonics measurements and instrumentation, for power supply systems and equipment connected thereto, Edition 2.1 2009-10*
- [6] IEEE Std 519-1992, *IEEE Recommended Practices and Requirements for Harmonic Control in Electrical Power Systems*
- [7] Ruthard Minkner, *A universal RC voltage transformer for High Voltage Networks: ETZ vol 22/2002, pp 22 - 29, VDE Verlag*
- [8] Par Dr. Joachim Schmid, Dr. Pascal Lequitte, *Measurement of Current and Voltage in MV and HV Switchgears with Low Power Instrument Transformers: Conference Matpost'03, 20-21 November 2003*
- [9] Alexander E. Emanuel, John A. Orr, *Current Harmonics Measurement by Means of Current Transformers: IEEE Transactions on Power Delivery, Vol. 22, No. 3, July 2007*
- [10] Eddy So, *Harmonic Measurements: Current and Voltage Transducers: Power Engineering Society General Meeting, 2003, IEEE, Volume 1, 13-17 July 2003*
- [11] Yao Xiao, Jun Fu, Bin Hu, Xiaoping Li, and Chunnian Deng, *Problems of Voltage Transducer in Harmonic Measurement: IEEE Transactions on Power Delivery, Vol. 19, No. 3, July 2004*
- [12] M. Sanaye-Pasand, A. Rezaei-Zare, H. Mohseni, Sh. Farhangi, and R. Iravani, *Comparison of Performance of Various Ferroresonance Suppressing Methods in Inductive and Capacitive Voltage Transformers: Power India Conference, 2006 IEEE*
- [13] Daqing Hou, Jeff Roberts, *Capacitive Voltage Transformer: Transient Overreach Concerns and Solutions For Distance Relaying: 1996 Canadian Conference, Volume 1, 26-29 May 1996*

- [14] Viraj Pradeep Mahadanaarachchi, Rama Ramakumar, *Analysis of Capacitive Voltage Transformer Transients with Wind Farm Integration*: Power Systems Conference 2009, 10-13 March 2009
- [15] Peter E. Sutherland, *Harmonic Measurements in Industrial Power Systems*: IEEE Transactions on Industry Applications, Vol. 31, No. 1, January/February 1995
- [16] Foroozan Ghassemi, Philip Gale, Tom Cumming, and Colin Coutts, *Harmonic Voltage Measurements Using CVTs*: IEEE Transactions on Power Delivery, Vol. 20, No. 1, January 2005
- [17] A. P. Sakis Meliopoulos, Fan Zhang, S. Zelingher, G. Stillman, G. J. Cokkinides, L. Coffeen, R. Burnett, J. McBride, *Transmission Level Instrument Transformers and Transient Event Recorders Characterization for Harmonic Measurements*: IEEE Transactions on Power Delivery, Vol. 8, No. 3, July 1993
- [18] H.Seljeseth, E. A. Saethre, T. Ohnstad, L. Lien, *Voltage Transformer Frequency Response. Measuring Harmonics in Norwegian 300 kV and 132 kV Power Systems*: 8<sup>th</sup> International Conference on Harmonics and Quality of Power, ICHQP '98, October 14-16, 1998, IEEE
- [19] Trench Group Switzerland AG, <http://www.trenchgroup.com/>, last visited on 20 January 2010
- [20] NxtPhase T&D Corporation, <http://www.nxtphase.com/>, last visited on 20 January 2010
- [21] NxtPhase T&D Corporation Presentation, January 2006
- [22] Farnoosh Rahmatian, Abraham Ortega, *Applications of Optical Current and Voltage Sensors in High-Voltage Systems*: Transmission & Distribution Conference and Exposition: Latin America, 2006. TDC '06. IEEE/PES 15-18 Aug. 2006
- [23] J. D. P. Hrabliuk, *Optical Current Sensors Eliminate CT Saturation*: Power Engineering Society Winter Meeting, 2002 IEEE. Volume 2, 27-31 Jan. 2002
- [24] T. Kumai, H. Nakabayashi, Y. Hirata, M. Takahashi, K. Terai, T. Kaminishi and K. Uehara, *Field Trial of Optical Current Transformer Using Optical Fiber as Faraday Sensor*: Power Engineering Society Summer Meeting, 2002 IEEE Volume 2, 25 July 2002
- [25] Patrick P. Chavez, Nicolas A. F. Jaeger, Farnoosh Rahmatian, *Accurate Voltage Measurement by the Quadrature Method*: IEEE Transactions on Power Delivery, Vol.18, No.1, January 2003
- [26] Farnoosh Rahmatian, Patrick P. Chavez, Nicolas A. F. Jaeger, *230 kV Optical Voltage Transducers Using Multiple Electric Field Sensors*: IEEE Transactions on Power Delivery, Vol.17, No.2, April 2002
- [27] Energy Market Regulatory Authority, <http://www.epdk.gov.tr/> , last visited on 25 April 2010

- [28] Turkish Electricity Transmission Inc. Co., <http://www.teias.gov.tr/> , last visited on 24 April 2010
- [29] Transmission System Supply Reliability and Quality Regulation, 10 Nov. 2004
- [30] Electricity Market Supply Regulation, 26 Nov. 2009
- [31] National Instruments, <http://www.ni.com/>, last visited on 27 April 2010
- [32] EMEK Electrical Industry Inc., <http://www.emek.com.tr/>, last visited on 28 April 2010

## **APPENDIX A**

### **ROUTINE TEST REPORT FOR RCVT by TRENCH GROUP**

The following document is prepared by Trench Group [19] and it is specific for the RCVT columns purchased for this work.



## Routine test report

Customer: **TUBITAK  
TR**

Your reference: **-**

Workorder: **0014104\_20**

Project: **National Power Quality Project of Turkey  
TR**

Object: **RC- Voltage Transformer 420 kV**

Quantity: **3**

Type: **RCVT 420 kV**

Serial No: **2071925 to 2071927**

Test specification: **IEC 60044-5**

Results: **All tests, listed on page 3, were successfully completed  
in accordance with the given test specification**

Written by: **L. Starck**

Test report contains **15 pages**

Saint-Louis, **February 11 th, 2008**

Trench France SA,  
Tests department **G. Maschio**

**TRENCH FRANCE S.A.**  
*Responsable plates-formes  
d'essais HT*  
**G. MASCHIO**

ROUTINE TEST REPORT

**TRENCH**

Project No: 0014104\_20

**Technical characteristics**

Rated System Voltage	$(U_r)$			<b>380</b> kV <sub>rms</sub>
Maximal Voltage for Equipment	$(U_m)$			<b>420</b> kV <sub>rms</sub>
Lowest Voltage for Equipment				<b>342</b> kV <sub>rms</sub>
Rated primary voltage	$(U_{pn})$			<b>380/√3</b> kV <sub>rms</sub>
Rated secondary voltage	$(U_{sn})$			<b>100/√3</b> V <sub>rms</sub>
Rated transformation ratio	$(K_N)$			<b>3800</b>
Rated frequency	$(f_N)$			<b>50</b> Hz
Dissipation factor at 20°C	$(\tan \delta)$	at $U_m/\sqrt{3}$	≤	<b>1,50%</b>
Rated voltage factor	$(xU_N)$	continuous		<b>1,2</b>
Rated voltage factor	$(xU_N)$	$t = 30$ s		<b>1,9</b>
Rated voltage factor	$(xU_N)$	$t = 100$ ms		<b>3</b>
Partial discharge	$(PD)$	at $1,2 U_m/\sqrt{3}$	≤	<b>5</b> pC
		at $1,2 U_m$	≤	<b>10</b> pC
		at $U_{Test}$	≤	<b>10</b> pC

**Rated insulation levels at standard atmospheric conditions**

Rated power frequency withstand voltage	$(U_{Test})$	<b>680</b> kV <sub>rms</sub>	<b>50</b> Hz	<b>60</b> s
Rated lightning impulse withstand voltage	$(U_{BIL})$	<b>1550</b> kV <sub>peak</sub>		
Rated switching impulse withstand voltage	$(U_{SIL})$	<b>1175</b> kV <sub>peak</sub>		
Rated power frequency withstand voltage on secondary winding		<b>4</b> kV <sub>rms</sub>	<b>50</b> Hz	<b>60</b> s

**Rated output and the corresponding accuracy class** (voltage ratio : **380/√3** kV :  $U_s$ )

terminal	$U_s$ [V]	burden impedance / capacitance	class
a-n	100/√3	108.4 kΩ / 896 pF	0,2 at 50 Hz

$U_s$ : Rated secondary voltage

**List of all required and performed tests**

Tests on capacitor(s), electromagnetic unit(s) and complete capacitor voltage transformer(s)

- 1) **Resistance measurement**  
before HVT
- 2) **Measurement of C- and  $\tan \delta$ - at power-frequency test**  
before and after HVT
- 3) **Measurement of partial discharge at power-frequency test**  
before and after HVT
- 4) **Power frequency withstand test on divider**  
HVT
- 5) **Resistance measurement**  
after HVT
- 6) **Power frequency withstand test on secondary winding**
- 7) **Test for accuracy at 50 Hz**
- 8) **Verification of terminal markings and check of rating plate**
- 9) **Magnitude and Phase error versus Frequency Test up to 50th harmonic**
- 10) **Magnitude versus Frequency Test over the entire bandwidth**

**Applied voltage on individual capacitor(s)**

$U_n/\sqrt{3}$ [kV]	$1,2 U_n/\sqrt{3}$ [kV]	$U_n$ [kV]	$1,2 U_n$ [kV]	$U_{test}$ [kV]
242	291	420	504	680



ROUTINE TEST REPORT

TRE

Project No: 0014104\_20

C-, tanδ-, PD-measurements and power-frequency withstand test at 50 Hz

Serial No.	U [kV <sub>rms</sub> ]	C [pF]	tan δ [10 <sup>-3</sup> ]	PD [pC]	t [s]	Limits of PD [pC]
2071927  PA 3	10	1041	8,1	-		-
	242	1041	8	-		≤ 5
	291	-	-	2		≤ 10
	420	-	-	7		≤ 10
	504	-	-	7		≤ 10
	680	-	-	8	60	≤ 10
	504	-	-	7		≤ 10
	420	-	-	7		≤ 10
	291	-	-	2		≤ 5
242	1041	8	-		-	
PD-ground level:						2 pC
PD-inception:						300 kV
PD-extinction:						320 kV

atm. conditions 1029 mbar 15 °C 43 % rel. humidity  
 measured by: Ameziane date: 15/12/2007

Power frequency withstand test on secondary winding

Serial No.	U [kV <sub>rms</sub> ]	f [Hz]	t [s]
2071927	4	50	60

measured by: Ameziane date: 15/12/2007

C-, tanδ-, PD-measurements and power-frequency withstand test at 50 Hz

Serial No.	U [kV <sub>rms</sub> ]	C [pF]	tan δ [10 <sup>-3</sup> ]	PD [pC]	t [s]	Limits of PD [pC]
2071925  PA 1	10	1037	8,3	-		-
	242	1037	8	-		≤ 5
	291	-	-	2		≤ 10
	420	-	-	3		≤ 10
	504	-	-	5		≤ 10
	680	-	-	8	60	≤ 10
	504	-	-	4		≤ 10
	420	-	-	2		≤ 10
	291	-	-	2		≤ 5
	242	1037	8	-		-
	PD-ground level:					
PD-inception:						630 kV
PD-extinction:						600 kV

atm. conditions 1022 mbar 14 °C 36 % rel. humidity  
 measured by: Schneberger date: 12/11/2007

Power frequency withstand test on secondary winding

Serial No.	U [kV <sub>rms</sub> ]	f [Hz]	t [s]
2071925	4	50	60

measured by: Ameziane date: 12/11/2007

ROUTINE TEST REPORT

**TRENCH**

Project No: 0014104\_20

**C-, tanδ-, PD-measurements and power-frequency withstand test at 50 Hz**

Serial No.	U [kV <sub>rms</sub> ]	C [pF]	tan δ [10 <sup>-3</sup> ]	PD [pC]	t [s]	Limits of PD [pC]
2071926  PA 2	10	1038	8,3	-		-
	242	1038	8	-		≤ 5
	291	-	-	2		≤ 10
	420	-	-	3		≤ 10
	504	-	-	6		≤ 10
	680	-	-	8	60	≤ 10
	504	-	-	5		≤ 10
	420	-	-	4		≤ 10
	291	-	-	2		≤ 5
	242	1040	8	-		-
PD-ground level:						2 pC
PD-inception:						480 kV
PD-extinction:						350 kV

atm. condition 1022 mbar

16 °C

34 % rel.humidity

measured by: Menweg

date: 12/11/2007

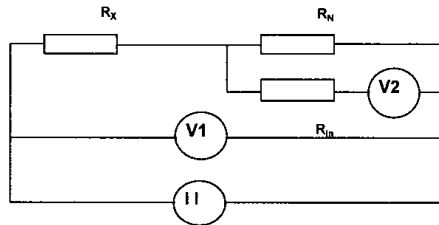
**Power frequency withstand test on secondary winding**

Serial No.	U [kV <sub>rms</sub> ]	f [Hz]	t [s]
2071926	4	50	60

measured by: Menweg

date: 12/11/2007

Resistance measurement after power frequency test



$R_x$  Measured resistance  
 $R_N$  Standard resistance  
 $R_{in}$  Input resistance of the voltmeter

$$R_x = \left( \frac{U_1}{U_2} - 1 \right) \times \left( \frac{R_N \cdot R_{in}}{R_N + R_{in}} \right)$$

$R_N = 1,000052 \text{ M}\Omega$   
 $R_{in} = 10 \text{ M}\Omega$

R1

Serial No.	Polarity	U1 (V)	U2 (V)	$R_x$ (M $\Omega$ )	R1 (M $\Omega$ )
2071925	+	967	2,3478	373,540336	373,518521
	-	972,9	2,3624	373,496706	
2071926	+	974,8	2,3668	373,530494	373,498917
	-	970,6	2,357	373,46734	
2071927	+	986,8	2,3953	373,629887	373,606588
	-	984,7	2,3905	373,583288	

R2

Serial No.	R2 (k $\Omega$ )
2071925	6366,80
2071926	6327,24
2071927	6301,86

V1 Measurement instrument: FLUKE 45  
 V2 Measurement instrument: FLUKE 45

atm. conditions: 1027 mbar 16 °C 40 % rel.humidity  
 measured by: Hoeltje date: 17/12/07

ROUTINE TEST REPORT

**TRENCH**

Project No: 0014104\_20

Tests for accuracy and check of polarity at 50 Hz

No.	U [kV]	Voltage error (ratio%)	$\delta$ (min.)	Limits	
				error	$\delta$
2071925	176 (80%)	+0,08	+0,4	$\pm 0,2 \%$	$\pm 10$ min
	219 (100%)	+0,08	+0,4	$\pm 0,2 \%$	$\pm 10$ min
	263 (120%)	+0,08	+0,3	$\pm 0,2 \%$	$\pm 10$ min

$\delta$  phase displacement

Measured by: Steinmann

date: 28/01/08

Check of rating plate

Verification of terminal marking

Checked by: Steinmann

date: 28/01/08

Tests for accuracy and check of polarity at 50 Hz

No.	U [kV]	Voltage error (ratio%)	$\delta$ (min.)	Limits	
				error	$\delta$
2071925	176 (80%)	+0,09	+0,3	$\pm 0,2 \%$	$\pm 10$ min
	219 (100%)	+0,08	+0,4	$\pm 0,2 \%$	$\pm 10$ min
	263 (120%)	+0,08	+0,4	$\pm 0,2 \%$	$\pm 10$ min

$\delta$  phase displacement

Measured by: Steinmann

date: 28/01/08

Check of rating plate

Verification of terminal marking

Checked by: Steinmann

date: 28/01/08

ROUTINE TEST REPORT

**TRENCH**

Project No: 0014104\_20

Tests for accuracy and check of polarity at 50 Hz

No.	U [kV]	Voltage error (ratio%)	$\delta$ (min.)	Limits	
				error	$\delta$
207192 <sup>7</sup>	176 (80%)	+0,13	+2,2.	± 0,2 %	± 10 min
	219 (100%)	+0,13	+2,2.	± 0,2 %	± 10 min
	263 (120%)	+0,12	+2,0	± 0,2 %	± 10 min

$\delta$  phase displacement

Measured by: Steinman

date: 28/01/08

Check of rating plate

Verification of terminal marking

Checked by: Steinman

date: 28/01/08.

ROUTINE TEST REPORT

**TRENCH**

Project No: 0014104\_20

**Magnitude and Phase error versus Frequency Test up to 50<sup>th</sup> harmonic**

Parameters: Burden Impedance: 108.4k $\Omega$   
 Burden Capacitance: 896pF  
 Rated Ratio: 3800  
 Cable: 400m Triax-Cable Huber&Suhner Type: G03332

No.	Frequency [Hz]	U <sub>in</sub> (V)	U <sub>out</sub> (mV)	$\delta$ [°]	Ratio [-]	$\Delta$ Ratio : $\epsilon$ [%]
2071925	50	1019,171	268,085	<b>0,415</b>	3801,671	<b>0,044</b>
	100	1003,157	263,868	<b>0,655</b>	3801,737	<b>0,046</b>
	150	983,876	258,802	<b>0,896</b>	3801,655	<b>0,044</b>
	500	979,821	257,752	<b>1,012</b>	3801,410	<b>0,037</b>
	1000	990,427	260,548	<b>1,156</b>	3801,321	<b>0,035</b>
	1500	994,446	261,65	<b>1,185</b>	3800,672	<b>0,018</b>
	2000	1012,102	266,35	<b>1,223</b>	3799,894	<b>-0,030</b>
	2500	985,913	259,5	<b>1,285</b>	3799,280	<b>-0,019</b>
5000	442,770	116,552	<b>1,286</b>	3798,908	<b>-0,029</b>	

$\delta$  phase displacement

Measured by: Weber & Hoeltje

date: 28/01/08

ROUTINE TEST REPORT

**TRENCH**

Project No: 0014104\_20

**Magnitude and Phase error versus Frequency Test up to 50<sup>th</sup> harmonic**

Parameters: Burden Impedance: 108.4kΩ  
 Burden Capacitance: 896pF  
 Rated Ratio: 3800  
 Cable: 400m Triax-Cable Huber&Suhner Type: G03332

No.	Frequency [Hz]	Uin (V)	Uout (mV)	$\delta$ [°]	Ratio [-]	$\Delta$ Ratio : $\epsilon$ [%]
2071926	50	994,425	261,543	<b>0,236</b>	3802,146	<b>0,056</b>
	100	990,484	260,512	<b>0,536</b>	3802,067	<b>0,054</b>
	150	994,188	261,502	<b>0,624</b>	3801,838	<b>0,048</b>
	500	983,431	258,705	<b>0,856</b>	3801,359	<b>0,036</b>
	1000	983,391	258,698	<b>0,936</b>	3801,310	<b>0,034</b>
	1500	987,805	259,891	<b>1,156</b>	3800,842	<b>0,022</b>
	2000	986,571	259,572	<b>1,296</b>	3800,761	<b>0,000</b>
	2500	994,425	261,653	<b>1,306</b>	3800,547	<b>0,014</b>
5000	480,859	126,539	<b>1,305</b>	3800,087	<b>0,002</b>	

$\delta$  phase displacement

Measured by: Weber & Hoeltje

date: 28/01/08

ROUTINE TEST REPORT

**TRENCH**

Project No: 0014104\_20

**Magnitude and Phase error versus Frequency Test up to 50<sup>th</sup> harmonic**

Parameters: Burden Impedance: 108.4k $\Omega$   
 Burden Capacitance: 896pF  
 Rated Ratio: 3800  
 Cable: 400m Triax-Cable Huber&Suhner Type: G03332

No.	Frequency [Hz]	Uin (V)	Uout (mV)	$\delta$ [°]	Ratio [-]	$\Delta$ Ratio : $\epsilon$ [%]
2071927	50	1005,507	265,023	<b>0,405</b>	3801,583	<b>0,042</b>
	100	994,525	261,615	<b>0,623</b>	3801,483	<b>0,039</b>
	150	993,124	261,251	<b>0,902</b>	3801,418	<b>0,037</b>
	500	986,150	259,435	<b>0,998</b>	3801,143	<b>0,030</b>
	1000	983,884	258,85	<b>1,103</b>	3800,980	<b>0,026</b>
	1500	985,070	259,202	<b>1,124</b>	3800,394	<b>0,010</b>
	2000	1019,171	268,251	<b>1,225</b>	3799,318	<b>-0,018</b>
	2500	990,512	260,791	<b>1,281</b>	3798,105	<b>-0,050</b>
5000	451,810	118,989	<b>1,283</b>	3797,072	<b>-0,077</b>	

$\delta$  phase displacement

Measured by: Weber & Hoeltje

date: 28/01/08

ROUTINE TEST REPORT

**TRENCH**

Project No: 0014104\_20

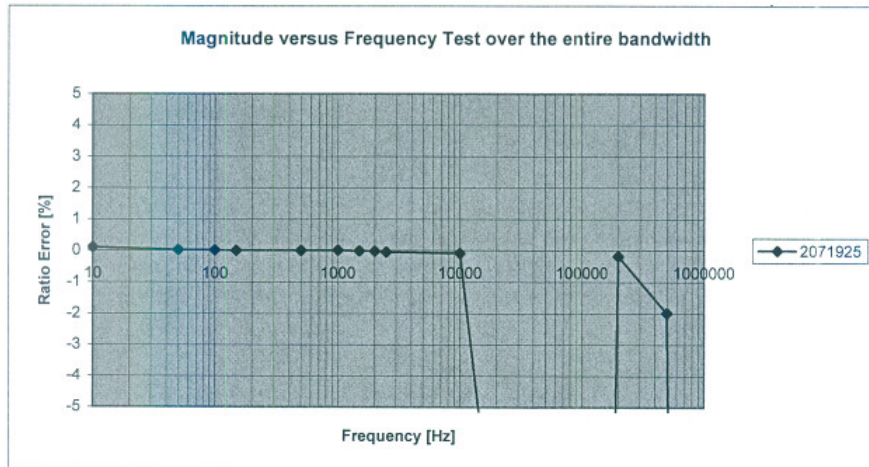
**Magnitude versus Frequency Test over the entire bandwidth**

Parameters: Burden Impedance: 108.4kΩ  
 Burden Capacitance: 896pF  
 Rated Ratio: 3800  
 Cable: 400m Triax-Cable Huber&Suhner Type: G03332

No.	Frequency [Hz]	Uin (V)	Uout (mV)	Ratio [-]	Δ Ratio : ε [%]
2071925	10	119,987	31,543	3803,918	0,103
	50	123,061	32,378	3800,76	0,02
	100	123,062	32,379	3800,673	0,018
	150	120,275	31,651	3800,038	0,001
	500	120,373	31,676	3800,133	0,003
	1000	120,469	31,699	3800,404	0,011
	1500	120,881	31,815	3799,497	-0,013
	2000	120,939	31,833	3799,171	-0,022
	2500	118,190	31,119	3798,001	-0,053
	10000	120,972	31,862	3796,748	-0,086
	50000	122,163	41,624	2934,917	-22,765
	100000	124,971	125,696	994,232	-73,836
	200000	126,057	33,235	3792,899	-0,187
	500000	57,268	15,376	3724,506	-1,987
750000	40,235	23,723	1696,033	-55,368	
1000000	35,689	36,929	966,422	-74,568	

Measured by: Weber & Hoeltje

date: 28/01/08



ROUTINE TEST REPORT

**TRENCH**

Project No: 0014104\_20

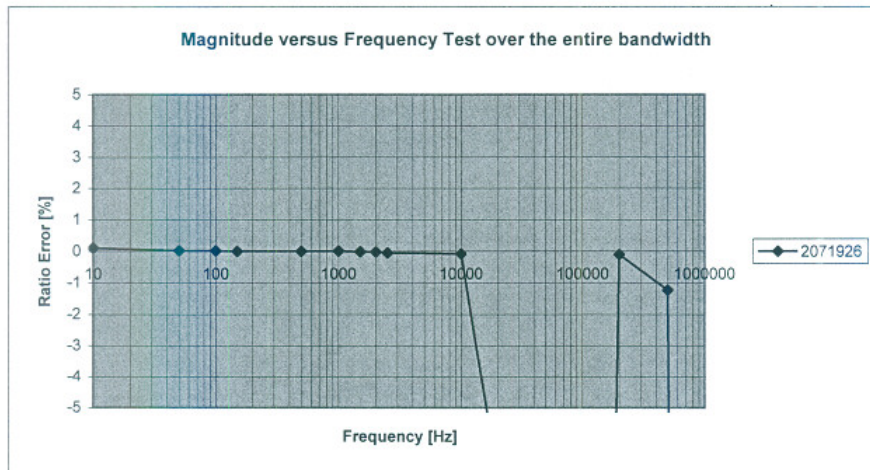
**Magnitude versus Frequency Test over the entire bandwidth**

Parameters: Burden Impedance: 108.4kΩ  
 Burden Capacitance: 896pF  
 Rated Ratio: 3800  
 Cable: 400m Triax-Cable Huber&Suhner Type: G03332

No.	Frequency [Hz]	Uin (V)	Uout (mV)	Ratio [-]	Δ Ratio : ε [%]
2071926	10	121,365	31,906	3803,839	0,101
	50	122,335	32,186	3800,876	0,023
	100	121,024	31,844	3800,528	0,014
	150	119,868	31,544	3800,025	0,001
	500	119,966	31,569	3800,12	0,003
	1000	120,025	31,582	3800,424	0,011
	1500	120,787	31,79	3799,528	-0,012
	2000	121,451	31,967	3799,262	-0,019
	2500	122,365	32,219	3797,914	-0,055
	10000	123,521	32,532	3796,908	-0,081
	50000	122,224	38,536	3171,676	-16,535
	100000	120,857	93,504	1292,533	-65,986
	200000	121,559	32,023	3795,99	-0,106
	500000	62,698	16,706	3753,023	-1,236
	750000	54,289	55,731	974,126	-74,365
1000000	42,322	25,697	1646,963	-56,659	

Measured by: Weber & Hoeltje

date: 28/01/08



ROUTINE TEST REPORT

**TRENCH**

Project No: 0014104\_20

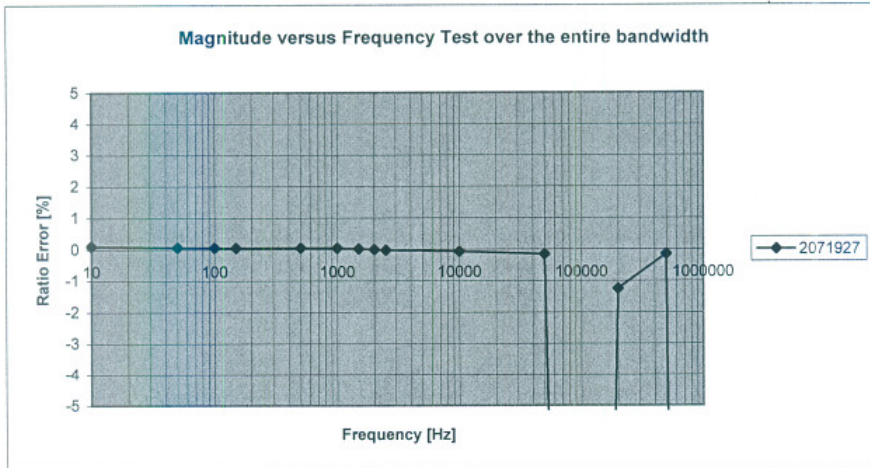
**Magnitude versus Frequency Test over the entire bandwidth**

Parameters: Burden Impedance: 108.4kΩ  
 Burden Capacitance: 896pF  
 Rated Ratio: 3800  
 Cable: 400m Triax-Cable Huber&Suhner Type: G03332

No.	Frequency [Hz]	Uin (V)	Uout (mV)	Ratio [-]	Δ Ratio : ε [%]
2071927	10	120,586	31,701	3803,855	0,101
	50	121,658	31,994	3802,525	0,066
	100	122,554	32,232	3802,246	0,059
	150	120,369	31,661	3801,807	0,048
	500	119,887	31,534	3801,833	0,048
	1000	119,364	34,397	3801,764	0,046
	1500	119,025	31,315	3800,894	0,024
	2000	120,487	31,707	3800,013	0,000
	2500	120,028	31,594	3799,076	-0,024
	10000	121,684	32,044	3797,404	-0,068
	50000	121,355	31,985	3794,122	-0,155
	100000	121,485	67,113	1810,156	-52,364
	200000	121,548	32,392	3752,408	-1,252
	500000	59,685	15,73	3794,342	-0,149
	750000	51,202	53,588	955,475	-74,856
1000000	41,253	13,632	3026,188	-20,363	

Measured by: Weber & Hoeltje

date: 28/01/08



## **APPENDIX B**

### **ROUTINE TEST REPORT FOR NXVCT**

**by NxtPhase T&D Corporation**

The following document is prepared by NxtPhase [20] and it is specific to the system NXVCT - 231 purchased for this work. Also, the other systems used throughout this work have similar specific routine test reports.

**ROUTINE TEST RESULTS  
NXVCT VOLTAGE & CURRENT SENSOR SYSTEM  
(CSA/IEC 60044-7 / CSA/IEC 60044-8 / IEEE C57.13-1993)**

**TYPE :** NXVCT-420  
**CUSTOMER :** TEIAS  
**PROJECT :** Teias Line Item #3, 420kV  
**CUSTOMER PO NUMBER :** TCOVCMT-1-07-01

**SYSTEM S/N :** NXVCT-0231

<b>COLUMN/SENSOR S/N :</b>	<b>Phase A</b>	<b>Phase B</b>	<b>Phase C</b>
	107114-008	107114-009	107114-010

**VCT SENSOR CHASSIS S/N :** 106928-031  
**TEMPERATURE SENSOR SN :** 07330004  
**CT SENSOR CHASSIS S/N:** 11682570015  
**CAPSU / PSU S/N :** 0307 2108 for VCT and 0307 2112 for CT  
**VT AMPLIFIER CHASSIS S/N :** N/A

**Rated Frequency (Hz) :** 50  
**Rated Primary Voltage (L-G) :** 230 kV  
**Rated Voltage Factor (ku) Cont. :** 1.2  
**Voltage Accuracy Class :** IEC 0.2 S & IEC 3P  
**VT Voltage Ratio (Main Output) :** 230000:2.3  
**VT Voltage Ratio (Second Output) :** N/A

**CT Fiber Turns (1st/2nd coils):** 44/2  
**Current Accuracy Class (1st coil):** IEC 0.2 S  
**Current Accuracy Class (2nd coil):** IEC 5P

<b>CT Rated Primary Current (A) :</b>	<b>C1 Output1</b>	<b>C1 Output2</b>	<b>C2 Output1</b>	<b>C2 Output2</b>
<b>CT Rated Secondary Output :</b>		450		2000
<b>CT RF or ALF</b>		4V		0.2V
		1.5		20

**1. Low-Voltage Components Withstand Test**

**Connections requiring 2.8 kVdc, applied for 1 minute**

– Sensor Chassis, CT Modulator Output	Pass
– Sensor Chassis, MR/DI Alarm Contacts	Pass
– Sensor Chassis, Outdoor Temperature	Pass
– CAPSU/PSU, Power Input	Pass

**Connections requiring 700 VDC, applied for 1 minute**

– Sensor Chassis, VT LEA	Pass
– Sensor Chassis, VT LEA2 (if installed)	Pass
– Sensor Chassis, CT LEA2 (if installed)	Pass
– CAPSU/PSU, CT HEA Output	N/A
– VT Amplifier, VT HEA Output	N/A

**2. Verification of terminal marking (Polarity Check)** Yes

**3. Tightness Test**

	Phase A	Phase B	Phase C
Leak Rate Pass Criteria < 0.5% a year	0.1%	0.1%	0.40%

**4. AC withstand test on primary terminals & measurement of partial discharge.**

– Refer to attached reports ( Routine HV Test Report NXVCT-0231) Pass

**5a. Accuracy Tests – CT Sensor / Chassis & Amplifier (HEA)** Pass

- Refer to attached reports (NXVCT-0231 Phase A CT Metering Accuracy Test Report.xls)
- Refer to attached reports (NXVCT-0231 Phase B CT Metering Accuracy Test Report.xls)
- Refer to attached reports (NXVCT-0231 Phase C CT Metering Accuracy Test Report.xls)

**5b. Accuracy Tests – VT Sensor / Chassis & Amplifier (HEA)** Pass

– Refer to attached reports ( Routine HV Test Report NXVCT-0231)

Thomas Lieu  
Production Engineer / Production Manager

12-Sep-07  
Date

**Type:** NXVCT-420  
**Project Name:** TEIAS  
**PO No.:** TCOVCMT-1-07-01  
**System S/N:** NXVCT-231  
**VCT Column A S/N:** 107114-008  
**VCT Column B S/N:** 107114-009  
**VCT Column C S/N:** 107114-010  
**VCT Sensor Chassis S/N:** 106928-031  
**Voltage Amplifier Chassis S/N:** N/A  
**Power Supply Type / S/N:** PSU / 0307 2108

**Insulation and VT Accuracy Specifications:**

Maximum System Voltage ( $U_m$ ) 420 kV  
 Basic Impulse Insulation Level 1550 kV  
 Wet Withstand Level (switching) 1175 kV  
 One-Minute Withstand Voltage 680 kV  
 One-Minute Wet Withstand Voltage 620 kV  
 Nominal Nitrogen Pressure (20 °C) 29 psig  
 Minimum Nitrogen Pressure (20 °C) 14 psig  
 Rated Primary Voltage (p-g) ( $U_{pn}$ ) 230 kV  
 Rated Secondary Voltage 1 (p-g) ( $U_{sn}$ ) 2.3 V  
 Rated Secondary Voltage 2 (p-g) ( $U_{sn}$ ) 2.3 V  
 System Frequency 50 Hz  
 VT Accuracy Class/Rated Burden 1 IEC 0.2 / 5kΩ  
 VT Accuracy Class/Rated Burden 2 IEC 3P / 5kΩ  
 Rated Voltage Factor ( $K_u$ ) 1.2 (continuous)  
 Rated Phase Offset 1 ( $\phi_{on}$ ) -0.36 °  
 Rated Phase Offset 2 ( $\phi_{on}$ ) -0.36 °  
 Rated Delay Time ( $t_{dn}$ ) 98 μs

**Test Facility:** Powertech Labs, Surrey, BC, Canada

<b>Test Name:</b>	<b>Test Standard:</b>	<b>Result:</b>
1. <u>AC Withstand Test and Partial Discharge Test</u> Date: 2007-08-26	IEC60044-7,8	Pass 

The VCT Columns were energized to the withstand voltage of 680 kV-rms with frequency 60 Hz for 60 seconds. The voltage was then decreased in steps and the partial discharge was measured at each step (requirements:  $\leq 5$  pC at 291 kV and  $\leq 10$  pC at 420 kV). The VT nitrogen pressure was at 14 psig (room temperature) for the duration of the test.

2. <u>VT Accuracy Test</u> Date: 2007-08-29	IEC60044-7,8	Pass
--	--------------	------

See Clause 2.1.31, IEC60044-7, for the definition of Voltage Error and Clause 3.1.29, IEC60044-8, for the definition of Phase Error. (Note that Clause B.5.1.2.2, IEC60044-7, specifies a logically incorrect/inconsistent definition of Phase Error.)

All accuracy measurements were taken with the customer-specified 100 kOhm burden applied.

**Routine HV Test Report #231**

**Phase A Output 1:**

% of Rated Primary Voltage	Voltage Applied (kV-rms)	Voltage Error (%)	Phase Error (minutes of arc)	0.2 Class Limits of Error
80	184	-0.04	2	±0.2% ; ±10 min
100	230	-0.06	2	±0.2% ; ±10 min
120	276	-0.06	10	±0.2% ; ±10 min

**Phase A Output 2:**

% of Rated Primary Voltage	Voltage Applied (kV-rms)	Voltage Error (%)	Phase Error (minutes of arc)	3P Class Limits of Error
2	4.6	0.38	5	±6% ; ±240 min
5	230	0.59	10	±3% ; ±120 min
100	230	-0.06	6	±3% ; ±120 min
150	345	-0.08	6	±3% ; ±120 min
190	437	-0.10	6	±3% ; ±120 min
300	680*	< 3	N/A	±3% ; ±120 min

**Phase B Output 1:**

% of Rated Primary Voltage	Voltage Applied (kV-rms)	Voltage Error (%)	Phase Error (minutes of arc)	0.2 Class Limits of Error
80	184	0.00	-1	±0.2% ; ±10 min
100	230	-0.01	-1	±0.2% ; ±10 min
120	276	-0.01	-1	±0.2% ; ±10 min

**Phase B Output 2:**

% of Rated Primary Voltage	Voltage Applied (kV-rms)	Voltage Error (%)	Phase Error (minutes of arc)	3P Class Limits of Error
2	4.6	-0.70	-5	±6% ; ±240 min
5	230	-0.18	-5	±3% ; ±120 min
100	230	0.00	-4	±3% ; ±120 min
150	345	0.01	-4	±3% ; ±120 min
190	437	0.00	-4	±3% ; ±120 min
300	680*	< 3	N/A	±3% ; ±120 min

**Phase C Output 1:**

% of Rated Primary Voltage	Voltage Applied (kV-rms)	Voltage Error (%)	Phase Error (minutes of arc)	0.2 Class Limits of Error
80	184	-0.01	-2	±0.2% ; ±10 min
100	230	-0.03	-2	±0.2% ; ±10 min
120	276	-0.03	-2	±0.2% ; ±10 min

**Phase C Output 2:**

% of Rated Primary Voltage	Voltage Applied (kV-rms)	Voltage Error (%)	Phase Error (minutes of arc)	3P Class Limits of Error
2	4.6	0.12	-4	±6% ; ±240 min

**Routine HV Test Report #231**

5	230	0.19	-5	±3% ; ±120 min
100	230	-0.02	-5	±3% ; ±120 min
150	345	0.00	-5	±3% ; ±120 min
190	437	-0.03	-5	±3% ; ±120 min
300	975 kV-peak*	< 3	N/A	±3% ; ±120 min

\* Verified VT Protection Accuracy at 300% using a ~1000 µs rise-time switching impulse and observing peak readings.

3. VT Frequency Response Characterization                      NxtPhase                      Characterization Tables  
Date: 2007-08-28

A variable-frequency, 14 kV signal was generated using a 120 V variable-frequency source connected to the secondary side of a distribution instrument transformer with turns ratio 14400:120. This signal was applied to the VCT Columns and a reference capacitive divider with a ratio of approximately 20000:1. The ratio and phase difference between each VT Output 1 of a phase and the reference were measured using a lock-in amplifier and recorded at different frequencies.

The ratio and phase readings are normalized with respect to the readings at the rated frequency of 50 Hz in the following tables. The uncertainty in the ratio and phase readings is ±1% and 1°, respectively.

**Phase A Output 1 Characterization Table:**

Applied Voltage (kV)	Frequency (Hz)	Normalized Ratio	Phase (°)
13.4	45	0.9985566	-2.3
13.5	50	1	-2.16
13.5	60	1.0018532	-2.16
13.5	100	1.0038115	-4.3
13.6	120	1.0033373	-5.2
13.6	150	1.0030693	-6.34
13.6	180	1.0034196	-7.6
13.6	200	1.0025221	-8.5
13.6	240	1.0023731	-10.2
13.8	400	0.9994281	-16.7
13.9	480	0.9988568	-20
14.3	650	0.9957952	-27.1
14.6	780	0.9943127	-32.4
14.7	800	0.9944087	-33.2
15.2	960	0.9896214	-39.7
11.9	1600	0.9758416	-66.6
15.3	1920	0.9659254	-79.8
14.5	2500	0.9419168	-104.2
10.8	3000	0.9169873	-125.3
11.0	3200	0.9057118	-133.9
12.2	3840	0.8596822	-161.2
10.5	4000	0.8453138	-167.9
8.4	4500	0.8007594	170.9
6.1	5000	0.7515311	150

**Phase B Output 1 Characterization Table:**

Applied Voltage (kV)	Frequency (Hz)	Normalized Ratio	Phase (°)
13.4	45	0.9975796	-2.15
14.5	50	1	-2.13
13.5	60	1.0028645	-2.43

**Routine HV Test Report #231**

13.5	100	1.0028659	-4.5
13.6	120	1.0024656	-5.38
13.6	150	1.0007149	-6.6
13.6	180	0.9993367	-7.95
13.6	200	1.0001565	-8.8
13.6	240	1.0000828	-10.5
13.8	400	0.9956819	-17.2
13.9	480	0.9944302	-20.7
14.3	650	0.9915121	-27.9
14.6	780	0.9867292	-33.4
14.7	800	0.9855047	-34.2
15.2	960	0.9817577	-41
15.9	1600	0.9635892	-68.5
16.5	1920	0.9241287	-82
14.5	2500	0.9239631	-106.9
14.1	3000	0.8960085	-128.3
12.6	3200	0.8839904	-137
12.3	3840	0.8356463	-164.8
12.6	4000	0.8208747	-171.6
8.4	4500	0.7750723	166.9
6.1	5000	0.7225561	145.7

**Phase C Output 1 Characterization Table:**

Applied Voltage (kV)	Frequency (Hz)	Normalized Ratio	Phase (°)
13.4	45	0.9993014	-2.7
13.4	50	1	-2.35
13.5	60	1.0012287	-2.8
13.5	100	1.0008427	-4.6
13.6	120	1.0003569	-5.4
13.6	150	0.9993878	-6.6
13.6	180	0.998716	-8
13.6	200	0.9981312	-8.8
13.6	240	0.9980489	-10.5
13.8	400	0.9943701	-17.2
13.9	480	0.9938351	-20.7
14.3	650	0.9908602	-28
14.6	780	0.9881645	-33.5
14.7	800	0.9874412	-34.4
15.2	960	0.9816674	-41
11.9	1600	0.9616226	-68.7
15.3	1920	0.9484301	-82.1
14.5	2500	0.9204518	-106.9
11.8	3000	0.8928716	-128.3
10.0	3200	0.8808314	-137
12.4	3840	0.8311186	-164.6
12.6	4000	0.8158278	-171.4
8.4	4500	0.7707033	167.2
6.1	5000	0.7194843	146

  
 Dr. Patrick Chavez, P.E.  
 Manager, High-Voltage Systems  
 NxtPhase T&D Corporation

*September 28, 2007*  
 Date



**NxtPhase TEST REPORT D1437R01.02**

**CT Accuracy (Linearity) Test Report**

Project		<b>TEIAS 420kV VCT</b>											
Test Date		<b>August 16, 2007</b>				Tested By		<b>Gang Chen</b>					
System Type		<b>NXVCT-420</b>				System Serial No.		<b>NXVCT-0231</b>					
Column (or Sensor head) Serial Number		<b>107114-008</b>				If NXCT-F3, No. of fiber turns in the test							
CT Sensor Chassis Serial Number		<b>106928-031</b>				CT No. in the chassis		<b>1</b>					
PSU Chassis Serial Number		<b>0307 2108</b>				Amplifier Channel		<b>N/A</b>					
Rated Primary Current		<b>450</b> A				Rated Secondary Output		<b>4.0</b> V					
RF		<b>1.5</b>		Accuracy Class		<b>IEC 0.2S</b>		Burden		<b>5k ohm</b>		CT Ratio = 450 A:4V	
Polarity Check		<input checked="" type="checkbox"/>		Rated Frequency		<b>50</b> Hz		Test Result		<b>PASS</b>			
Notes:													
Nominal Current (A)	% of Rated Current	Ratio Error (±%)	Phase Error (±min)	TCF (IEEE/CSA)	Arbiter Ratio (RCF)	Arbiter Phase (°)	Measured Current (A)					Result	
675	150	0.02	-22.8	1.0086	<b>0.9998</b>	<b>-0.38</b>	<b>675.59</b>					<b>Pass</b>	
450	100	0.00	-23.4	1.0090	<b>1.0000</b>	<b>-0.39</b>	<b>450.16</b>					<b>Pass</b>	
225	50	-0.01	-23.4	1.0091	<b>1.0001</b>	<b>-0.39</b>	<b>225.24</b>					<b>Pass</b>	
90	20	0.07	-24.0	1.0085	<b>0.9993</b>	<b>-0.40</b>	<b>90.045</b>					<b>Pass</b>	
45	10	0.05	-25.2	1.0092	<b>0.9995</b>	<b>-0.42</b>	<b>44.758</b>					<b>Pass</b>	
22.5	5	-0.03	-25.2	1.0100	<b>1.0003</b>	<b>-0.42</b>	<b>22.785</b>					<b>Pass</b>	
0													

Notes:  
 Arbiter 931A or 933A is set up so that  
 CH1 is connected to reference CT (Knopp),  
 CH2 is connected to CT under test,  
 CH1/CH2 = RCF (Ratio Correction Factor) = 1 - Ratio Error  
 Phase (CH2 - CH1) = Phase error in degree

- Arbiter 931 A accuracy 0.05% and 3 minutes of phase from 40 mA to 20 A
- Arbiter 933 A accuracy 0.05% and 0.6 minutes of phase from 50 mA to 20 A
- Arbiter 933 A accuracy 0.10% and 3 minutes of phase from 10 mA to 50 mA
- Reference Knopp CT ratio set to 1000:1

**NXTPHASE** Protection CT Calibration Record

Project		TEIAS 420kV VCT		
Test Date	July 24, 2007	Tested By	Gang Chen	
System Type	NXVCT-420	System Serial No.	NXVCT-0231	
Column (or Sensor head) Serial Number	107114-008	If NXCT-F3, No. of fiber turns in the test		
CT Sensor Chassis Serial Number	11682570015	CT No. in the chassis	1	
CAPSU Chassis Serial Number	0307 2112	Amplifier Channel	N/A	
Rated Primary Current (A)	N/A	Rated Secondary LEA Output (V)	N/A	
RF	N/A	Rated Frequency (Hz)	50 Hz	
Polarity Check	YES	CT Ratio	N/AA:N/AV	
Accuracy Class	IEC 5P	Burden	5 kOhm	
Light Source Current (mA)	60.7422	LEA Phase Advance	Disable	
Rated Primary Current for Optional LEA (A)	2000	Optional LEA Phase Advance	Disable	
Rated Output Voltage for Optional LEA (V)	0.2	Optional LEA RF	20	
CT Ratio for Optional LEA (A:V)	2000 : 0.2			
Rated current data*	LEA Arbiter Ratio	LEA Arbiter Phase (°)	Optional LEA Arbiter Ratio	Optional LEA Arbiter Phase (°)
	N/A	N/A	1.0001	-0.37

NXVCT-0231 Phase A CT Protection Test.xls



**NxtPhase TEST REPORT D1437R01.02**

**CT Accuracy (Linearity) Test Report**

Project		<b>TEIAS 420kV VCT</b>											
Test Date		<b>August 17, 2007</b>			Tested By		<b>Peter Shen</b>						
System Type		<b>NXVCT-420</b>			System Serial No.		<b>NXVCT-0231</b>						
Column (or Sensor head) Serial Number		<b>107114-009</b>			If NXCT-F3, No. of fiber turns in the test								
CT Sensor Chassis Serial Number		<b>106928-031</b>			CT No. in the chassis		<b>2</b>						
PSU Chassis Serial Number		<b>0307 2108</b>			Amplifier Channel		<b>N/A</b>						
Rated Primary Current		<b>450</b> A			Rated Secondary Output		<b>4.0</b> V						
RF		<b>1.5</b>		Accuracy Class		<b>IEC 0.25</b>		Burden		<b>5k ohm</b>		CT Ratio = 450 A:4V	
Polarity Check		<input checked="" type="checkbox"/>		Rated Frequency		<b>50</b> Hz		Test Result		<b>PASS</b>			
Notes:		no phase compensation											
Nominal Current (A)	% of Rated Current	Ratio Error (±%)	Phase Error (±min)	TCF (IEEE/CSA)	Arbiter Ratio (RCF)	Arbiter Phase (°)	Measured Current (A)						Result
675	150	-0.01	-22.8	1.0089	<b>1.0001</b>	<b>-0.38</b>	<b>675.73</b>						<b>Pass</b>
450	100	-0.02	-23.4	1.0092	<b>1.0002</b>	<b>-0.39</b>	<b>450.5</b>						<b>Pass</b>
225	50	-0.01	-24.0	1.0093	<b>1.0001</b>	<b>-0.40</b>	<b>225.09</b>						<b>Pass</b>
90	20	0.08	-24.0	1.0084	<b>0.9992</b>	<b>-0.40</b>	<b>90.018</b>						<b>Pass</b>
45	10	0.16	-23.4	1.0074	<b>0.9984</b>	<b>-0.39</b>	<b>44.691</b>						<b>Pass</b>
22.5	5	0.08	-24.6	1.0087	<b>0.9992</b>	<b>-0.41</b>	<b>22.675</b>						<b>Pass</b>
0													

Notes:  
 Arbiter 931A or 933A is set up so that  
 CH1 is connected to reference CT (Knopp),  
 CH2 is connected to CT under test,  
 CH1/CH2 = RCF (Ratio Correction Factor) = 1 - Ratio Error  
 Phase (CH2 - CH1) = Phase error in degree

- Arbiter 931 A accuracy 0.05% and 3 minutes of phase from 40 mA to 20 A
- Arbiter 933 A accuracy 0.05% and 0.6 minutes of phase from 50 mA to 20 A
- Arbiter 933 A accuracy 0.10% and 3 minutes of phase from 10 mA to 50 mA
- Reference Knopp CT ratio set to 1000:1



**Protection CT Calibration Record**

Project		TEIAS 420kV VCT		
Test Date	July 24, 2007	Tested By	Gang Chen	
System Type	NXVCT-420	System Serial No.	NXVCT-0231	
Column (or Sensor head) Serial Number	107114-009	If NXCT-F3, No. of fiber turns in the test		
CT Sensor Chassis Serial Number	11682570015	CT No. in the chassis	2	
CAPSU Chassis Serial Number	0307 2112	Amplifier Channel	N/A	
Rated Primary Current (A)	N/A	Rated Secondary LEA Output (V)	N/A	
RF	N/A	Rated Frequency (Hz)	50 Hz	
Polarity Check	YES	CT Ratio	N/AA:N/AV	
Accuracy Class	IEC 5P	Burden	5 kOhm	
Light Source Current (mA)	62.4447	LEA Phase Advance	Disable	
Rated Primary Current for Optional LEA (A)	2000	Optional LEA Phase Advance	Disable	
Rated Output Voltage for Optional LEA (V)	0.2	Optional LEA RF	20	
CT Ratio for Optional LEA (A:V)	2000 : 0.2			
Rated current data*	LEA Arbiter Ratio	LEA Arbiter Phase (°)	Optional LEA Arbiter Ratio	Optional LEA Arbiter Phase (°)
	N/A	N/A	1.0002	-0.36

NXVCT-0231 Phase B CT Protection Test.xls



**NxtPhase TEST REPORT D1437R01.02**

**CT Accuracy (Linearity) Test Report**

Project		<b>TEIAS 420kV VCT</b>											
Test Date		<b>August 20, 2007</b>			Tested By		<b>Gang Chen</b>						
System Type		<b>NXVCT-420</b>			System Serial No.		<b>NXVCT-0231</b>						
Column (or Sensor head) Serial Number		<b>107114-010</b>			If NXCT-F3, No. of fiber turns in the test								
CT Sensor Chassis Serial Number		<b>106928-031</b>			CT No. in the chassis		<b>3</b>						
PSU Chassis Serial Number		<b>0307 2108</b>			Amplifier Channel		<b>N/A</b>						
Rated Primary Current		<b>450</b> A			Rated Secondary Output		<b>4.0</b> V						
RF		<b>1.5</b>		Accuracy Class		<b>IEC 0.2S</b>		Burden		<b>5k ohm</b>		CT Ratio = 450 A:4V	
Polarity Check		<input checked="" type="checkbox"/>		Rated Frequency		<b>50</b> Hz		Test Result		<b>PASS</b>			
Notes:		no phase compensation											
Nominal Current (A)	% of Rated Current	Ratio Error (±%)	Phase Error (±min)	TCF (IEEE/CSA)	Arbiter Ratio (RCF)	Arbiter Phase (°)	Measured Current (A)						Result
675	150	0.01	-22.8	1.0087	<b>0.9999</b>	<b>-0.38</b>	<b>675.47</b>						<b>Pass</b>
450	100	0.01	-22.8	1.0087	<b>0.9999</b>	<b>-0.38</b>	<b>450.35</b>						<b>Pass</b>
225	50	-0.02	-22.8	1.0090	<b>1.0002</b>	<b>-0.38</b>	<b>225.17</b>						<b>Pass</b>
90	20	0.01	-23.4	1.0089	<b>0.9999</b>	<b>-0.39</b>	<b>90.078</b>						<b>Pass</b>
45	10	-0.02	-24.0	1.0094	<b>1.0002</b>	<b>-0.40</b>	<b>44.648</b>						<b>Pass</b>
22.5	5	0.01	-22.8	1.0087	<b>0.9999</b>	<b>-0.38</b>	<b>22.637</b>						<b>Pass</b>
0													

Notes:  
 Arbiter 931A or 933A is set up so that  
 CH1 is connected to reference CT (Knopp),  
 CH2 is connected to CT under test,  
 CH1/CH2 = RCF (Ratio Correction Factor) = 1 - Ratio Error  
 Phase (CH2 - CH1) = Phase error in degree

- Arbiter 931 A accuracy 0.05% and 3 minutes of phase from 40 mA to 20 A
- Arbiter 933 A accuracy 0.05% and 0.6 minutes of phase from 50 mA to 20 A
- Arbiter 933 A accuracy 0.10% and 3 minutes of phase from 10 mA to 50 mA
- Reference Knopp CT ratio set to 1000:1

**NXTPHASE** Protection CT Calibration Record

Project		TEIAS 420kV VCT		
Test Date	July 24, 2007	Tested By	Gang Chen	
System Type	NXVCT-420	System Serial No.	NXVCT-0231	
Column (or Sensor head) Serial Number	107114-010	If NXCT-F3, No. of fiber turns in the test		
CT Sensor Chassis Serial Number	11682570015	CT No. in the chassis	3	
CAPSU Chassis Serial Number	0307 2112	Amplifier Channel	N/A	
Rated Primary Current (A)	N/A	Rated Secondary LEA Output (V)	N/A	
RF	N/A	Rated Frequency (Hz)	50 Hz	
Polarity Check	YES	CT Ratio	N/AA:N/AV	
Accuracy Class	IEC 5P	Burden	5 kOhm	
Light Source Current (mA)	61.9088	LEA Phase Advance	Disable	
Rated Primary Current for Optional LEA (A)	2000	Optional LEA Phase Advance	Disable	
Rated Output Voltage for Optional LEA (V)	0.2	Optional LEA RF	20	
CT Ratio for Optional LEA (A:V)	2000 : 0.2			
Rated current data*	LEA Arbiter Ratio	LEA Arbiter Phase (°)	Optional LEA Arbiter Ratio	Optional LEA Arbiter Phase (°)
	N/A	N/A	1.0001	-0.37

NXVCT-0231 Phase C CT Protection Test.xls



NxtPhase T&D Corporation  
2635 Lillooet Street  
Vancouver, BC, V5M 4P7

Tel. (604) 215 9822  
Fax. (604) 215 9833  
[www.nxtphase.com](http://www.nxtphase.com)

**TEST REPORT**  
**NXVCT CT Bandwidth**

<b>Test Date:</b> September 13, 2007	<b>Project:</b> CT Frequency Response
<b>Sample Data:</b>	System Serial Number: NXVCT-0231 Column S/N and Phase: 107114-008, Phase A Sensor Chassis Serial Number: 106928-031 (Current Sensor 1)
<b>Test Witness:</b>	Gang Chen, Peter Shen
<b>Test Standard:</b>	IEC 60044-8 (guideline)
<b>Test Procedure:</b>	Signals from 50 Hz to 20 kHz at about 10% of rated current were applied to the primary terminals of an NXVCT, and the LEA output of the CT was compared with the signal from a reference current source, using an Arbiter 931A. At above 3 kHz SR805 Lock-in amplifier and Agilent 34401A digital multi-meter was used for the comparison of the rms values (Arbiter 931A is limited to 3 kHz). Ratio and phase errors from the measurements are given below. .
<b>Test Criteria:</b>	The CT LEA output has a 3-dB bandwidth in excess of 20 kHz.
CT Rated Delay Time = 30.7 $\mu$ s	



NxtPhase T&D Corporation  
2635 Lillooet Street  
Vancouver, BC, V5M 4P7

Tel. (604) 215 9822  
Fax. (604) 215 9833  
[www.nxtphase.com](http://www.nxtphase.com)

Rated delay time		30.7 micro seconds		
Test Freq (Hz)	RCF, Metering CT	Phase Measured, Metering CT (degrees)	Ratio Error %	Phase Error (degrees)
50	1.000082	-0.398467	-0.01	0.15
100	0.999497	-1.061237	0.05	0.04
150	0.999642	-1.634823	0.04	0.02
200	0.999836	-2.220202	0.02	-0.01
250	0.999835	-2.756353	0.02	0.01
300	1.000003	-3.316527	0.00	0.00
350	0.999901	-3.879967	0.01	-0.01
400	1.000011	-4.435487	0.00	-0.01
450	1.00021	-4.982275	-0.02	-0.01
500	1.000106	-5.543637	-0.01	-0.02
550	1.000153	-6.086685	-0.02	-0.01
600	1.000332	-6.653243	-0.03	-0.02
650	1.000517	-7.20008	-0.05	-0.02
700	1.000278	-7.754892	-0.03	-0.02
750	1.000414	-8.301265	-0.04	-0.01
800	1.000423	-8.855422	-0.04	-0.01
850	1.000509	-9.413137	-0.05	-0.02
900	1.000366	-9.962053	-0.04	-0.02
950	1.000452	-10.520692	-0.05	-0.02
1000	1.000853	-11.051978	-0.09	0.00
1500	1.002263	-16.591595	-0.23	-0.01
2000	1.003969	-22.108652	-0.40	0.00
2500	1.005944	-27.726737	-0.59	-0.10
3000	1.008836	-33.232602	-0.88	-0.08
3000	1.010215	-33.828383	-1.0	-0.67
3500	1.013707	-39.4833	-1.4	-0.80
4000	1.017415	-45.13565	-1.7	-0.93
4500	1.021115	-50.7984	-2.1	-1.06
5000	1.024914	-56.449483	-2.4	-1.19
10000	1.076024	-112.4535	-7.1	-1.93
15000	1.163602	-168.837	-14.1	-3.06
20000	1.290245	-226.955833	-22.5	-5.92

**Overall test results:** The optical CT meets and exceeds its frequency performance requirements.

**Remarks:**

- The uncertainty of measurements is about 1% for ratio and 0.5° for phase.
- The equivalent phase corresponding to the rated time delay of 30.7 μs was taken into account for calculating phase error as defined in IEC 60044-8.

Prepared by:

*Thomas Lieu*

Thomas Lieu, P. Eng.  
Operation Manager



NxtPhase T&D Corporation  
2635 Lillooet Street  
Vancouver, BC, V5M 4P7

Tel. (604) 215 9822  
Fax. (604) 215 9833  
[www.nxtphase.com](http://www.nxtphase.com)

**TEST REPORT**  
**NXVCT CT Bandwidth**

<b>Test Date:</b> September 13, 2007	<b>Project:</b> CT Frequency Response
<b>Sample Data:</b>	System Serial Number: NXVCT-0231 Column S/N and Phase: 107114-008, Phase A Sensor Chassis Serial Number: 11682570015 (Current Sensor 1)
<b>Test Witness:</b>	Gang Chen, Peter Shen
<b>Test Standard:</b>	IEC 60044-8 (guideline)
<b>Test Procedure:</b>	Signals from 50 Hz to 20 kHz at about 10% of rated current were applied to the primary terminals of an NXVCT, and the LEA output of the CT was compared with the signal from a reference current source, using an Arbiter 931A. At above 3 kHz SR805 Lock-in amplifier and Agilent 34401A digital multi-meter was used for the comparison of the rms values (Arbiter 931A is limited to 3 kHz). Ratio and phase errors from the measurements are given below. .
<b>Test Criteria:</b>	The CT LEA output has a 3-dB bandwidth in excess of 20 kHz.
CT Rated Delay Time = 30.7 $\mu$ s	



NxtPhase T&D Corporation  
 2635 Lillooet Street  
 Vancouver, BC, V5M 4P7

Tel. (604) 215 9822  
 Fax. (604) 215 9833  
[www.nxtphase.com](http://www.nxtphase.com)

Rated delay time		30.7 micro seconds		
Test Freq (Hz)	RCF, Metering CT	Phase Measured, Metering CT (degrees)	Ratio Error %	Phase Error (degrees)
50	1.001001	-0.496287	-0.10	0.06
100	0.999258	-1.116585	0.07	-0.01
150	1.001847	-1.644618	-0.18	0.01
200	1.000965	-2.112775	-0.10	0.10
250	1.000072	-2.905093	-0.01	-0.14
300	0.998915	-3.601117	0.11	-0.29
350	1.000129	-4.106732	-0.01	-0.24
400	0.997252	-4.49242	0.28	-0.07
450	1.001397	-4.998977	-0.14	-0.03
500	0.998869	-5.4636	0.11	0.06
550	0.995402	-5.998688	0.46	0.08
600	0.996073	-6.581317	0.39	0.05
650	0.996935	-7.331968	0.31	-0.15
700	0.993693	-7.998023	0.63	-0.26
750	0.994281	-8.357742	0.58	-0.07
800	0.997326	-8.917882	0.27	-0.08
850	0.992695	-9.563028	0.74	-0.17
900	0.993267	-9.740068	0.68	0.21
950	0.988227	-10.493632	1.19	0.01
1000	1.003495	-11.032018	-0.35	0.02
1500	1.001992	-16.720673	-0.20	-0.14
2000	0.999512	-22.29264	0.05	-0.19
2500	0.998022	-28.004803	0.20	-0.37
3000	1.002151	-33.466762	-0.21	-0.31
3000	1.016965	-33.7854	-1.7	-0.63
3500	1.01922	-39.457267	-1.9	-0.78
4000	1.024791	-44.965117	-2.4	-0.76
4500	1.027452	-50.7958	-2.7	-1.06
5000	1.033358	-56.431233	-3.2	-1.17
10000	1.10894	-111.350667	-9.8	-0.83
15000	1.244166	-166.033667	-19.6	-0.25
20000	1.469842	-220.779167	-32.0	0.26

**Overall test results:** The optical CT meets and exceeds its frequency performance requirements.

**Remarks:**

- The uncertainty of measurements is about 1% for ratio and 0.5° for phase.
- The equivalent phase corresponding to the rated time delay of 30.7 μs was taken into account for calculating phase error as defined in IEC 60044-8.

Prepared by:

*Thomas Lieu*

Thomas Lieu, P. Eng.  
 Operations Manager



NxtPhase T&D Corporation  
2635 Lillooet Street  
Vancouver, BC, V5M 4P7

Tel. (604) 215 9822  
Fax. (604) 215 9833  
[www.nxtphase.com](http://www.nxtphase.com)

**TEST REPORT**  
**NXVCT CT Bandwidth**

<b>Test Date:</b> September 13, 2007	<b>Project:</b> CT Frequency Response
<b>Sample Data:</b>	System Serial Number: NXVCT-0231 Column S/N and Phase: 107114-009, Phase B Sensor Chassis Serial Number: 106928-031 (Current Sensor 2)
<b>Test Witness:</b>	Gang Chen, Peter Shen
<b>Test Standard:</b>	IEC 60044-8 (guideline)
<b>Test Procedure:</b>	Signals from 50 Hz to 20 kHz at about 10% of rated current were applied to the primary terminals of an NXVCT, and the LEA output of the CT was compared with the signal from a reference current source, using an Arbiter 931A. At above 3 kHz SR805 Lock-in amplifier and Agilent 34401A digital multi-meter was used for the comparison of the rms values (Arbiter 931A is limited to 3 kHz). Ratio and phase errors from the measurements are given below. .
<b>Test Criteria:</b>	The CT LEA output has a 3-dB bandwidth in excess of 20 kHz.
CT Rated Delay Time = 30.7 $\mu$ s	



NxtPhase T&D Corporation  
2635 Lillooet Street  
Vancouver, BC, V5M 4P7

Tel. (604) 215 9822  
Fax. (604) 215 9833  
[www.nxtphase.com](http://www.nxtphase.com)

Rated delay time 30.7 micro seconds				
Test Freq (Hz)	RCF, Metering CT	Phase Measured, Metering CT (degrees)	Ratio Error %	Phase Error (degrees)
50	0.999663	-0.410928	0.03	0.14
100	0.999247	-1.07943	0.08	0.03
150	0.999257	-1.633645	0.07	0.02
200	0.999523	-2.208942	0.05	0.00
250	0.9994	-2.76327	0.06	0.00
300	0.999397	-3.31347	0.06	0.00
350	0.999587	-3.893693	0.04	-0.03
400	0.999774	-4.447298	0.02	-0.03
450	0.999753	-5.007463	0.02	-0.03
500	0.99976	-5.561798	0.02	-0.04
550	0.999665	-6.125603	0.03	-0.05
600	0.999862	-6.662488	0.01	-0.03
650	0.999935	-7.228023	0.01	-0.04
700	0.999869	-7.775838	0.01	-0.04
750	1.000138	-8.333027	-0.01	-0.04
800	1.000125	-8.892017	-0.01	-0.05
850	1.000428	-9.453862	-0.04	-0.06
900	1.000218	-10.007723	-0.02	-0.06
950	1.000353	-10.551642	-0.04	-0.05
1000	1.001401	-11.078695	-0.14	-0.03
1500	1.002659	-16.616023	-0.27	-0.04
2000	1.004387	-22.151737	-0.44	-0.05
2500	1.006299	-27.697477	-0.63	-0.07
3000	1.009023	-33.22104	-0.89	-0.07
3000	1.011071	-33.4195	-1.1	-0.26
3500	1.013976	-39.002833	-1.4	-0.32
4000	1.017175	-44.5823	-1.7	-0.37
4500	1.020967	-50.1721	-2.1	-0.44
5000	1.025409	-55.75155	-2.5	-0.49
10000	1.096619	-111.279333	-8.8	-0.76
15000	1.223135	-166.541333	-18.2	-0.76
20000	1.429162	-221.530167	-30.0	-0.49

**Overall test results:** The optical CT meets and exceeds its frequency performance requirements.

**Remarks:**

- The uncertainty of measurements is about 1% for ratio and 0.5° for phase.
- The equivalent phase corresponding to the rated time delay of 30.7 μs was taken into account for calculating phase error as defined in IEC 60044-8.

Prepared by:

*Thomas Lieu*

Thomas Lieu, P. Eng.  
Operation Manager



NxtPhase T&D Corporation  
2635 Lillooet Street  
Vancouver, BC, V5M 4P7

Tel. (604) 215 9822  
Fax. (604) 215 9833  
[www.nxtphase.com](http://www.nxtphase.com)

**TEST REPORT**  
**NXVCT CT Bandwidth**

<b>Test Date:</b> September 13, 2007	<b>Project:</b> CT Frequency Response
<b>Sample Data:</b>	System Serial Number: NXVCT-0231 Column S/N and Phase: 107114-009, Phase B Sensor Chassis Serial Number: 11682570015 (Current Sensor 2)
<b>Test Witness:</b>	Gang Chen, Peter Shen
<b>Test Standard:</b>	IEC 60044-8 (guideline)
<b>Test Procedure:</b>	Signals from 50 Hz to 20 kHz at about 10% of rated current were applied to the primary terminals of an NXVCT, and the LEA output of the CT was compared with the signal from a reference current source, using an Arbiter 931A. At above 3 kHz SR805 Lock-in amplifier and Agilent 34401A digital multi-meter was used for the comparison of the rms values (Arbiter 931A is limited to 3 kHz). Ratio and phase errors from the measurements are given below. .
<b>Test Criteria:</b>	The CT LEA output has a 3-dB bandwidth in excess of 20 kHz.
CT Rated Delay Time = 30.7 $\mu$ s	



NxtPhase T&D Corporation  
2635 Lillooet Street  
Vancouver, BC, V5M 4P7

Tel. (604) 215 9822  
Fax. (604) 215 9833  
[www.nxtphase.com](http://www.nxtphase.com)

Rated delay time		30.7 micro seconds		
Test Freq (Hz)	RCF, Metering CT	Phase Measured, Metering CT (degrees)	Ratio Error %	Phase Error (degrees)
50	0.993425	-0.798108	0.66	-0.25
100	0.991092	-0.865928	0.90	0.24
150	1.002667	-1.500507	-0.27	0.16
200	0.998374	-2.701488	0.16	-0.49
250	1.005264	-3.15881	-0.52	-0.40
300	0.991836	-3.481797	0.82	-0.17
350	0.997337	-4.598663	0.27	-0.73
400	0.987124	-4.27125	1.30	0.15
450	0.991739	-5.433112	0.83	-0.46
500	0.99744	-6.179627	0.26	-0.65
550	0.997892	-6.574058	0.21	-0.50
600	0.993469	-7.238862	0.66	-0.61
650	0.994168	-7.087298	0.59	0.10
700	0.984707	-8.308038	1.55	-0.57
750	0.99168	-8.467343	0.84	-0.18
800	0.985466	-9.039242	1.47	-0.20
850	0.99138	-9.693017	0.87	-0.30
900	0.98667	-10.685822	1.35	-0.74
950	0.987292	-11.005317	1.29	-0.51
1000	1.053039	-11.55397	-5.04	-0.50
1500	1.035814	-17.206505	-3.46	-0.63
2000	1.026844	-23.022493	-2.61	-0.92
2500	1.022174	-28.938193	-2.17	-1.31
3000	1.027557	-34.903763	-2.68	-1.75
3000	0.989033	-33.177333	1.1	-0.02
3500	0.989688	-38.6018	1.0	0.08
4000	0.99274	-44.332267	0.7	-0.12
4500	0.992676	-49.778883	0.7	-0.04
5000	1.006596	-55.351817	-0.7	-0.09
10000	1.064464	-110.494	-6.1	0.03
15000	1.194812	-165.786167	-16.3	-0.01
20000	1.384434	-220.226833	-27.8	0.81

**Overall test results:** The optical CT meets and exceeds its frequency performance requirements.

**Remarks:**

- The uncertainty of measurements is about 1% for ratio and 0.5° for phase.
- The equivalent phase corresponding to the rated time delay of 30.7 μs was taken into account for calculating phase error as defined in IEC 60044-8.

Prepared by:

*Thomas Lieu*

Thomas Lieu, P. Eng.  
Operations Manager



NxtPhase T&D Corporation  
2635 Lillooet Street  
Vancouver, BC, V5M 4P7

Tel. (604) 215 9822  
Fax. (604) 215 9833  
[www.nxtphase.com](http://www.nxtphase.com)

**TEST REPORT**  
**NXVCT CT Bandwidth**

<b>Test Date:</b> September 13, 2007	<b>Project:</b> CT Frequency Response
<b>Sample Data:</b>	System Serial Number: NXVCT-0231 Column S/N and Phase: 107114-010, Phase C Sensor Chassis Serial Number: 106928-031 (Current Sensor 3)
<b>Test Witness:</b>	Gang Chen, Peter Shen
<b>Test Standard:</b>	IEC 60044-8 (guideline)
<b>Test Procedure:</b>	Signals from 50 Hz to 20 kHz at about 10% of rated current were applied to the primary terminals of an NXVCT, and the LEA output of the CT was compared with the signal from a reference current source, using an Arbiter 931A. At above 3 kHz SR805 Lock-in amplifier and Agilent 34401A digital multi-meter was used for the comparison of the rms values (Arbiter 931A is limited to 3 kHz). Ratio and phase errors from the measurements are given below. .
<b>Test Criteria:</b>	The CT LEA output has a 3-dB bandwidth in excess of 20 kHz.
CT Rated Delay Time = 30.7 $\mu$ s	



NxtPhase T&D Corporation  
2635 Lillooet Street  
Vancouver, BC, V5M 4P7

Tel. (604) 215 9822  
Fax. (604) 215 9833  
[www.nxtphase.com](http://www.nxtphase.com)

Rated delay time 30.7 micro seconds				
Test Freq (Hz)	RCF, Metering CT	Phase Measured, Metering CT (degrees)	Ratio Error %	Phase Error (degrees)
50	1.000933	-0.386503	-0.09	0.17
100	1.00006	-1.065323	-0.01	0.04
150	1.000296	-1.59192	-0.03	0.07
200	1.000632	-2.126417	-0.06	0.08
250	0.99994	-2.732083	0.01	0.03
300	1.000852	-3.25226	-0.09	0.06
350	0.999684	-3.845352	0.03	0.02
400	0.999921	-4.357772	0.01	0.06
450	1.000303	-4.955072	-0.03	0.02
500	1.000067	-5.4783	-0.01	0.05
550	1.00043	-6.028617	-0.04	0.05
600	1.000383	-6.60784	-0.04	0.02
650	1.00025	-7.174287	-0.02	0.01
700	0.999868	-7.686702	0.01	0.05
750	1.000335	-8.243018	-0.03	0.05
800	0.999179	-8.775908	0.08	0.07
850	0.999314	-9.35166	0.07	0.04
900	1.000113	-9.9358	-0.01	0.01
950	0.999518	-10.472595	0.05	0.03
1000	1.000761	-10.991473	-0.08	0.06
1500	1.002022	-16.48763	-0.20	0.09
2000	1.004157	-21.98527	-0.41	0.12
2500	1.006623	-27.471798	-0.66	0.16
3000	1.010471	-32.993087	-1.04	0.16
3000	1.017751	-33.463783	-1.7	-0.31
3500	1.02146	-39.010683	-2.1	-0.33
4000	1.025864	-44.6252	-2.5	-0.42
4500	1.03076	-50.231983	-3.0	-0.50
5000	1.034016	-55.8127	-3.3	-0.55
10000	1.104893	-111.153167	-9.5	-0.63
15000	1.233026	-166.509	-18.9	-0.73
20000	1.435862	-221.14	-30.4	-0.10

**Overall test results:** The optical CT meets and exceeds its frequency performance requirements.

**Remarks:**

- The uncertainty of measurements is about 1% for ratio and 0.5° for phase.
- The equivalent phase corresponding to the rated time delay of 30.7 μs was taken into account for calculating phase error as defined in IEC 60044-8.

Prepared by:

*Thomas Lieu*

Thomas Lieu, P. Eng.  
Operations Manager



NxtPhase T&D Corporation  
2635 Lillooet Street  
Vancouver, BC, V5M 4P7

Tel. (604) 215 9822  
Fax. (604) 215 9833  
[www.nxtphase.com](http://www.nxtphase.com)

**TEST REPORT**  
**NXVCT CT Bandwidth**

<b>Test Date:</b> September 13, 2007	<b>Project:</b> CT Frequency Response
<b>Sample Data:</b>	System Serial Number: NXVCT-0231 Column S/N and Phase: 107114-010, Phase C Sensor Chassis Serial Number: 11682570015 (Current Sensor 3)
<b>Test Witness:</b>	Gang Chen, Peter Shen
<b>Test Standard:</b>	IEC 60044-8 (guideline)
<b>Test Procedure:</b>	Signals from 50 Hz to 20 kHz at about 10% of rated current were applied to the primary terminals of an NXVCT, and the LEA output of the CT was compared with the signal from a reference current source, using an Arbiter 931A. At above 3 kHz SR805 Lock-in amplifier and Agilent 34401A digital multi-meter was used for the comparison of the rms values (Arbiter 931A is limited to 3 kHz). Ratio and phase errors from the measurements are given below. .
<b>Test Criteria:</b>	The CT LEA output has a 3-dB bandwidth in excess of 20 kHz.
CT Rated Delay Time = 30.7 $\mu$ s	



NxtPhase T&D Corporation  
 2635 Lillooet Street  
 Vancouver, BC, V5M 4P7

Tel. (604) 215 9822  
 Fax. (604) 215 9833  
[www.nxtphase.com](http://www.nxtphase.com)

Rated delay time 30.7 micro seconds				
Test Freq (Hz)	RCF, Metering CT	Phase Measured, Metering CT (degrees)	Ratio Error %	Phase Error (degrees)
50	0.954087	-0.604073	4.81	-0.05
100	0.946359	-0.893993	5.67	0.21
150	0.949794	-1.433597	5.29	0.22
200	0.949331	-1.90268	5.34	0.31
250	0.947085	-2.772582	5.59	-0.01
300	0.948629	-3.299007	5.42	0.02
350	0.944546	-3.87985	5.87	-0.01
400	1.130979	-4.512835	-11.58	-0.09
450	0.937925	-4.525482	6.62	0.45
500	0.93142	-5.598928	7.36	-0.07
550	0.942558	-6.379573	6.09	-0.30
600	0.939071	-6.21301	6.49	0.42
650	0.933293	-7.28149	7.15	-0.10
700	0.932187	-7.952852	7.27	-0.22
750	0.93971	-8.958967	6.42	-0.67
800	0.926799	-8.136513	7.90	0.71
850	0.925213	-9.618063	8.08	-0.22
900	0.916468	-9.828092	9.11	0.12
950	0.929838	-10.537878	7.55	-0.04
1000	1.013311	-11.085667	-1.31	-0.03
1500	1.008626	-16.534152	-0.86	0.04
2000	0.99639	-22.4614	0.36	-0.36
2500	0.985778	-27.73412	1.44	-0.10
3000	0.989631	-33.389745	1.05	-0.23
3000	1.035652	-33.411683	-3.4	-0.26
3500	1.044736	-38.612217	-4.3	0.07
4000	1.038967	-44.23075	-3.8	-0.02
4500	1.051734	-49.93385	-4.9	-0.20
5000	1.062087	-55.8596	-5.8	-0.60
10000	1.128684	-109.953667	-11.4	0.57
15000	1.245999	-164.382667	-19.7	1.40
20000	1.414973	-218.810333	-29.3	2.23

**Overall test results:** The optical CT meets and exceeds its frequency performance requirements.

**Remarks:**

- The uncertainty of measurements is about 1% for ratio and 0.5° for phase.
- The equivalent phase corresponding to the rated time delay of 30.7 μs was taken into account for calculating phase error as defined in IEC 60044-8.

Prepared by:

*Thomas Lieu*

Thomas Lieu, P. Eng.  
 Operations Manager